THE SYNTHESIS OF [16,17-^{14}C]GERANYLGERANYL PYROPHOSPHATE

To My Husband, Hieu D. Lieu

THE SYNTHESIS OF [16,17-^{14}C]GERANYLGERANYL PYROPHOSPHATE AS A PROBE FOR THE BIOSYNTHESIS OF TAXOL

By

TRAM NGOC THUY HUYNH, B.Sc.

A Thesis

Submitted to the School of Graduate Studies

in Partial Fulfilment of the Requirements

for the Degree

Master of Science

McMaster University

December 1992

MASTER OF SCIENCE (1992) McMASTER UNIVERSITY

(Chemistry) Hamilton, Ontario

TITLE: The Synthesis of [16,17-^{14}C]Geranylgeranyl Pyrophosphate as a Probe for The Biosynthesis of Taxol.

AUTHOR: Tram Ngoc Thuy Huynh, B.Sc. (McMaster University)

SUPERVISOR: Dr. Paul H.M. Harrison

NUMBER OF PAGES: xi, 99

Abstract

Taxol, a highly functionalized and complex diterpene belonging to the taxane group, possesses strong antitumor activity against various cancers, especially in cases of advanced ovarian and breast cancers. Because of the unique mechanism of action and the unusual chemical structure, taxol may represent the prototype of a new class of chemotherapeutic agents. The non-clinical work up to date on taxol is described in this thesis, including natural resources, chemical synthesis and chemical manipulation of taxol.

The biosynthesis of taxol has not yet been studied. The hypothesis proposed for the biosynthetic sequence involves cyclization of geranylgeranyl pyrophosphate (GGPP) into hydrocarbon intermediates, which are then further transformed into taxol. In order to study the biosynthesis of taxol, [^{14}C]-labelled GGPP was prepared. Through the use of this labelled precursor in incubations with cell-free extract of yew labelled biosynthetic intermediates which are formed can be isolated and identified, hence leading to further understanding of the biosynthesis of taxol.

The synthesis of [16,17-^{14}C]geranylgeranyl pyrophosphate was achieved in eight steps starting from commercially available geranylgeraniol. The alcohol was protected as the acetate derivative and the terminal double bond selectively epoxidized. The epoxide was opened to the diol, which was then cleaved. The resulting aldehyde was coupled to [^{14}C] isopropyltriphenylphosphonium ylid in a Wittig reaction, giving [16,17-

^{14}C]geranylgeraniol after deprotection of the acetate group. The alcohol was converted into the chloride derivative and subsequently to [16,17-^{14}C]geranylgeranyl pyrophosphate.

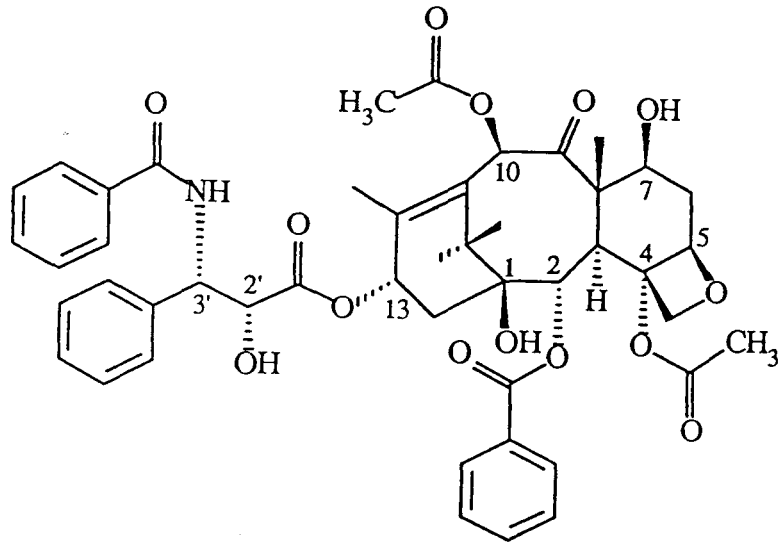

Taxol

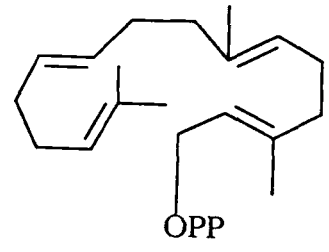

Geranylgeranyl Pyrophosphate (GGPP)

Acknowledgements

I would like to express my gratitude to my supervisor, Dr. Paul H.M. Harrison, for his patient assistance and guidance throughout the course of this research.

I wish to thank the members of our research group Karen Bell, Gerri M^{ac}Eachern, Endang Saepudin and Sengen Sun for all their help in the lab, especially Gerri M^{ac}Eachern for the very helpful discussion about my project.

I would also like to offer a very special thank to my parents for everything that they have given me in my life. Finally, I would like to thank my husband, Hieu for supporting me throughout the research, especially the writing up of this thesis.

Financial assistance from the Natural Sciences and Engineering Research Council of Canada and McMaster University are gratefully acknowledged.

TABLE OF CONTENTS

LIST OF FIGURES

LIST OF TABLES

LISTS OF ABBREVIATIONS

Ac	CH_3CO
CI	chemical ionization
DCQB	dihydroquinidine-4-chlorobenzoate
(+)DET	(+) diethyltartrate
DMAP	dimethylaminopyridine
DPC	di-2-pyridyl carbonate
e.e.	enantiomeric excess
EI	electron impact ionization
Et	ethyl
G_2	post synthetic phases of the mitotic cycle
GGPP	geranylgeranyl pyrophosphate
GTP	guanosine triphophate
IR	infrared
M	metaphase of the mitotic cycle
MAPs	microtubule associated proteins
m-CBPA	*m*-chloroperbenzoic acid
Me	methyl
MS	mass spectrometry
NMNO	N-methylmorpholine-N-oxide

NMR	nuclear magnetic resonance
Ph	phenyl
PPNO	4-phenylpyridine N-oxide
RT	room temperature
t-Boc	*tert*-butoxycarbonyl
t-Bu	*tert*-butyl
THF	tetrahydrofuran
TLC	thin layer chromatography
TMS	tetramethylsilane
troc	2,2,2-trichloroethyloxy carbonyl
Ts	*p*-toluenesulfonyl
UV	ultraviolet

I. INTRODUCTION

Taxol (Figure 1) is a complex diterpene isolated from the bark of the Pacific yew *Taxus brevifolia*, a very slow growing understory tree found in the old growth forest of the Pacific Northwest. Taxol possesses high cytotoxicity, strong antitumor activity and is currently being tested in Phase II clinical trials in the United States. Taxol is presently considered to be one of the most exciting leads in cancer chemotherapy due to its promising results in the treatment of cases of advanced ovarian, breast and other cancers.

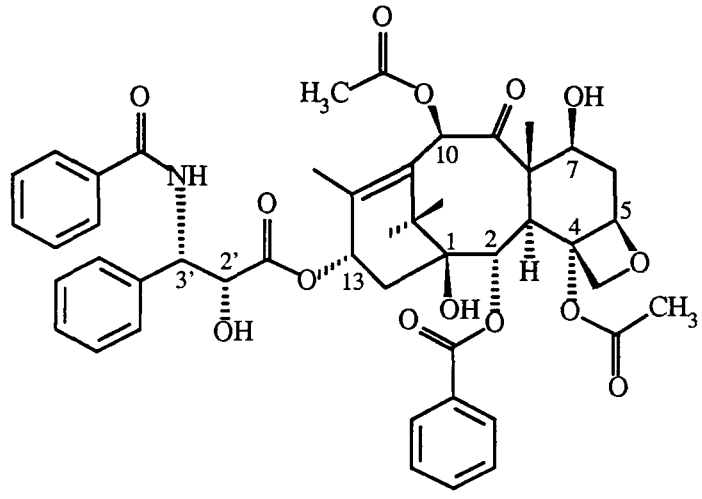

Figure 1. Taxol

1.0 Isolation

In a large-scale screening program sponsored by the National Cancer Institute and the U.S. Department of Agriculture during the late 1960s, a crude extract from the dried

bark stripped from the Pacific yew *Taxus brevifolia* was found to possess cytotoxic activity (the ability to kill tumor cells in culture) against several murine tumors. Taxol was later isolated and identified as the active constituent of the extract by Wall and coworkers[1] in 1971. There was only limited interest in taxol at the time of its discovery because its significant cytotoxic activity appeared to be mainly against leukemias (L1210, P388, P1534 leukemias, Walker 256 carcinosarcoma, Sarcoma 180, and the Lewis lung tumors) in mice and also the extreme insolubility of taxol suggested that finding a suitable dosage form would be difficult. It was not until the observation of its strong antineoplastic activity[2] against murine B16 melanoma cells and several human tumor xenograft systems (MX-1 mammary tumor, CX-1 colon and LX-1 lung xenografts) and the discovery[3] of taxol's unique mechanism of cytotoxic action that taxol was selected for preclinical developments in 1977. Progress in developing taxol as a drug toward clinical trials was very slow due largely to its scarcity, the difficulty of large-scale isolation, extraction and preparation and the poor aqueous solubility which made formulation difficult.

2.0 Mechanism of Action of Taxol

In 1977, interest in taxol was heightened due to the discovery that taxol has a unique mode of action[3]: namely, it acts as a promoter of microtubule assembly and inhibitor of microtubule disassembly.

Microtubules are self-assembling and self-disassembling intracellular polymeric protein structures, which have crucial functions in living cells. Microtubules

are responsible for a variety of structural and functional roles in the cell such as intracellular organelle transport, and formation of the mitotic spindle and the cytoplasmic cytoskeleton. The cytoplasmic cytoskeleton is an intricate three-dimensional array of interconnected microtubules, microfilaments (actin filaments) and intermediate filaments, of which microtubules are the largest element. The cytoplasmic microtubules define and maintain the shape of the cell, determine the distribution of the other components of the cytoskeleton, and are involved in many of the cell's movements. The mitotic spindle is formed during mitosis, and is responsible for separation of the chromosomes prior to cell division. The spindle consists of organized bundles of polar microtubules originating from the spindle poles (centrioles) at either ends and extending toward the equator of the dividing cell, and the chromosomal microtubules originating from the kinetochores (specialized structures that form on opposite side of the centromere (center) of the chromosomes) and extending toward the spindle poles. During metaphase of mitosis, the chromosomes are split apart as they move toward opposite poles, by the depolymerized chromosomal microtubules.

Microtubules are not static organelles but rather are in a state of dynamic equilibrium with their components, the tubulin proteins (the dimeric protein consists of two protein subunits α and β tubulins). The direction of their equilibrium toward microtubule assembly or disassembly appears to be determined by signals generated during specific cell cycle phases by intracellular regulators like calcium and guanosine triphosphate (GTP)[4,5]. Studies of microtubule assembly *in vitro* have shown that the polymerization requires a critical concentration of tubulin dimers, magnesium ion, GTP,

microtubule-associated proteins (MAPs), organic buffer and heat (37°C).

Taxol was found to inhibit the division of exponentially growing HeLa cells at the late G_2 (the postsynthetic phase) and metaphase (M, where depolymerization of the mitotic spindle splits the chromosomes in 2 halves of the dividing tumor cell) at a low concentration of 0.25 μM[3,6]; there were no significant effects on DNA, RNA or protein synthesis. Examination of the cells accumulated in the G_2 and M phases showed shorter microtubules and bundles of microtubules, all of which have the same structure as normal microtubules. It was concluded that taxol acts to block cells in mitotic stages of the cell cycle by catalyzing rapid microtubule formation and then stabilizing them against depolymerization[3,6,7]. Cancer cells are uncontrolled and rapidly growing cells that result in the loss of tissue stability, reduce tissue function and often lead to a fatal outcome. Antimitotic agents act to disrupt the control of microtubule dynamics which then would disrupt cell division as well as other cellular activities in which microtubules are involved. Taxol alters the normal equilibrium of microtubules, shifting the equilibrium in favour of microtubules by lowering the critical concentration of tubulins required to form microtubules[3], enhancing the rate of polymerization and stabilizing them against depolymerization. In contrast, all other known agents which exert effects on microtubules such as colchinine, podophyllotoxin and vinblastine inhibit the assembly of microtubules.

Experiments with purified tubulin *in vitro* demonstrated that taxol enhanced the rate and extent of polymerization of tubulins[3,8] to microtubules, even in the absence of factors that are normally essential for microtubule assembly such as GTP or MAPs[9]. Taxol also stimulated polymerization of tubulins without MAPs, in the presence of Ca^{2+},

inhibited by colchicine[10]. Taxol-treated microtubules are relatively insensitive to low temperature (4°C) and calcium chloride (Ca^{2+})[3,7], conditions that would usually promote disassembly. The resistance to depolymerization suggested that the binding site for taxol is on the intact microtubules[3] rather than on tubulin dimers. Optimal effect of the drug was observed when taxol was one equivalent to tubulin dimers: the binding constant is approximately 0.9 μmol/L and the binding is reversible[3]. The binding site of taxol is different from the binding sites for exchangeable GTP, colchinine, podophyllotoxin or vinblastine, and taxol did not competitively inhibit the binding of colchinine, podophyllotoxin or MAPs[10]. At the present time, the mechanism by which taxol interacts with microtubules at the molecular level and blocks cell mitosis is poorly understood, and it is being investigated extensively.

Phase I trials of taxol which began in 1983, were aimed at determining the maximum tolerated dosage in humans and any dose-limited toxicities. The trials were nearly aborted due to high incidence of severe acute hypersensitivity reactions[11,12]: one patient died from sudden hypotension. These reactions also occurred more frequently when taxol was infused over shorter duration. Due its high hydrophobicity, taxol was formulated in cremaphore EL, a polyethoxylated castor oil necessary to solubilize the drug. Earlier toxicology work had shown that this surfactant could produce hypersensitive reactions in animals[13,14]. Therefore the infusion duration was increased from 6 to 24 hours, and "anti-allergic" medications including steroids and antihistamines were used. These measures resulted in a dramatic reduction of the allergic reactions, and permitted the completion of phase I studies in 1988. The major dose-limiting toxicities of taxol

found were neotropenia[15,16,17] and peripheral neuropathy (numbness and tingling of extremities)[18]. The trials also indicated aneoplastic activity in several tumor types, especially activities against melanoma, renal and ovarian cancer[15-24].

Phase II trials[25-31] in which the drug effectiveness is tested on a larger number of patients is now being conducted in the United States. The results available to date have shown that taxol has excellent activity against advanced and refractory ovarian carcinoma[25,29,30], and breast cancer[31,32], moderate response rate in melanoma[28] and non-small cell lung carcinoma[33,34], but low activity in renal cell carcinoma.[26] For example, McGuire and coworkers[25] reported that there was a 30% rate of improvement (combined partial and complete responses) among patients with advanced ovarian cancer, who had not responded to standard treatments. Another Phase II trial was reported to have an overall 37% response rate to advanced and refractory ovarian carcinoma. Another study[30] showed tumor shrinkage in 48% of patients with advanced breast cancer whose prior chemotherapy had failed. However the limited supply of taxol has prevented a more extensive clinical study to broaden the scope of the trials to other disease sites.

3.0 Supply Problems

Ongoing clinical trials of taxol have been slow because taxol is in very short supply. The shortage of taxol has sparked unusually widespread research efforts, with scientists in medicine, chemistry, and several other fields trying to find ways to increase the drug's availability. Various strategies being studied include total synthesis from simple starting materials, partial synthesis from readily available taxol precursors,

extraction from *Taxus* needles, cultivation of *Taxus* plants, cell culture production and identification of simpler drug analogues.

3.1 Natural Resources

3.1.0 Current Source of Taxol

Presently, taxol is extracted from the bark of the Pacific yew, *Taxus brevifolia* which grows in forests of the northwestern United States and in western Canada. The current approach to large-scale isolation of taxol from the bark consists of methanol extraction of the crushed, dried bark, a CH_2Cl_2-H_2O partition step, a precipitation step and several silica and Florisil chromatographies on the preparative scale. One of the difficulties in the scheme is the separation of taxol and cephalomannine (Figure 2), a closely related taxane.

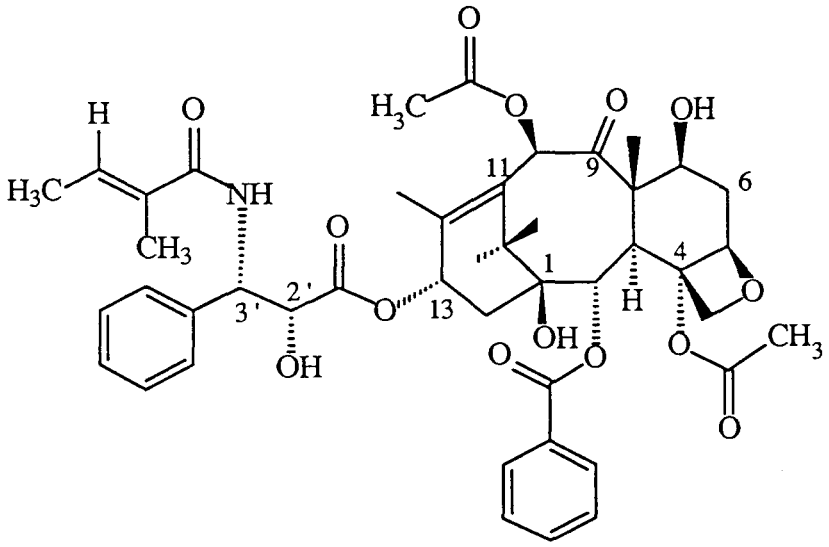

Figure 2. Cephalomannine

The purification of taxol is effected by very careful chromatography under low resolution conditions (separation is carried out using a CH_2Cl_2/*n*-BuOH solvent system

on silica gel or by HPLC, which adds significantly to the costs of the isolation process). However, a recent method[35] using the difference of the side chains of the two compounds to effect the separation was described. The double bond in cephalomannine can be selectively oxidized with osmium tetraoxide under mild conditions, yielding a diastereomeric mixture of diol derivatives while taxol remains unchanged. The resulting mixture then can be readily separated by simple flash chromatography on silica gel, giving taxol in good yield. Taxol was initially obtained in 0.02% yield[1], but large-scale isolations have given somewhat lower yield: in one case 27300 kg of bark yielded 1900 g of taxol, i.e. about 0.007%. At the present time, the only large scale source of taxol is the bark of *Taxus brevifolia* and it is expected to continue to be the chief source for the next 3 to 5 years, but the natural supply cannot be expected to meet the long term future demand. The isolation process from the dried bark is tedious, expensive and low yielding. Producing a gram of taxol requires the harvesting of 3 to 4 trees, either by stripping the bark off the tree or cutting the tree down and collecting the bark. The demand for taxol has already started to escalate: in Phase I clinical trials in 1987-1988, 60,000 lbs of dried bark was collected; for Phase II trials in 1991, a collection of 750,000 lbs of dried bark was obtained to yield 25 kg of taxol, resulting in the destruction of 38,000 trees[36]. The average quantity of taxol required for 1 course of treatment in the clinic is 300 mg, and generally a minimum of 4 courses of treatments are given. But if the responses are positive, then the treatments can be increased to 10 or more courses. Given that 12,000 women each year die from ovarian cancer in the United States[37], treatments of these patients alone would require a minimum of 15 - 25 kg of taxol per

year. Furthermore if taxol proves to be effective against other type of cancers, then the demand for taxol can be estimated to reach 250 kg per year. With the current isolation procedure, that demand would require 7.5 million pounds of dried bark from 380,000 trees. An accurate inventory of the abundance of the Pacific yew has not been undertaken, but an estimated population of 130 million yew trees occur on the National Forest land in Washington and Oregon Cascades, and the Pacific yew occurs on at least 2.5 millions acres from northern California to Alaska[37]. The Pacific yew is a slow-growing tree which takes up to 200 years to reach maturity, and while it is not currently threatened or endangered, continued harvesting of the plant for commercial preparation of taxol is untenable. Therefore an alternative solution to the taxol supply problem needs to be found.

3.1.1 Renewable Sources: Yew Needles

Since harvesting the yew bark essentially destroys the tree (either by stripping the bark off the tree or cutting the tree down to collect the bark), an obvious solution to the problem would be to look for taxol in other parts of the yew tree such as the needles. The needles of the yew are renewable each year and can be easily collected from the tree without damaging it if its taxol content is found to be as significant as that of the bark. A survey for the occurrence of taxol in other parts of the yew tree based on the analysis of several plant samples, showed that the taxol content is highly variable[38] (Table 1). The bark samples gave a range of 0.0001% - 0.069% (Table 1). The needles gave less significant yields in the range of 0.00003% - 0.003%, although one sample was reported to yield 0.006% of taxol, so the range is probably wider than the data shown. The other

significant yield of taxol comes from the seedlings at 0.0058%.

Table 1: Dry Weight Percent of Taxol in Various Parts of *Taxus brevifolia*[38]
s = Standard Deviation.

Plant Material	Average % Taxol	Range of %
Bark	0.015, s = 0.018	0.0001 - 0.0690
Roots	0.004, s = 0.004	0.0008 - 0.0100
Wood	0.0006, s = 0.0004	0.0001 - 0.0012
Wood with bark	0.0003, s = 0.0002	0.00003 - 0.004
Branches	0.0017, s = 0.0020	0.0001 - 0.0050
Leaves/Needles	0.0015, s = 0.0012	0.00003 - 0.003
Twigs	0.0012, s = 0.0013	0.0002 - 0.0034
Seedlings	0.0058, s = 0.0040	0.0007 - 0.0150

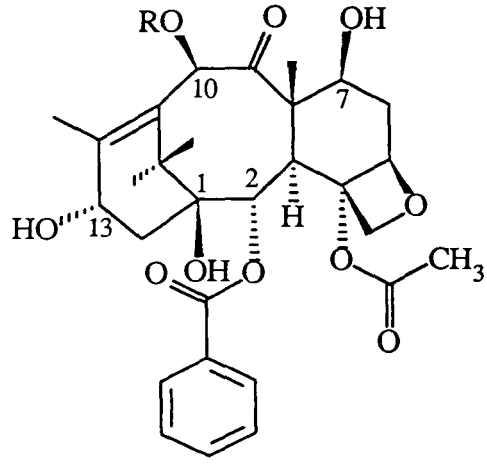

Baccatin III , R = Ac

10- Deacetylbaccatin III , R = H

Figure 3. Taxol analogues

Taxol has also been detected in other *Taxus* species. Wall's original paper[1] reported that taxol had been isolated from *T. cuspidata* and *T. baccata*. The taxanes baccatin III (**2**) and 10-deacetylbaccatin III (**3**)(Figure 3) can both be converted to taxol in high yield and so their availabilities are as important as that of taxol. Baccatin III was originally isolated from the heartwood of *T. baccata* with a yield of 0.0002%, and from the leaves, roots and stems of *T. wallichiana* with an unspecified yield. A survey on the contents of taxol and 10-deacetylbaccatin III in six *Taxus* species[39] was carried out in an attempt to find an alternate supply for taxol. The taxol content of both needles and stems was determined by HPLC (Table 2)[39] and the highest amount by weight was found in the needles of *Taxus x media* cv. Hicksii (0.01%). Other comparable amounts were found in the needles of *T. canadensis* (0.009%), *T. cuspidata* cv. Capitata (0.008%) and *T. brevifolia* (0.006%). The taxol content in the stems was no more than one half of that found in the needles. The weight percentage of taxol from the CH_2Cl_2 partition fraction was about 0.2% versus the 2% obtained from the bark of *T. brevifolia*. This result indicated that the CH_2Cl_2-H_2O partition step is less efficient in concentrating taxol in the needle extract due to the higher amount of waxy, non polar components in the needles. The percentage weight of 10-deacetylbaccatin III (Table 3)[39] showed that the highest amount was obtained from the needles of *T. baccata* (0.02%), although there was one reported yield[36] of 0.1% (1 g/kg of dried needles). In summary, there are four *Taxus* species whose needles contain amounts of taxol and 10-deacetylbaccatin III which are comparable to the quantities reported from the bark of *T. brevifolia*. The taxol content in the needles might be lower than the taxol content in the bark, but the amount of leaves

on a tree is at least 3 or 4 times the weight of the bark, so about the same amount of taxol is isolable from each tree. In addition, the isolation process can also be modified to co-isolate 10-deacetylbaccatin III (key precursor in the partial synthesis of taxol, Section 3.3.1), therefore utilizing all possible routes to taxol.

Table 2: Summary of Percent of Taxol in Six *Taxus* species[39]

Taxus species	Taxol Content (%)		
	Plant part	Dry weight	CH_2Cl_2 solubles
Taxus baccata cv. Repandens	Needles	0.003	0.05
	Stems	0.001	0.1
Taxus brevifolia	Needles	0.006	0.2
Taxus canadensis	Needles	0.009	0.3
	Stems	0.002	0.3
Taxus cuspidata cv. Capitata	Needles	0.008	0.2
	Stems	0.004	0.3
Taxus x media cv. Densiformis	Needles	0.002	0.03
	Stems	0.003	0.2
Taxus x media cv. Hicksii	Needles	0.01	0.2
	Stems	0.005	0.3

Beside the wild yew species in the forest, millions of ornamental *Taxus* species are available in some major U.S. nurseries. The *Taxus* plants are usually raised for 6 to 12 years before they are sold, and every year the needles are trimmed from the trees. These yew clippings can be collected and utilized. However, more extensive research and development needs to be done before taxol production from yew needles for clinical use

can be implemented.

Table 3. Summary of Percent 10-Deacetylbaccatin III in Six *Taxus* species[39]

Taxus species	10-Deacetylbaccatin III (%)		
	Plant part	Dry weight	CH_2Cl_2 solubles
Taxus baccata cv. Repandens	Needles	0.02	0.4
	Stems	-	-
Taxus brevifolia	Needles	0.01	0.3
Taxus canadensis	Needles	0.002	0.09
	Stems	0.005	0.6
Taxus cuspidata cv. Capitata	Needles	0.002	0.05
	Stems	0.002	0.1
Taxus x media cv. Densiformis	Needles	0.007	0.1
	Stems	0.002	0.1
Taxus x media cv. Hicksii	Needles	0.009	0.2
	Stems	0.002	0.1

A number of studies on the variation of content of taxol and its derivatives in different cultivars and wild species are being carried out[40], as is the propagation of a number of high yielding varieties by some major nurseries and lumber companies in the U.S.. The needles of the various *Taxus* species can represent a renewable source for taxol and its key precursor (10-deacetylbaccatin III). The optimum method for harvesting and storage of the needles prior to extraction and processing remains to be determined. Analytical data[40] has shown that taxol and its derivatives are highly unstable at room temperature, implying that they would undergo extensive degradation during longterm

storage of needles. In contrast to the needles, the taxol content was found to remain constant in the dried bark irrespective of the duration of storage. Also the analysis of the needle foliage is more difficult due to the presence of large amounts of photosynthetic pigments and cuticular waxes, so several conditions in the extraction (tissue size, solvent system, solvent temperature, length of extraction, etc..) need to be optimized.

3.1.2 The Heartwood

Another source of supply of taxol to be considered is the heartwood of the yew tree. Although its taxol content (0.0006%) (Table 1) appears to be much less than that of the bark of the tree, the bark only consists of 1/8 inch of the tree outer layer and there is much more of the heartwood in the tree. It has been speculated that the heartwood of the tree can contain between 50 to 100 times the total of taxol in the bark[41]. At the present time, the optimum method of extraction has not yet been determined for the isolation of taxol from the heartwood. Three procedures are being considered for the extraction from the heartwood:

1. Reduction of the size of the wood particles and use of the conventional extraction method which may improve the yield.
2. Improvement of the solubility of taxol by adding various chemical couplers.
3. Improvement of the access to taxol by swelling the wood fiber to make it more porous.

3.2 Cell Cultures

Taxol production in cell cultures is also being considered as an alternative source for the bark of the yew trees. In this process, cell lines are selected from tissue of a

Taxus species and grown in large vessels containing artificial growth medium. The advantages of this process are that the cell line can be selected from high yielding plants, and that the growth can be optimized to produce taxol and/or its key precursor (10-deacetylbaccatin III) by applying metal salt or microbial pathogens to the growth medium. The adaptation of cell cultures to large-scale production can be associated with several problems, in particular in respect of the need for an economically viable process. Phyton Catalytic (Ithaca, NY) has the exclusive license to produce and optimize the cell culture process to produce taxol and like compounds. These researchers reported that *T. brevifolia* bark or cambrial tissue forms callus in tissue culture and secretes taxol (with several other new compounds) into the supernatant[42]. Taxol can be recovered by ether extraction. The growth rate can be enhanced by adding ammonium nitrate, and elicitors such as *Cytospora abietis*, *Penicillium minioluteum* or vandyl sulfate. Each liter of supernatant produces 1 to 3 mg of taxol[43], which would be equivalent to the yield from 20 g of dried bark in a conventional extraction method. A continuous flow system in which taxol is continuously filtered from the supernatant, while supplying fresh media, may increase the yield and can be adapted to scale up the procedure to production level. However, there are problems associated with this method as with other large-scale cell cultures. The slow-growing callus is vulnerable to fungal and bacterial infection, and antibiotic treatment of the infection may interfere with the growth. The callus cells are sensitive and unstable and need constant monitoring. The process is reported to be just 2 to 5 years away from commercial production. The prospects for cell culture are uncertain at the present, but this method may prove to be a possible alternative for the

source of taxol.

3.3 Synthesis

Taxol (**1**) has a complex, highly functionalized carbon framework with 11 chiral centers, posing a difficult task for total synthesis of the compound. Although the total synthesis has not been achieved, several groups have reported progress with some innovative approaches including the use of pinene, camphor, baccatin III and 10-deacetyl baccatin III as the backbone for the taxol core.

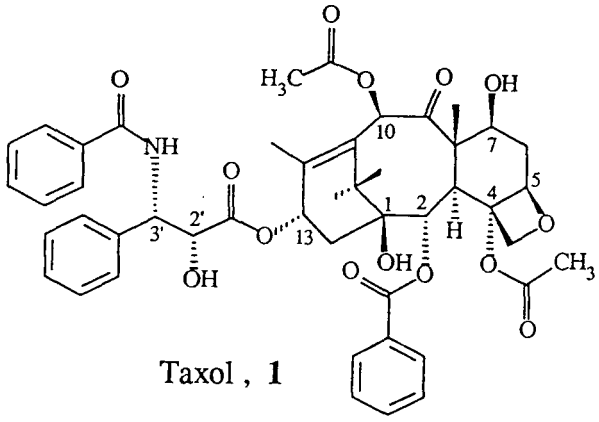

Taxol , **1**

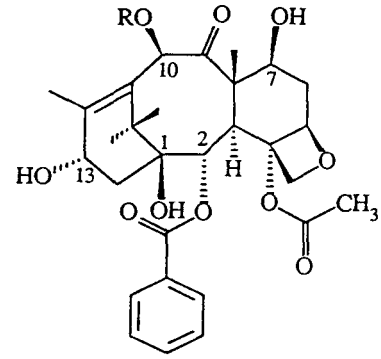

Baccatin III , R = Ac

10- Deacetylbaccatin III , R = H

3.3.0 Partial Syntheses with Vicinal Oxyamination Reaction

The partial syntheses to taxol started from the simpler diterpenoid 10-deacetylbaccatin III (**3**) which is available in high yield[44] from the renewable yew needles (1g/kg of dried needles), and from baccatin III (isolable from the heartwood of *T. baccata*)[45]. The key step in these partial syntheses of taxol is to esterify the C-13 hydroxyl group with a suitably protected derivative of the acid side chain. The order of reactivity[46] of the 3 hydroxyl groups in 10-deacetylbaccatin III is 7 > 10 >> 13. Baccatin III and 10-deacetylbaccatin III have folded structures in which the α hydroxyl group at

C-13 is in a hindered position and may be hydrogen bonded to the 4α acetyl group. Acylation at C-13 thus is a very difficult step. The conversion of 10-deacetylbaccatin III to baccatin III was accomplished by protection of the C-7 hydroxyl group with a suitable protecting group, and then acetylation at C-10 (Scheme 1).

One partial synthesis of taxol was designed from 7-(2,2,2-trichloroethyloxy carbonyl) baccatin III (troc-baccatin III)[47]. This protecting group can be removed under mild conditions at the end of the synthesis, therefore avoiding the destruction of the rest of the taxol molecule. Thus the troc derivative of **2** was esterified with *trans*-cinnamic acid, dicyclohexylcarbodiimide (DCC) and 4-(dimethylamino)pyridine (DMAP)(Scheme 1). To obtain the 2'*R*,3'*S* configuration as in taxol, a cis addition is required on the 2'-3' double bond of the *trans* cinnamate ester. Using the classical catalytic procedure (*t*-butyl-N-chloro-N-argentocarbamate, osmium tetraoxide in acetonitrile) with the addition of a chiral amine, the ester was converted to the desired product in 25% yield, with 80% stereocontrol, along with three other compounds which were its stereoisomer and regioisomers. Presumably, the chiral amine forms a stable adduct with OsO_4, thereby improving the oxyamination and inducing chirality in the amino-alcohol product. The yield was still low because of the low regioselectivity of the reaction. Deprotection of the amine, benzoylation, and removal of the troc group completed the partial synthesis of taxol, giving an overall yield of 14%. The *t*-Boc derivative of 10-deacetyltaxol (the compound was named Taxotère and/or RP56976 (Figure 4)) prepared as shown above was discovered to have excellent antitumor activity,[48] and was as potent as taxol: it inhibits cell replication, promotes the *in vivo* assembly of stable microtubules

Scheme 1

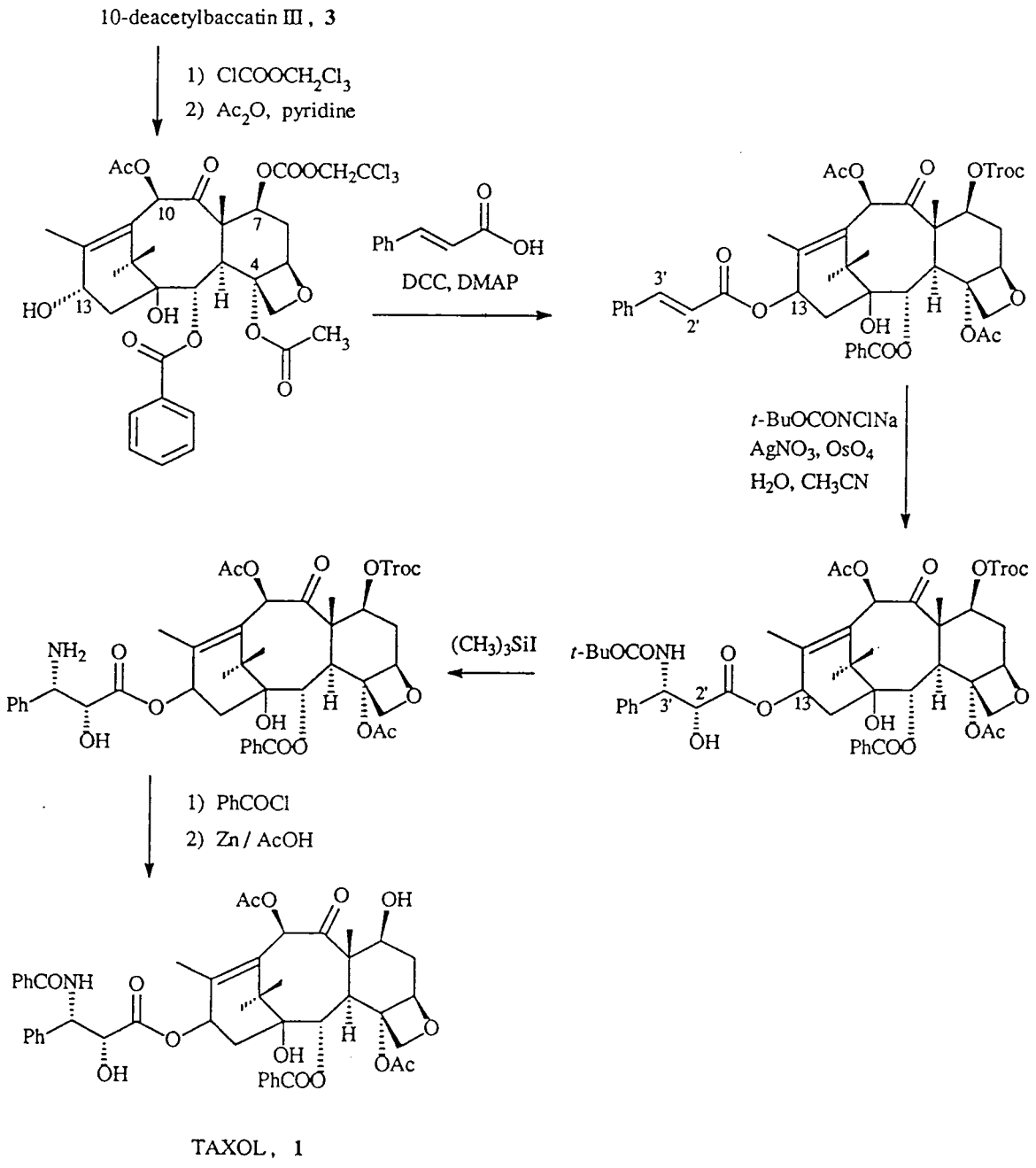
10-deacetylbaccatin III, 3
1) ClCOOCH2Cl3
2) Ac2O, pyridine
DCC, DMAP
t-BuOCONClNa
AgNO3, OsO4
H2O, CH3CN
(CH3)3SiI
1) PhCOCl
2) Zn / AcOH
TAXOL, 1

in the absence of GTP and it induces microtubule-bundle formation in cells. Taxotère is currently undergoing development as a drug for clinical trials[49].

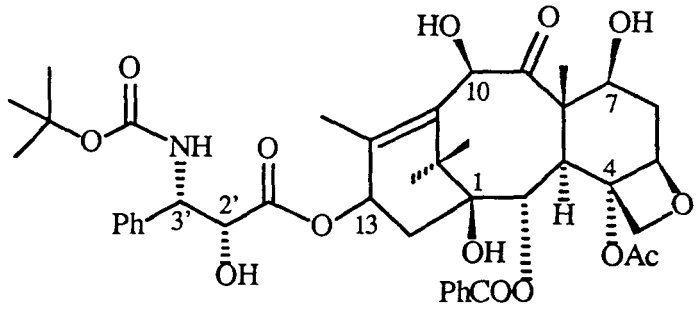

Figure 4. Taxotère

3.3.1 Syntheses of Acid Side Chain

The second major pathway to taxol involves the direct acylation of a protected baccatin III with a protected acid side chain under forcing conditions. The acid side chain has been synthesized by many methods, one of which is based on an asymmetric epoxidation[50] of *cis*-cinnamoyl alcohol, followed by cleavage of the epoxide by a nitrogen nucleophile as shown in Scheme 2. The alcohol was epoxidized using *t*-butyl hydroperoxide in the presence of titanium isopropoxide and (+)-diethyl tartrate (Sharpless epoxidation) in 65% yield and 78% enantiomeric excess (e.e.). The epoxy alcohol was oxidized and the resulting carboxylic acid methylated prior to cleavage of the epoxide to avoid the need to protect the free hydroxyl group. The epoxyester then underwent a regio- and stereospecific ring opening with trimethylsilyl azide and a catalytic amount of zinc chloride. Benzoylation of the azido alcohol yielded the azidobenzoate as indicated. The final reduction of the azide accompanied by O to N acyl migration, was achieved to

give the final acid side chain as its methyl ester **4b** in 23% overall yield. The alcohol was protected with ethyl vinyl ether and the ester cleaved to yield the free carboxylic acid **4c**, ready to be coupled to baccatin III in the final step to taxol.

Scheme 2

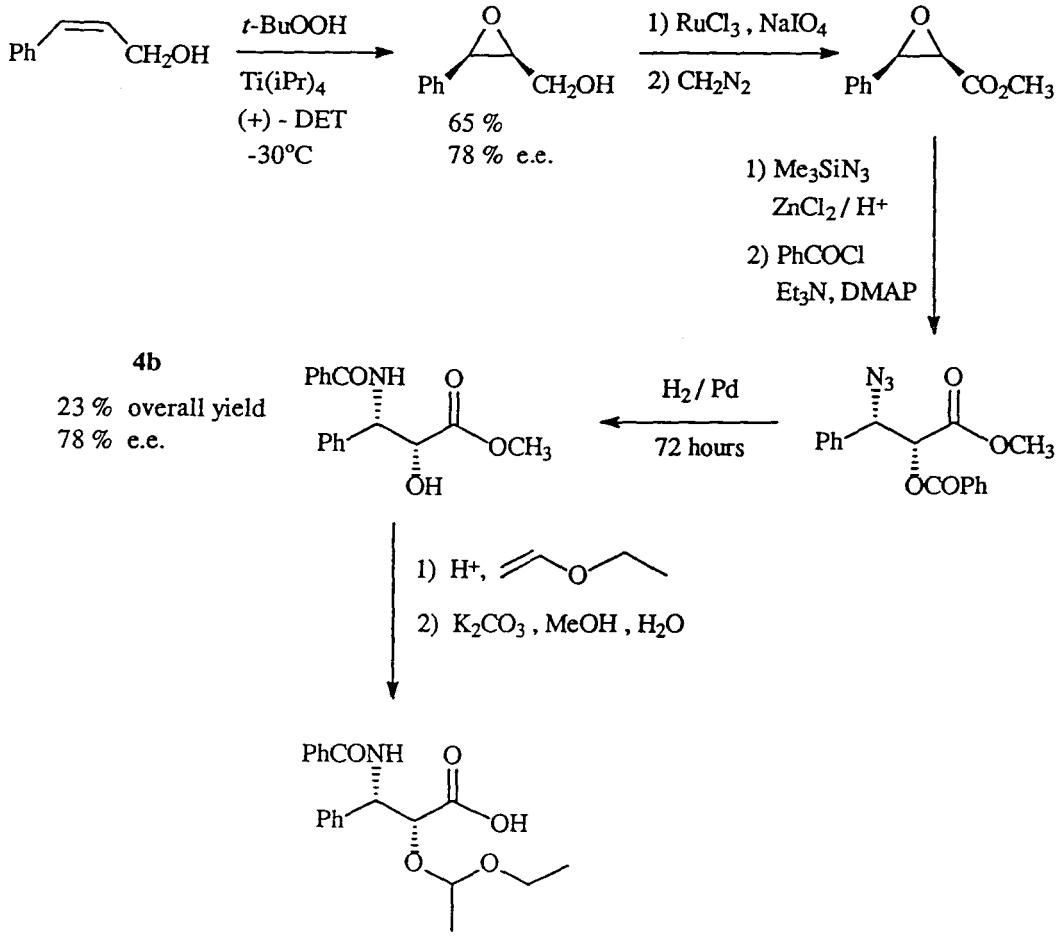

4c , (2*R*,3*S*)-N-Benzoyl-O-(1-ethoxyethyl)
-3-phenylisoserine

An improved synthesis of the acid side chain by the same author[51] involves the Sharpless dihydroxylation reaction. The inexpensive methyl cinnamate in aqueous acetone was dihydroxylated with dihydroquinidine-4-chlorobenzoate (DCQB) as the added

alkaloid, N-methylmorpholine-N-oxide (NMNO) as co-oxidant, and a catalytic amount of osmium tetraoxide (Scheme 3). The 2*S*,3*R* diol was obtained in 51% yield and 98% e.e.. Next, monotosylation of the diol gave exclusively the 2-tosylate which was converted to the 2*R*,3*R* epoxide with potassium carbonate in 91% yield. The remaining steps were modified slightly from the previous synthesis, giving a better overall yield of 35% for the final ester **4b**.

Scheme 3

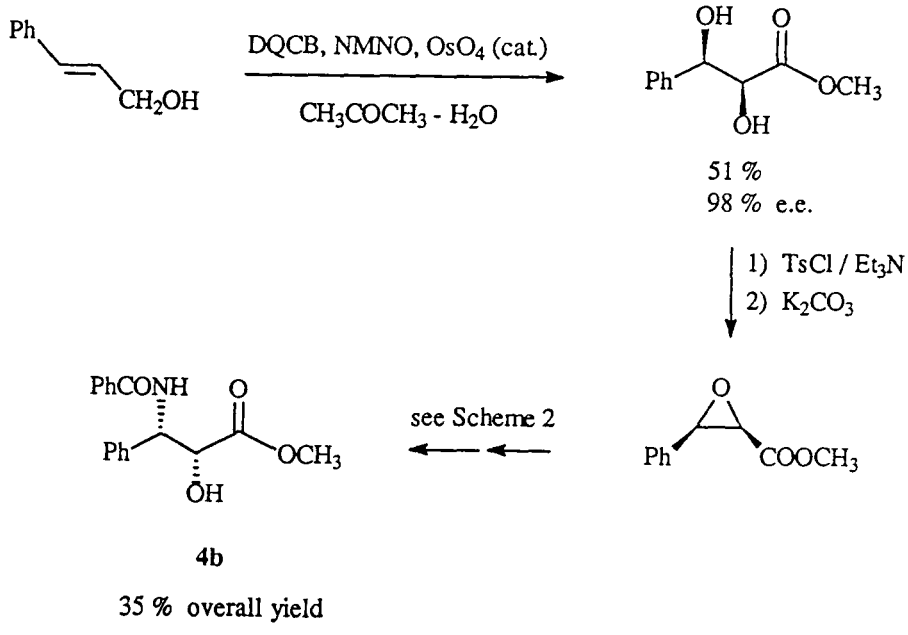

4b

35 % overall yield

One other synthesis of the acid side chain using a similar concept to the above was reported[52] recently, using the readily available (salen)Mn(III) complex **5** as the catalyst along with 4-phenylpyridine N-oxide (4-PPNO) for the epoxidation of *cis*-ethylcinnamate (Scheme 4). The starting material was easily obtained from reduction of ethyl phenylacetylenecarboxylate. The *cis* epoxide was obtained in 97% e.e. and 57%

yield along with 13% of the *trans* isomer. The N-oxide coordinates with the mildly acidic Mn species, and inhibits the catalyst decomposition (the catalyst decomposes by complexing with the epoxide). Without purification, the mixture of *cis* and *trans* isomers was treated with ammonia in ethanol to generate 3-phenylisoseriamide regioselectively. Impurities from the *trans*-epoxide ring opening were removed by recrystallization. Hydrolysis of the amide and acidification was effected to yield (2*R*,3*S*)-3-phenylisoserine. Benzoylation gave the acid side chain of taxol **4a** in 25% overall yield from *cis*-ethyl cinnamate.

Scheme 4

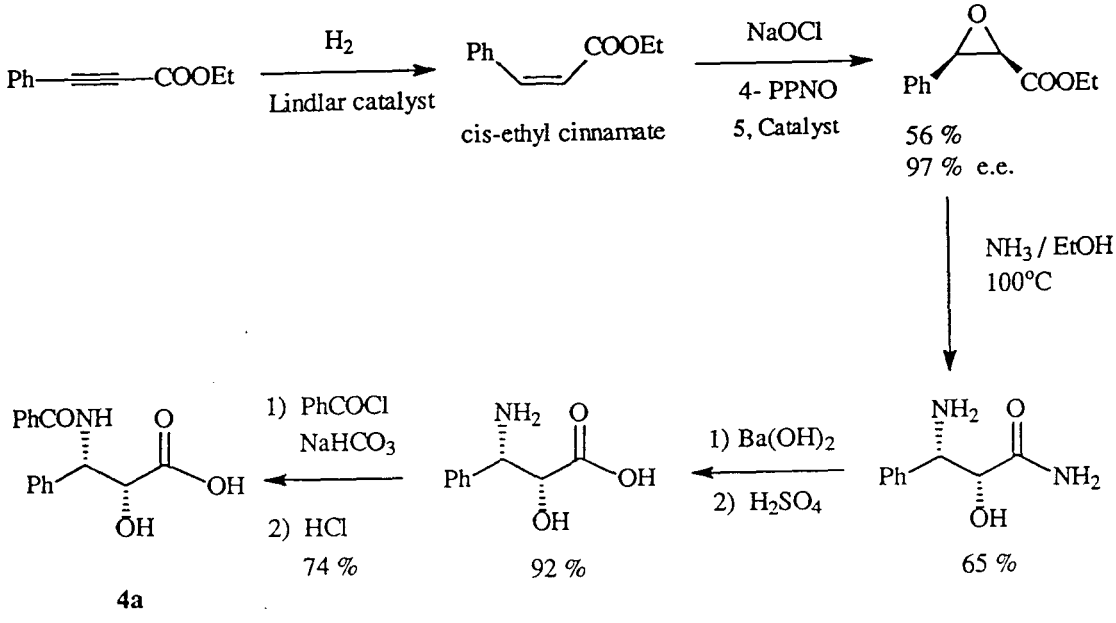

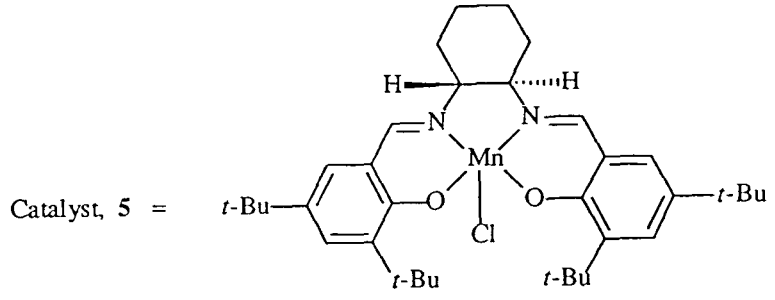

Another efficient approach to the acid side chain was developed using a β-lactam as the key intermediate[53,54]. The β-lactam was enantioselectively synthesized using a lithium-chiral ester enolate-imine cyclocondensation reaction (Scheme 5). First, the chiral lithium ester enolate was generated in situ from silyloxy acetate and reacted with N-trimethylsilylimine. The chiral auxiliary effectively directs the approach of the imine to the *si* face of the *E*-enolate in the transition state, therefore forming the *cis*-β-lactam upon cyclization with 97% e.e.. The β-lactam was deprotected with tetrabutylammonium fluoride and hydrolyzed with concentrated hydrochloric acid. Next, benzoylation of the hydrochloric acid salt afforded the product **4a** in 70% yield. The side chain was thus synthesized in 4 steps with higher overall yield than the other syntheses described (30 - 40%), and an enantiomeric excess of greater than 96%.

Scheme 5

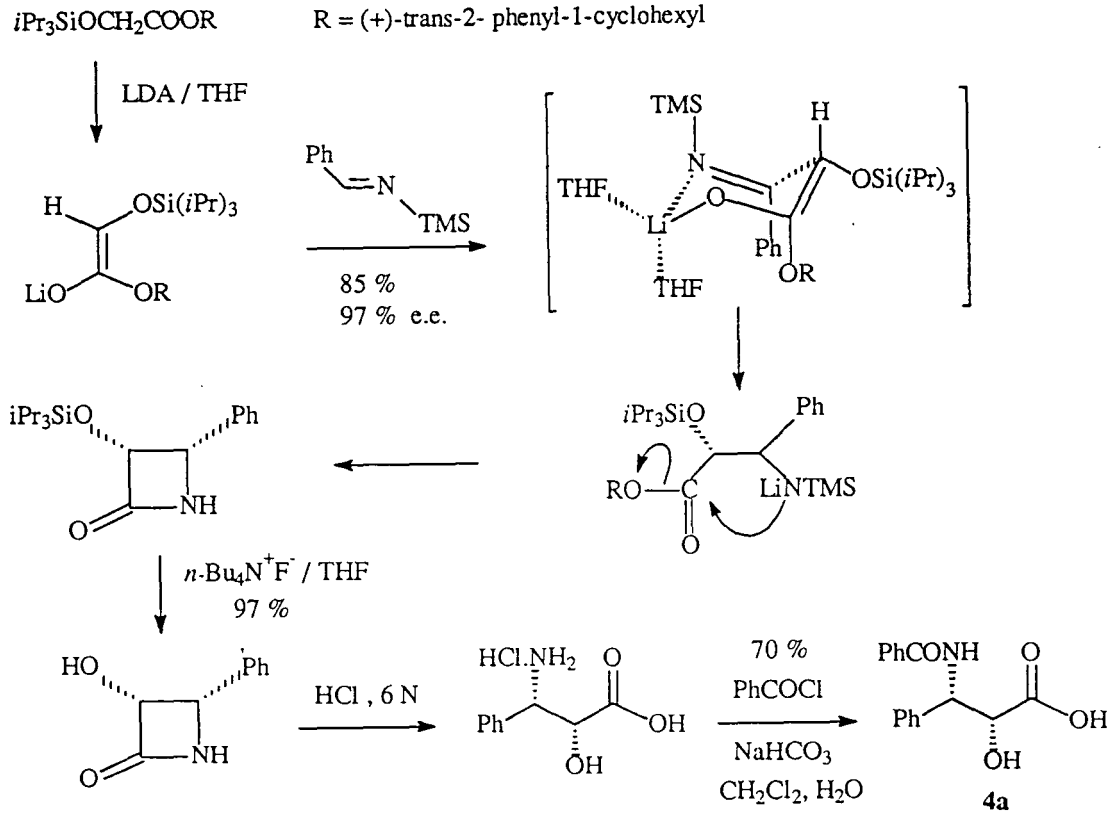

Another strategy for synthesizing the acid side chain was developed based on chelation controlled carbonyl addition[55]. The efficient conversion of (*S*)-phenylglycine to the amino alcohol was achieved by lithium aluminum hydride reduction (Scheme 6), which was then benzoylated to give the N-benzoyl derivative. Next, the tandem Swern oxidation-carbonyl addition sequence was used to yield the *syn* product in 62% yield with good diastereoselection (9:1) and with complete retention of enantiomeric purity. The hydroxyl group was protected with ethyl vinyl ether in the presence of pyridinium-p-toluenesulfonate. The double bond was oxidized with ruthenium chloride and sodium periodate in the presence of sodium bicarbonate to yield the protected acid side chain of taxol (**4c**). The total yield was 30% for the four steps.

Scheme 6

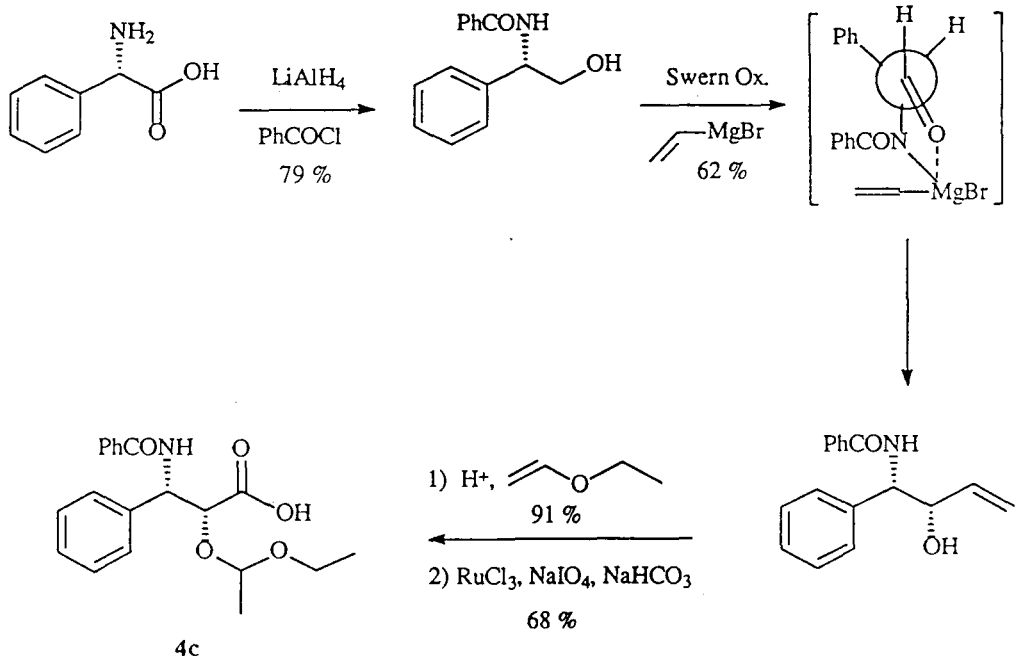

There also has been a chemoenzymatic synthesis of a derivative of N-benzoyl-(2R,3S)-3-phenylisoserine, in which the racemic mixture was resolved by enzymatic hydrolysis[56] (Scheme 7).

Scheme 7

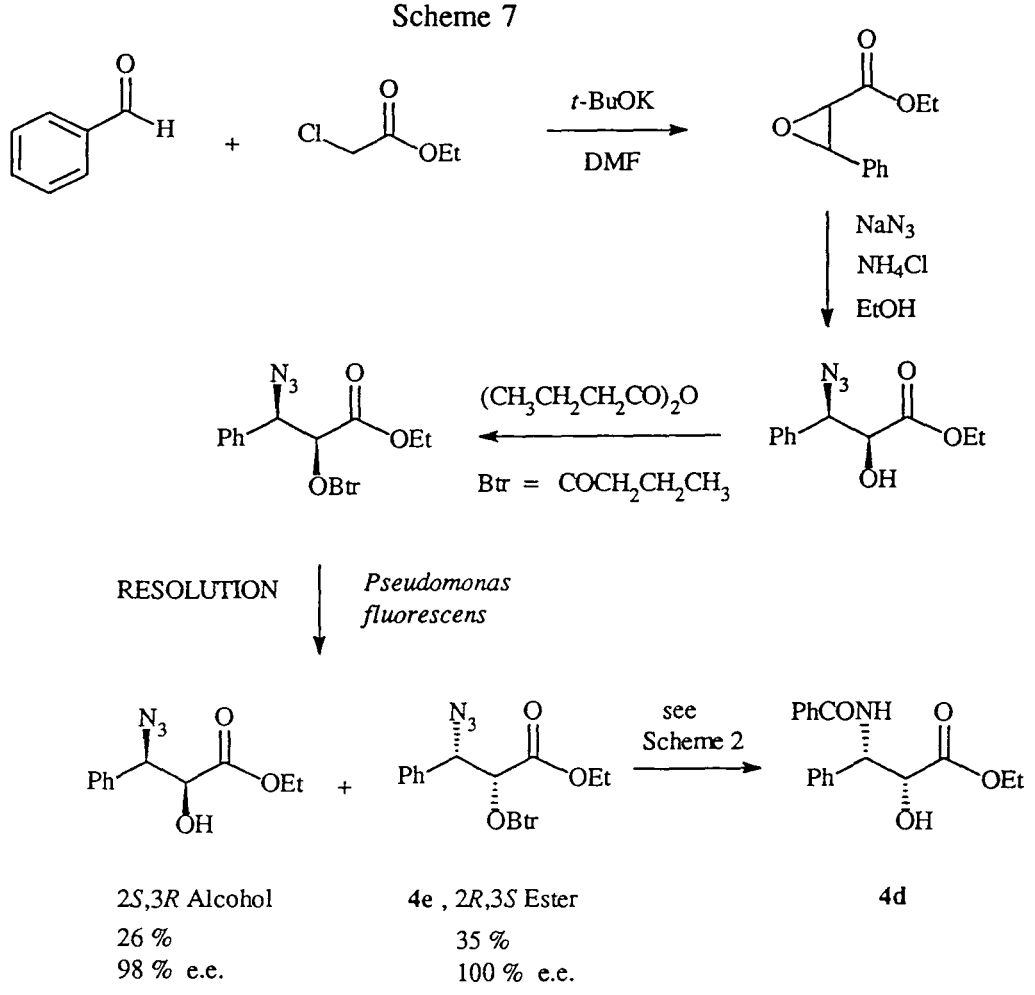

In the reaction sequence, *cis*-ethyl phenylglycidate was prepared by condensation of benzaldehyde and ethyl chloroacetate with potassium *t*-butoxide in DMF. Next, the direct opening of the epoxide ring was effected with azide ion, followed by acylation of the resulting azido alcohol by a standard procedure with butyric anhydride and pyridine, giving the protected hydroxyl compound ready to be separated by enzyme catalyzed

hydrolysis. Lipases from *Pseudomonas fluorescens* were used to resolve the racemic mixture. The alcohol product with the 2*S*,3*R* configuration was obtained in 26% yield and 98% e.e.. The remaining ester **4e** (2*R*,3*S* isomer) was also isolated from the product mixture in 35% yield and 100% e.e.. The ester then can be used to furnish the acid side chain **4d** used in the partial synthesis of taxol (see Scheme 2).

The final step in the partial synthesis of taxol involves the coupling of the protected acid side chain **4c** to the protected baccatin III. Compound **2** was protected with triethylsilyl chloride[57] (20 equivalents of triethylsilyl chloride, 50 mL of pyridine per mmol of 10-deacetylbaccatin III, 23°C, 20 hours, Ar). The esterification step was achieved in the presence of di-2-pyridyl carbonate (DPC), and DMAP in toluene solution at 73°C for 100 hours (50% conversion), giving C-2', C-7 protected taxol derivative **7** in 40% yield (Scheme 8). The protecting groups were removed with 0.5% Hcl in ethanol, giving taxol in 38% yield from 10-deacetylbaccatin III (**3**). The coupling reaction was postulated[58] to proceed through the intermediate **6**. The 5,6-dihydro-6-ketooxazine (**6**) acts as the cyclic version of the activated ester and would be less sterically demanding.

3.3.2 Total Synthesis

Several groups of researchers have been investigating many different approaches to the taxane skeleton involving total synthesis. Only one total synthesis of a taxane, the unnatural enantiomer of taxusin has been reported. Some of the approaches to build up the strained and highly functionalized tricyclic framework of taxane include cyclization reactions, ring enlargements, ring contractions, rearrangements and fragmentations.

Scheme 8

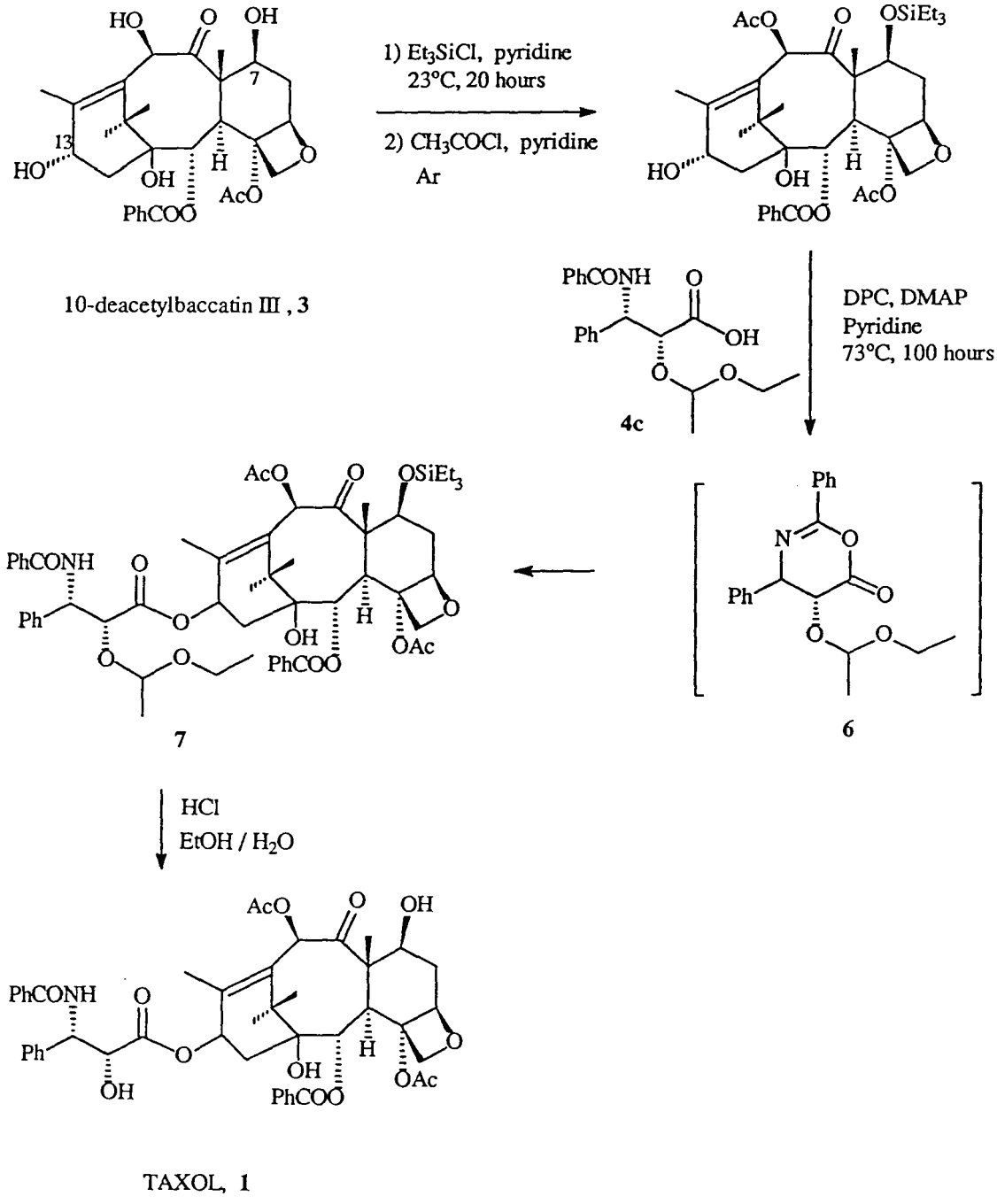

10-deacetylbaccatin III , 3

4c

6

7

TAXOL, 1

Recently, a strategy for the total synthesis of taxol from pinene was reported[59]. In the synthesis, the tricyclic core of taxol was assembled in 5 steps from verbenone (the air oxidized form of pinene) (Scheme 9). Then, in 3 more steps the two rings A and B were functionalized with the same functional groups found in taxol. The next step(s) in the sequence would involve functionalization of the C ring. At present, the reaction sequence offers promise for the total synthesis of taxol in the near future, and it is currently being used to synthesize analogues that are required for molecular mode of action and drug development studies.

Scheme 9

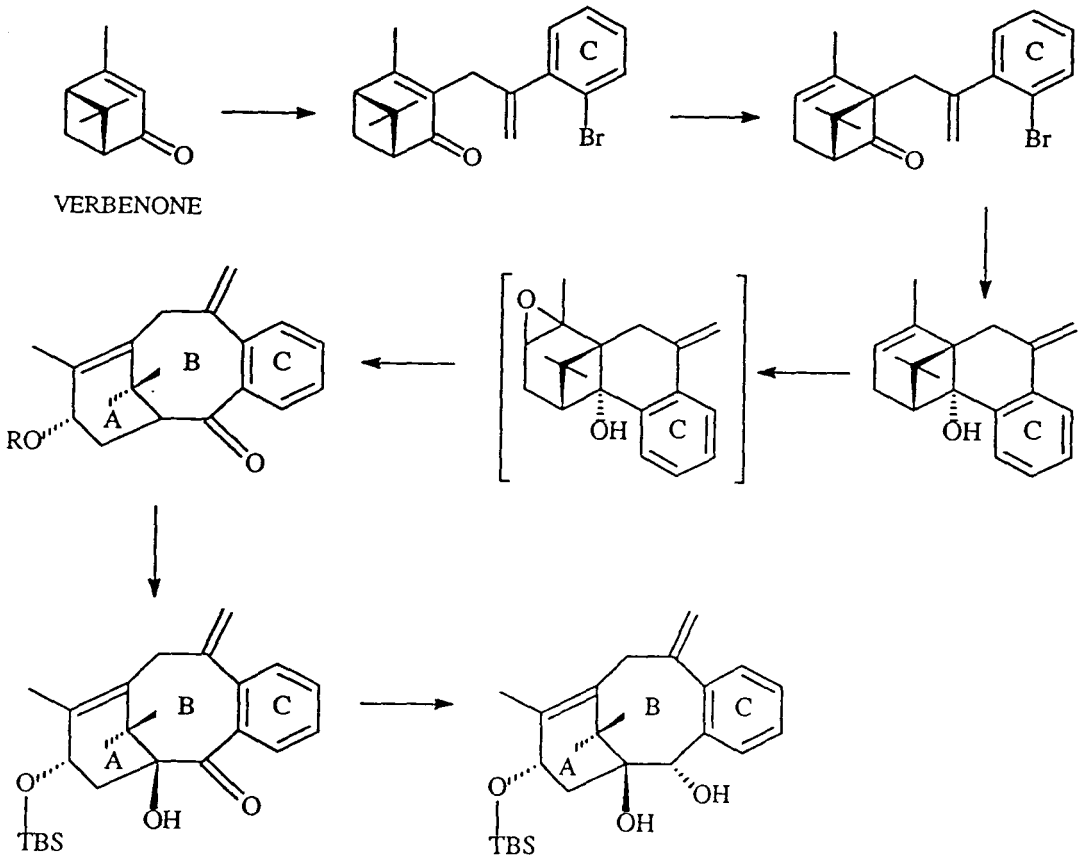

3.4 Taxol Analogues

The final approach to solving the supply problems involves the study of taxol analogues. This approach may lead to an analog that possesses antitumor activity comparable to or better than that of taxol itself, which may be able to supplant taxol altogether in the future. The structure-activity studies being carried out also may lead to modified taxol analogues with enhanced aqueous solubility, or with simpler structure which would be accessible by synthesis or modification of readily available taxanes, therefore eliminating the problem of depleting the yew population.

These structure-activity studies used cytotoxicity in cell culture systems as the major criterion for activity of the taxanes because the assay only requires a small amount of material and cytotoxicity correlates well with other measures of activity such as tubulin assembly, disassembly and binding.

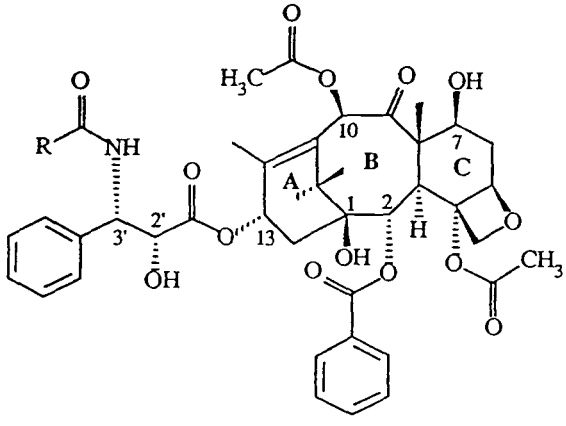

Taxol , **1** , R = Ph

Cephalomannine , R =

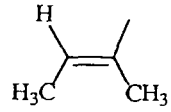

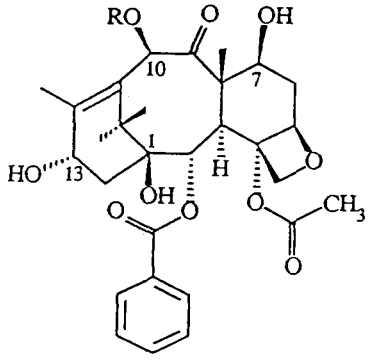

BACCATIN III , R = Ac

10- DEACETYLBACCATIN III , R = H

The results are summarized as follows:

1. The C-13 ester side chain is absolutely required for cytotoxicity, but even if the side chains are structurally very different from that of taxol the compound is still active.

Taxol and cephalomannine are both active while the cytotoxicities of baccatin III and 10-deacetylbaccatin III are reduced 322-fold.[60,61,62,63]

2. The hydroxyl group at C-2' of taxol and its derivatives is necessary for maximum biological activity. Acylation of taxol at the 2' position diminishes its cytotoxicity considerably. When the acyl group is labile and can be hydrolyzed *in vivo* to the corresponding 2'-hydroxyl compound, then the compound possesses comparable cytotoxicity to taxol.[62,64]

3. The removal of the 3'-N-benzoyl group results in loss of cytotoxic activity. However, the group can be replaced with other N-acyl groups: cephalomannine possesses comparable activity to taxol, while taxotère has slightly increased cytotoxic activity compared to taxol.[62,65]

4. A major stereochemical effect is observed when the configurations of the 2' and 3' groups are interchanged. The compound with the natural configuration is 11-fold more active than the one with the unnatural configuration in the tubulin disassembly assay.[65]

5. Acylation at C-7 in the ring of taxol does not significantly reduce the tubulin disassembly inhibition activity or its cytotoxicity, while attachment at C-7 of a polar sugar residue increases the activity.[61,62,64,65]

6. The stereochemistry of the C-7 hydroxyl group does not make a large difference in activity: taxol and 7-*epi*-taxol have comparable activities.[62,66]

7. Deacetylation at the C-10 position, as in 10-deacetyltaxol, does not reduce the cytotoxicity of the compound very much. However, the 10-deacetyltaxol derivative is actually more active than taxol in tubulin disassembly activity and cytotoxicity, so there

is an interplay between the side chain and ring effects.[61,62,65,66]

8. Attachment of polar groups at C-7 and C-10 slightly reduces the activity.[65]

9. Oxidation at C-7 reduces activity significantly.[60,65]

10. Opening of the oxetane ring reduces significantly the cytotoxicity and tubulin disassembly activity. The change is presumably due to the changed polarity of the ring-opened product or to some specific tubulin-binding feature of the oxetane ring.[60,67]

11. Contraction of ring A does not reduce activity very much in spite of the change in structure.[60,67]

12. A change in the 2-benzoyl group to a 2-(3-hydroxybenzoyl) group does not affect tubulin-disassembly activity but it does reduce the cytotoxicity.[65]

In summary, changes (with a few exceptions) in the taxane skeleton appear to reduce the activity of taxol derivatives. The conformation of the side chain is not strongly influenced by the taxane skeleton, and it is proposed that the taxol recognition site on microtubules possesses a hydrophobic cleft designed to accept a side chain with the functionality similar to that found in taxol, cephalomannine or taxotère.

3.5 Summary of the Supply Problem

The search for alternate or additional supplies of taxol is proceeding very intensively at the present. All approaches have problems associated with them. The renewable needle sources seem to be the most likely answer to the limited supply of taxol compared to the others such as cell cultures, synthesis and modification of taxol. The main source of taxol is still expected to be from the bark of *Taxus brevifolia* for the next 3 to 5 years.

4.0 Biosynthesis of Taxol

Biogenetic-type synthesis has often been used and has been proven to be a successful approach to achieve syntheses of complex natural compounds such as vinblastine, ervatamine and colchicine. The biosynthesis of taxol (**1**) and its derivatives can lend insight to the formation of this complex diterpene and may help in the total chemical synthesis of taxol. Although biosynthetic studies of taxol have not been reported, some work has been done on the C-13 side chain of taxol. Some biogenetic hypotheses were proposed for the biosynthesis of taxanes as well as taxol.

4.1 Biosynthesis of Taxane Framework

The most commonly accepted hypothesis[68,69] is that the taxane carbon framework is formed through cyclization of geranylgeranyl pyrophosphate (**8**), the universal precursor for diterpenes (Scheme 10). It was postulated that the diterpenes cembrene or verticillene could act as intermediates in the biosynthetic scheme for taxanes since a similar biogenesis has been suggested for cembrene and verticillene. Loss of the pyrophosphate group from **8** could be followed by cyclization yielding intermediate **9**. From the cation, two different pathways could be envisioned to give cembrene (**11**) or intermediate **10**. Hydrogen elimination forms verticillene (**12a**). Another cyclization is proposed to take place, forming the second six-membered ring of the taxane framework. Hydrogen elimination leads to the formation of the exocyclic double bond. Another cyclization pathway can take place through a different conformation of verticillene (**12b**). The second six-membered ring is formed, giving a taxane framework with an endocyclic double bond (**17**). However, attempts to effect the transannular electrophilic cyclization

Scheme 10

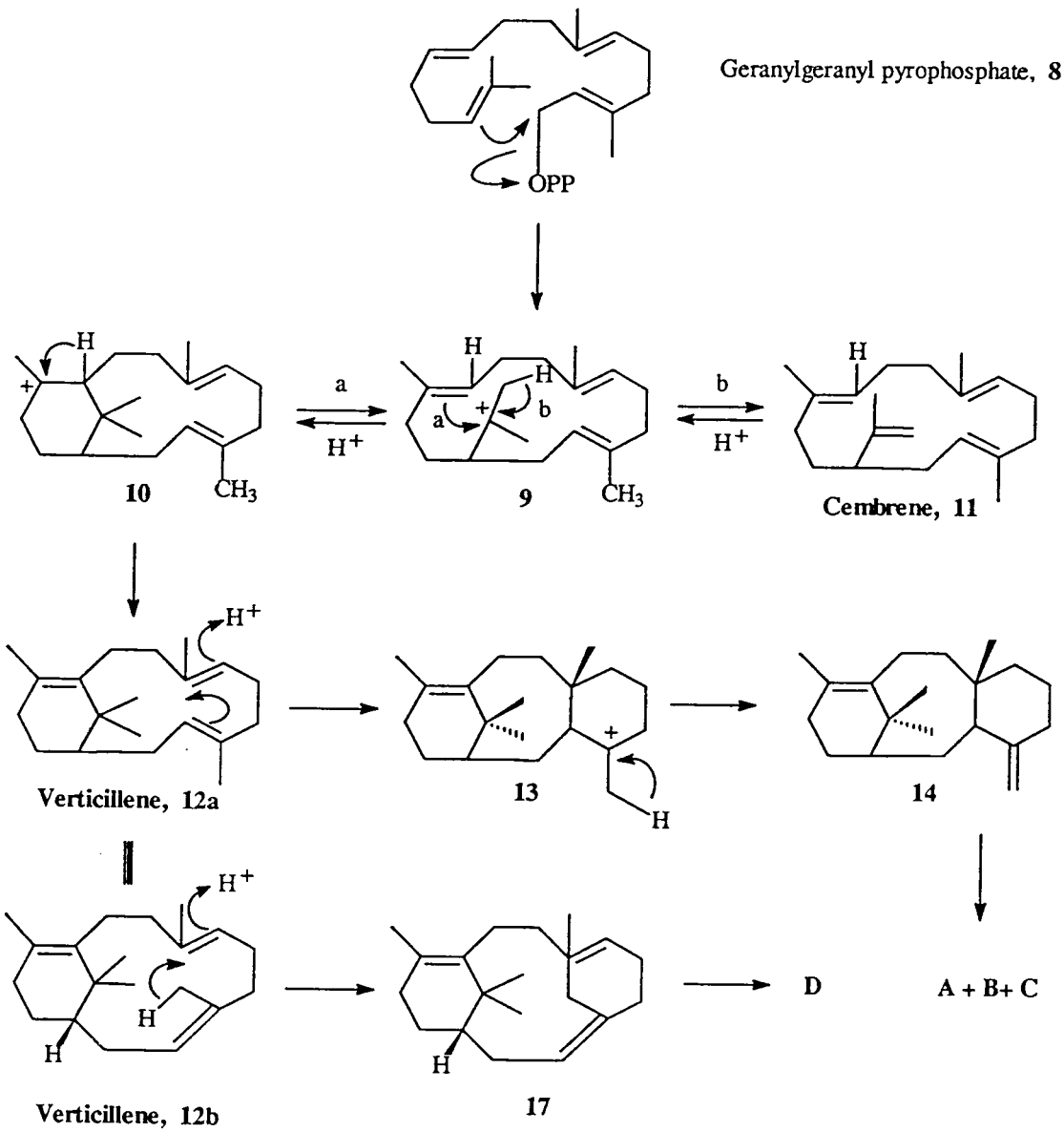
OPP
Geranylgeranyl pyrophosphate, 8
H
a
H+
b
H+
10
9
CH3
Cembrene, 11
H+
Verticillene, 12a
13
14
H+
H
H
Verticillene, 12b
17
D
A + B+ C

of cembrene[70] (**11**) or verticillene[71] (**12**) and its epoxides by chemical means, failed to produce compounds with the taxane carbon framework. These results do not disprove the involvement of these intermediates in the biosynthetic sequence of the taxane ring system, but they suggest that the sequence may involve an alternative pathway or perhaps involve a different geometric and/or positional isomer of GGPP.

4.2 Biosynthesis of The Four Structural Groups of Taxanes

All of the taxane compounds isolated from various yew species can be categorized into four groups[69] according to their structural differences and their chemical reactivities (Scheme 11a,b). The four groups are:

1. Group A consists of taxanes having an exocyclic methylene group at C-4.
2. Group B consists of compounds with a C-4 and C-20 epoxide.
3. Group C consists of compounds having an oxetane ring at C-4, C-5 and C-20.
4. Group D consists of one compound having an endocyclic double bond between C-4 and C-20.

The biosynthesis for the compounds of group A is proposed to start from the intermediate **14** (Scheme 11a). The carbon framework can be oxidized at various positions to form a polyol intermediate. Next, esterification of the various hydroxyl groups in the molecule would complete the biosynthesis of compounds of group A.

The carbon framework for compounds of group B is proposed to be derived from **14**, by epoxidation of the exocyclic double bond, giving **15**. Similar transformations by oxidation and esterification would lead to the final structures with all of the functionalities in place.

Scheme 11a

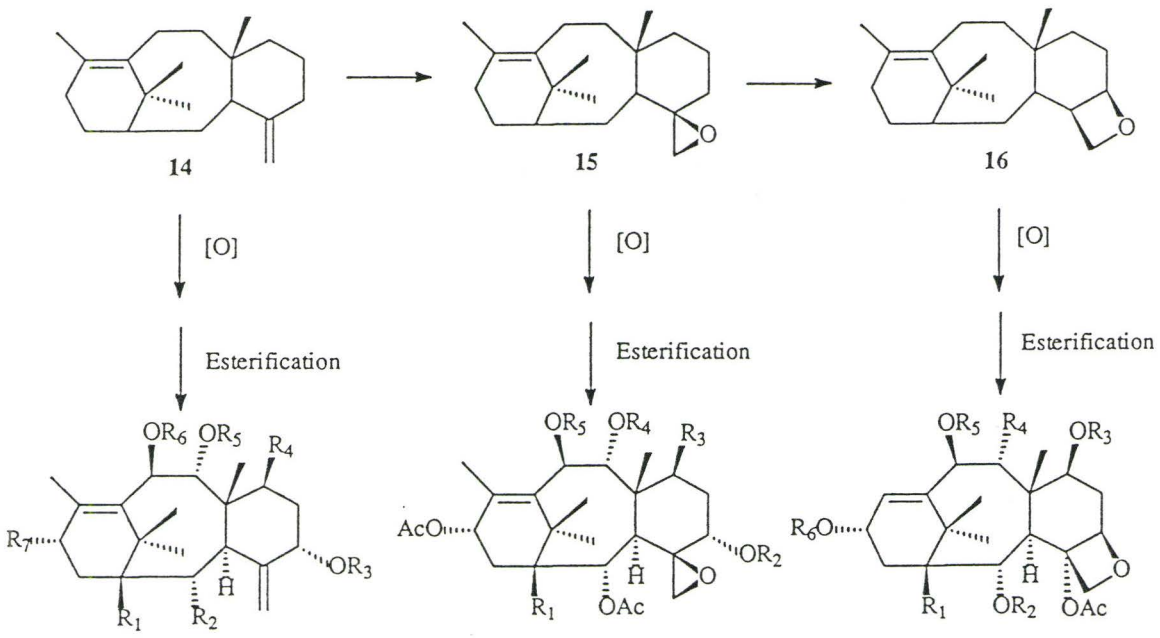

Group A

R_1 = H, OH, OAc
R_2 = H, OH,OAc, OR
R_3 = H, Ac, R
R_4 = H, OAc
R_5 = H, Ac
R_6 = H, Ac
R_7 = H, OH, OAc or Ketone

Group B

R_1 = H, OH
R_2 = H, Ac, R
R_3 = H, OAc, OR
R_4 = H, Ac
R_5 = H, Ac

Group C

R_1 = H, OH
R_2 = H, Ac, R
R_3 = H, Ac
R_4 = OH, OAc or Ketone
R_5 = H, Ac
R_6 = H, Ac, R

Scheme 11b

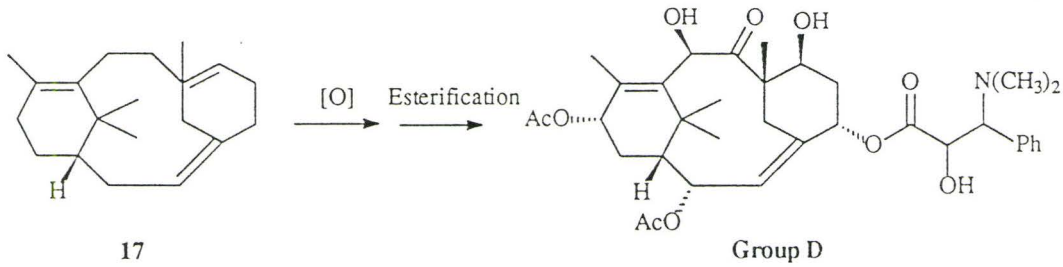

17

Group D

For compounds of group C, the hypothesis proposes that the epoxide ring could be opened and rearrange to form the oxetane ring. Oxidations and esterification of **16** would elaborate compounds of group C, which include taxol.

From the above biosynthetic hypothesis, the formation of the oxetane ring in taxol was proposed to start from a compound having a double bond at C-4 and C-20. Many of the group A taxanes contain an ester group at C-5 that is structurally related to the side chain in taxol. There was a recent discovery of new exocyclic methylene compounds containing a 2-hydroxy-3-dimethylamino-3-phenylpropionic ester at C-5 such as **18** (Scheme 12). It was proposed[69,72] that the C-13 side chain in taxol is derived from an intramolecular transfer of the ester group of C-5. The 3-dimensional structure of taxol shows a folding in which the α-hydroxyl group at C-13 is very close to the ester at C-5. One of the conformations of **18** can be represented as **19**. The formation of the ortho ester **20** could occur as an intramolecular reaction. This intermediate (**20**) could then break down to yield product **21**, resulting from an intramolecular transesterification. Through epoxidation of the allylic alcohol and then acylation to protect the free hydroxyl group, compound **22** could be formed. The epoxide ring opening assisted by nucleophilic attack of the carbonyl oxygen then could convert **22** into the intermediate **23**. The oxetane ring could be formed by nucleophilic attack of the primary hydroxyl group and the acyl transfer from C-5 to C-4 would yield taxol-like derivatives such as compound **24**.

4.3 Biosynthesis of Related Taxol Side Chain

The biosynthesis of an acid related to the C-13 side chain of taxol, Winterstein's

Scheme 12

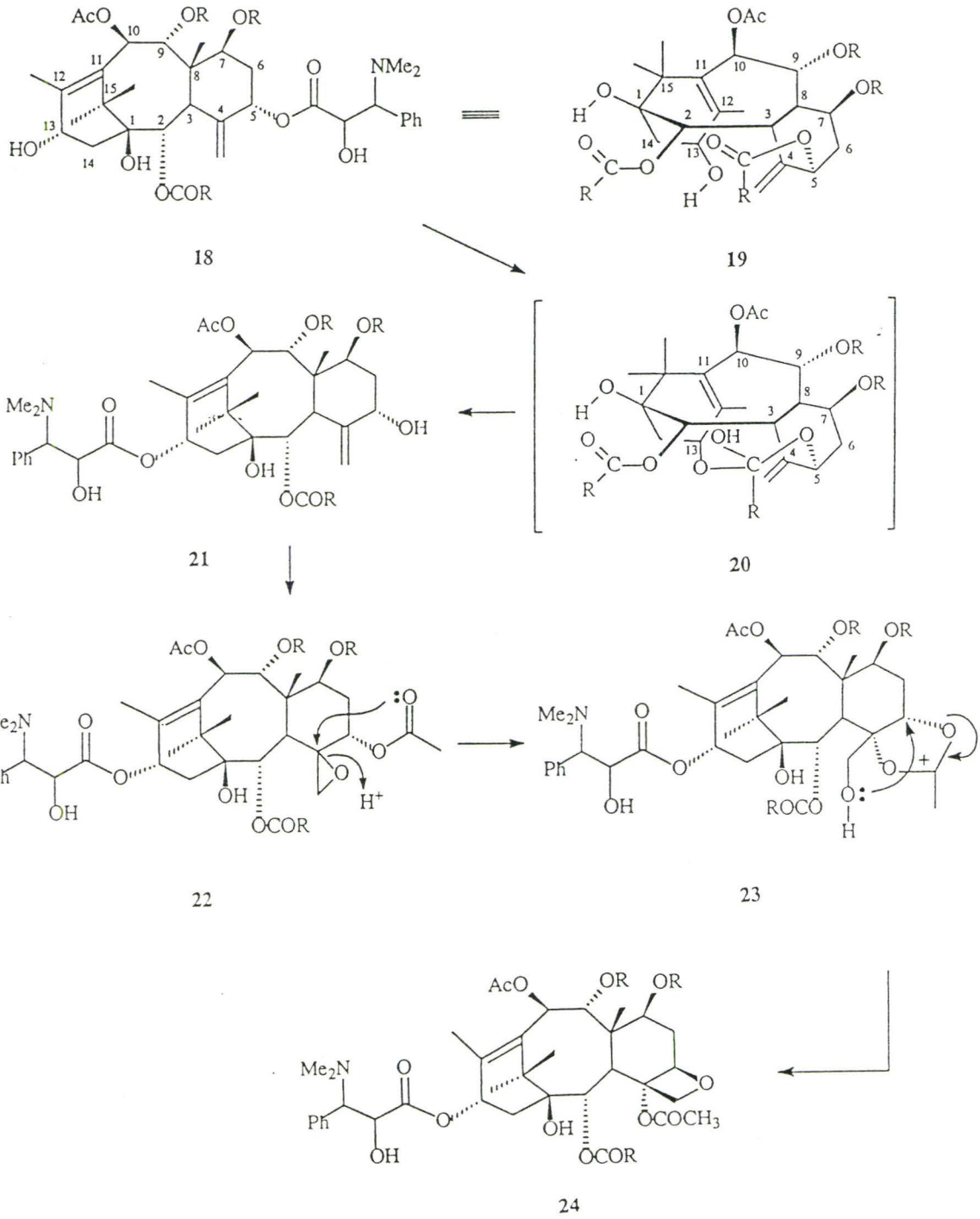

18 19 20 21 22 23 24

acid ((3R)-3-dimethylamino-3-phenylpropionic acid) has been reported. The acid was isolated as the hydrolysis product of taxine. It has been demonstrated[73,74] that in *Taxus baccata*, Winterstein's acid is biosynthesized from (2*S*)-phenylalanine, and that the conversion occurs stereospecifically with the loss of the 3-pro *R* proton (see Table 4). There is an inversion of configuration at C-3 (Scheme 13) in the final product. In the same studies, it was observed that cinnamic acid (both 2 and 3-^{14}C labelled) was incorporated 10-100 times less efficiently then (2*S*)-phenylalanine, even though cinnamic acid is a known metabolite of phenylalanine. It is possible that the taxol side chain (**4a**) is biosynthesized by a similar pathway: the intermediate of the conversion (β-phenylalanine) could be oxidized and then benzoylated to yield **4a**.

Scheme 13

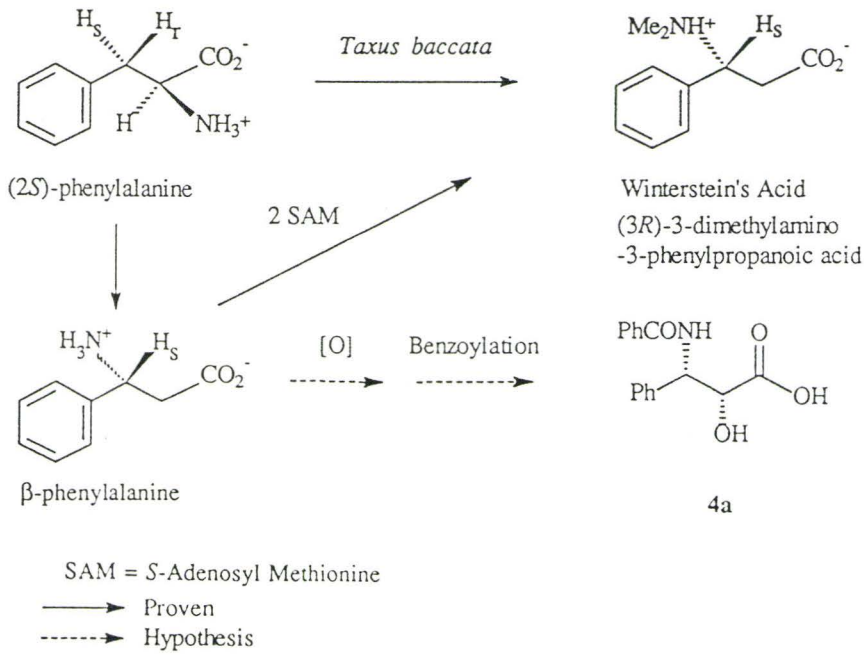

Table 4. Incorporation of (2S)-phenylalanine into (3R)-3-dimethyl--amino-3-phenylpropionic acid in *Taxus baccata*[48]

Expt no	Incorporation of ^{14}C (%)	Loss of ^{3}H (%)
	(2S)-Phenyl[2-^{14}C, 3R-$^{3}H_1$]alanine	
1	0.013	91
2	0.014	89
	(2S)-Phenyl[2-^{14}C, 3S-$^{3}H_1$]alanine	
1	0.014	33
2	0.020	33

4.4 Enzymatic Approach to Taxol

The biosynthesis of taxol is an intriguing problem, since the molecule has a very complex structure with diverse functionalities. We have taken on the challenge of studying the biosynthesis of taxol by investigating the enzymatic conversion of the precursor geranylgeranyl pyrophosphate (GGPP) to taxol. Cell-free extracts of the yew needles are expected to contain the key enzyme(s) which can catalyze the cyclization of GGPP to some hydrocarbon intermediates on the pathway to taxol (see Scheme 10,11a). Radioactively labelled GGPP would be used to label the intermediates of the cyclization sequence, thereby leading to their isolation and identification. These intermediates may be useful in the effort toward total synthesis of taxol, for they would have the taxane framework and chiralities as well as some of the functionalities present in taxol. On the other hand, any enzyme found in the cell-free extract can be cloned and used in a

bioreactor to scale up production of the intermediates which can be manipulated into taxol.

II. RESULTS AND DISCUSSION

In order to study the biosynthesis of taxol, the precursor geranylgeranyl pyrophosphate isotopically labelled with ^{14}C at either position 16 or 17 was synthesized. Carbon-14 is required as the labelled radioactive isotope instead of tritium because the hydrogen atoms could be lost during enzymic conversion from the acyclic diterpene to product. The labelled pyrophosphate was prepared from geranylgeraniol (Scheme 14) by adapting the strategy used by Cane[75] to synthesize the sesquiterpene precursor [12,13-^{14}C]farnesyl pyrophosphate .

1.0 Synthesis of Geranylgeranyl Acetate (26).

Commercially available geranylgeraniol (**25**) was converted to the corresponding acetate (**26**) by stirring with acetic anhydride in pyridine at room temperature overnight (Scheme 15).

Scheme 15

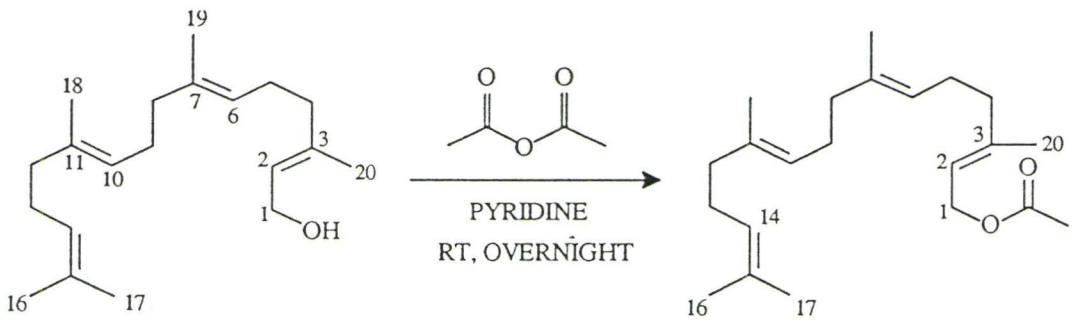

25 **26**

Scheme 14

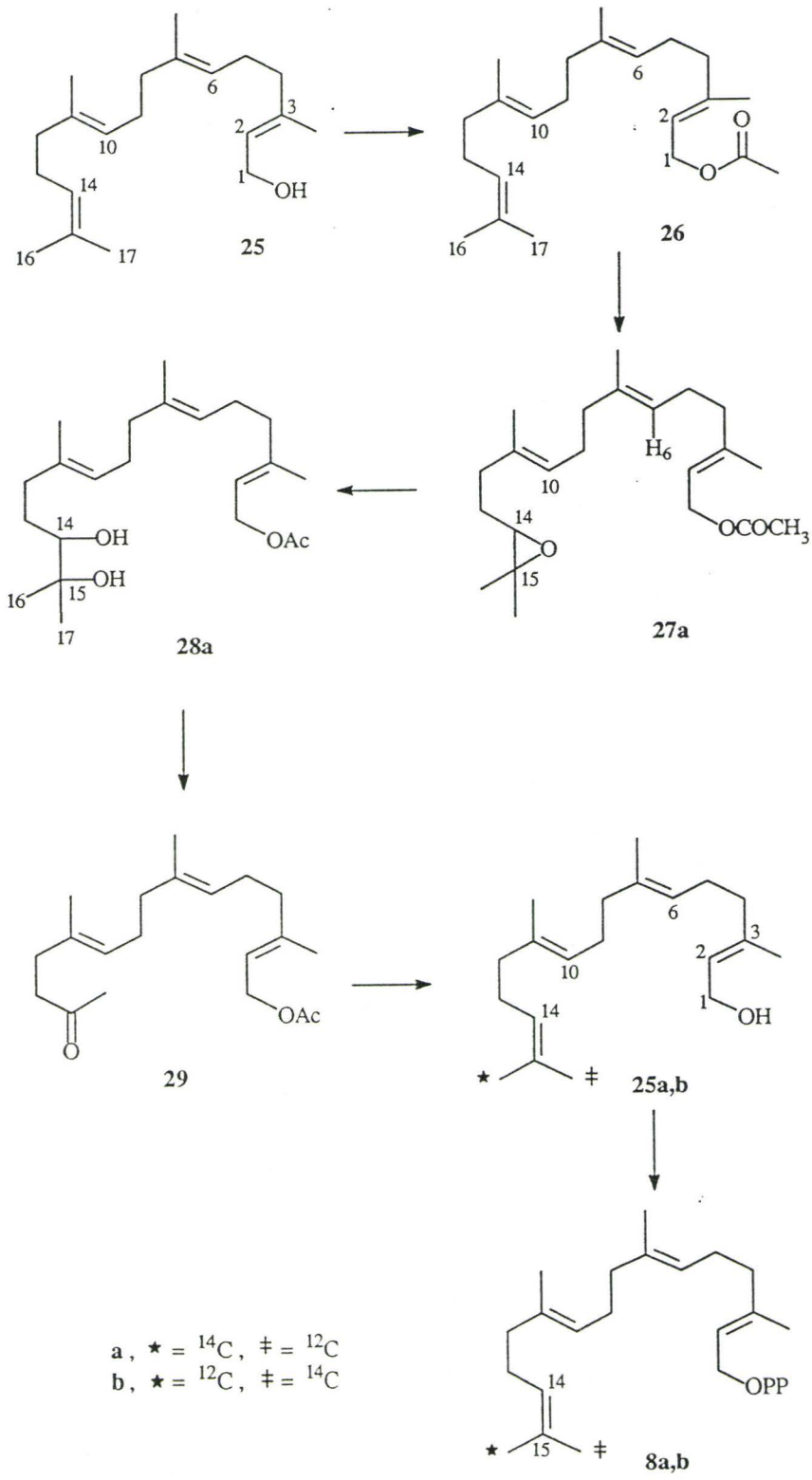

a, ★ = ^{14}C, ‡ = ^{12}C
b, ★ = ^{12}C, ‡ = ^{14}C

Geranylgeranyl acetate was obtained in 79% yield and was characterized by proton nuclear magnetic resonance (^{1}H NMR), carbon-13 nuclear magnetic resonance (^{13}C NMR), infrared (IR) spectroscopy and mass spectrometry (MS). The ^{1}H NMR spectrum of **26** (Figure 6) is similar to that of geranylgeraniol (Figure 5) except for the downfield shift of the doublet assigned to the methylene protons at C-1 from 4.15 ppm to 4.59 ppm. The spectrum contains the characteristic signals for an acyclic isoprenoid compound with the triplet of the vinyl proton H-2 which is bonded to C-2, at 5.34 ppm. This proton is shifted upfield 0.08 ppm from that of geranylgeraniol due to the acetate group, but remains shifted downfield from the other vinyl protons in the isoprenoid chain. The multiplet centered at 5.08 ppm, which consists of overlapping triplets is assigned to the three other vinylic protons (H-2, H-6, H-10). The allylic protons on the methylene groups give rise to the multiplet centered at 2.03 ppm and overlap the singlet of the methyl from the acetate group. The signals at 1.60, 1.68 and 1.71 ppm are assigned to the five methyl groups of **26**. The signal at 1.71 ppm is not present in the spectrum of geranylgeraniol, therefore suggesting its assignment to the protons of the C-20 methyl group, due to the influence of the acetate group. The ^{13}C NMR spectrum of geranylgeranyl acetate was assigned based on comparison with available data for related compounds[76,77]. The signals at 142.04, 135.30, 134.77 and 131.04 ppm are assigned to the sp^2 carbons of the trisubstituted double bonds at position 3, 7, 11 and 15, assuming a progression in shift along the chain. The signals at 124.28, 124.06, 123.51 and 118.05 ppm are assigned to the other vinylic carbons at position 2, 6, 10 and 14, where the progression in shift is in the reverse direction. The relatively small differences in chemical shifts render the

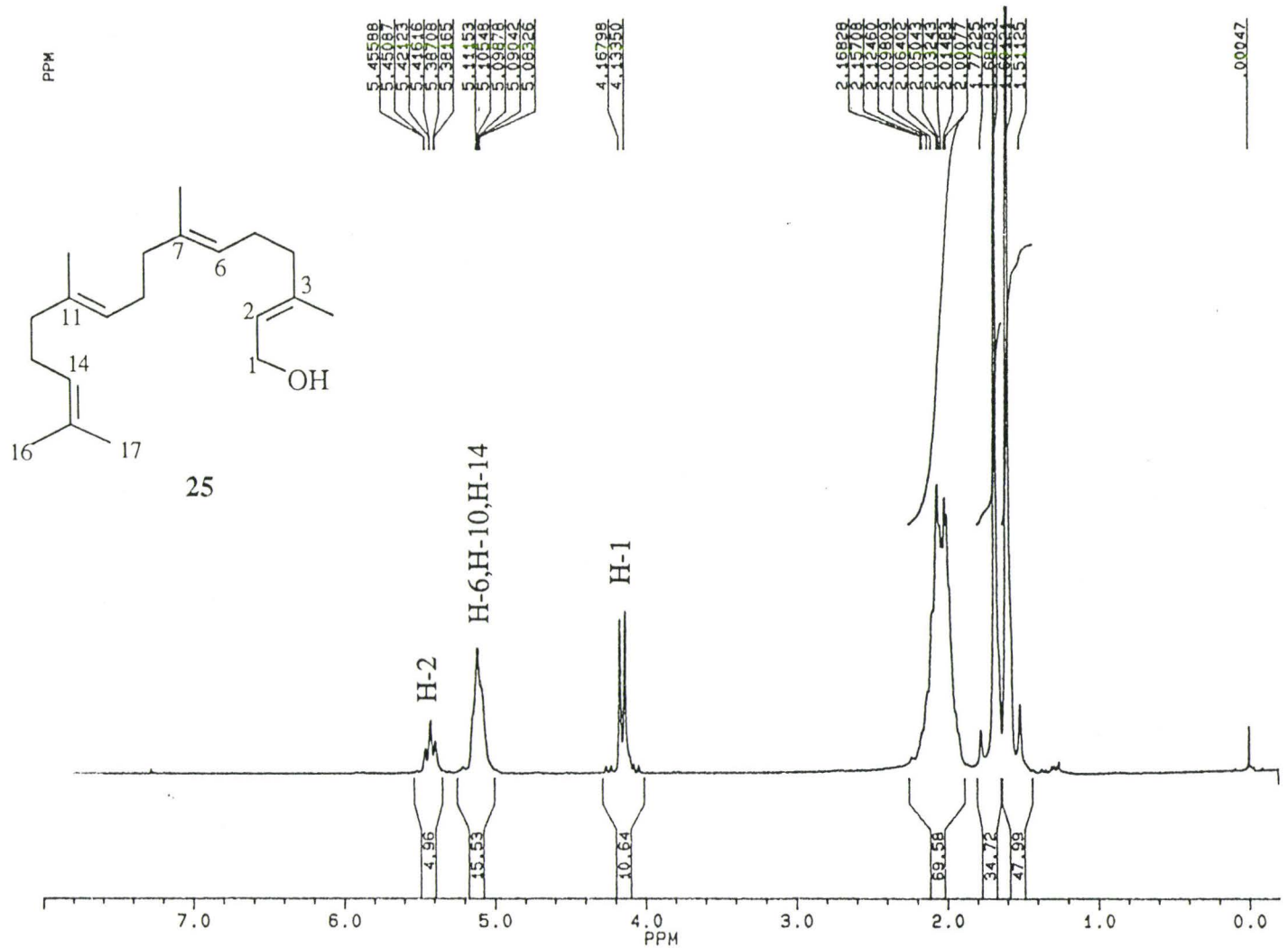

Figure 5. The ^{1}H NMR Spectrum of Geranylgeraniol (**25**)

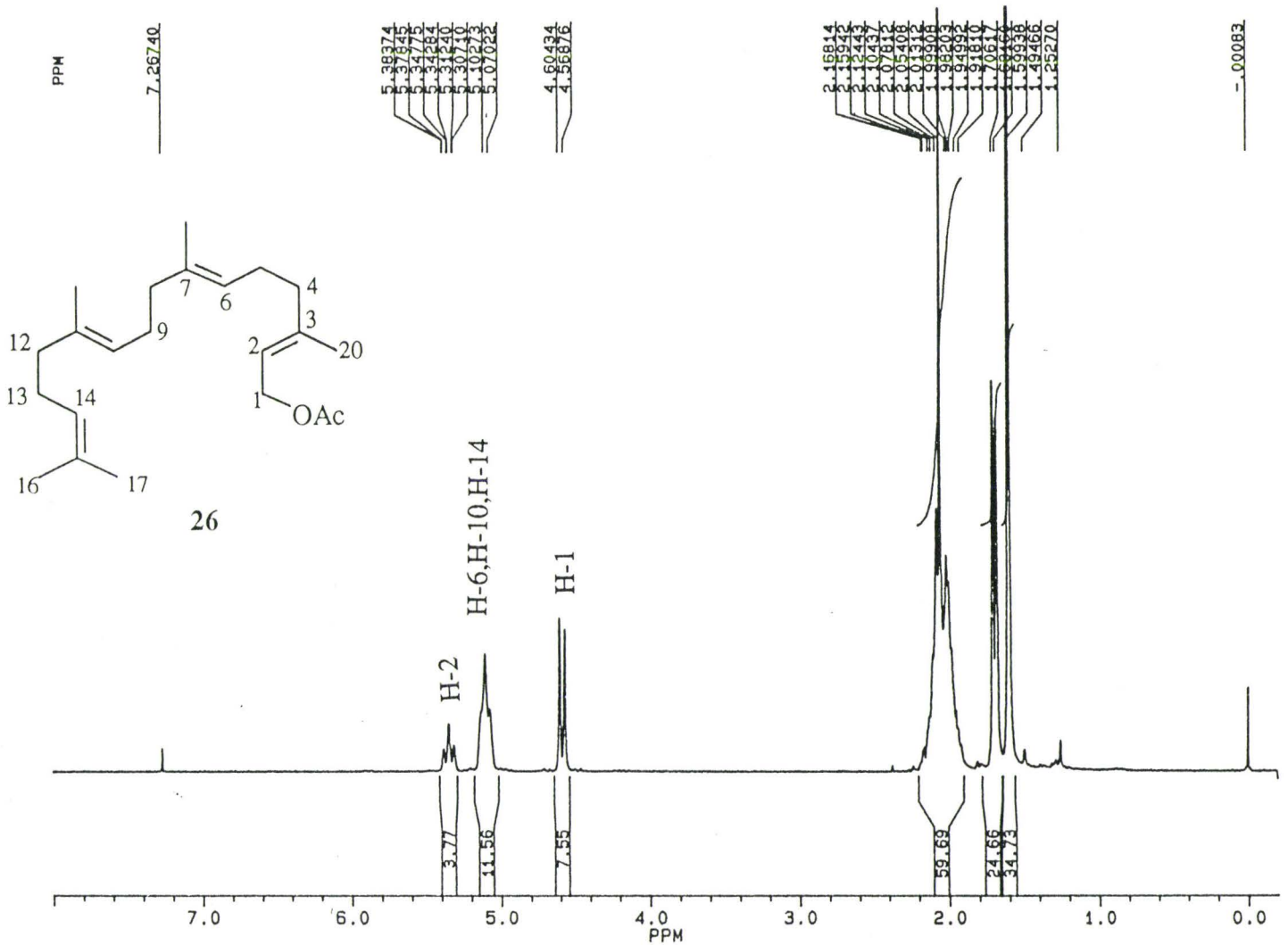

Figure 6. The ^{1}H NMR Spectrum of Geranylgeranyl Acetate (**26**)

individual assignments uncertain. The signal at 61.24 ppm is assigned to the C-1 carbon which is attached to the acetate group. The resonances of the internal methylene groups attached to the trisubstituted double bonds separate into two groups: one at lower field (at around 26 ppm) for the methylene carbons *cis* to the hydrogen (C-4, C-8 and C-12), and the other group at higher field (at around 39 ppm) for the methylene carbons *cis* to the methyl (C-5, C-9 and C-13). The assignments within the groups are arbitrary. The carbon of the terminal *trans*-methyl group resonates at 25.57 ppm, while the carbon of the terminal *cis*-methyl group and the other methyl groups in the molecule are assigned to resonances at 15 to 17 ppm.

The mass spectrum of **26** shows a weak molecular ion at *m/z* 332, and the other major peaks of the spectrum reflect the structure of the compound (Figure 7). The base peak of the spectrum is at *m/z* 69, which is characteristic of acyclic terpenoids and arises from the allylic cleavage of the terminal isopentenyl group. The protecting group of **26** (acetate) is readily eliminated generating the signal at *m/z* 272, which then loses an isoprene unit (mass 69) producing the signal at *m/z* 204 (11% of the intensity of the base peak). Further loss of another isoprene unit from *m/z* 204 generates the signal at *m/z* 136. The prominent peaks in the lower mass region (*m/z* 81,93,107,121) are hydrocarbon fragments from the unsaturated ion at *m/z* 136 (loss of butyl, propyl, ethyl and methyl groups). Likewise, *m/z* 161 and 189 are signals of ions derived from fragmentations of the ion at *m/z* 204 (loss of propyl and methyl groups).

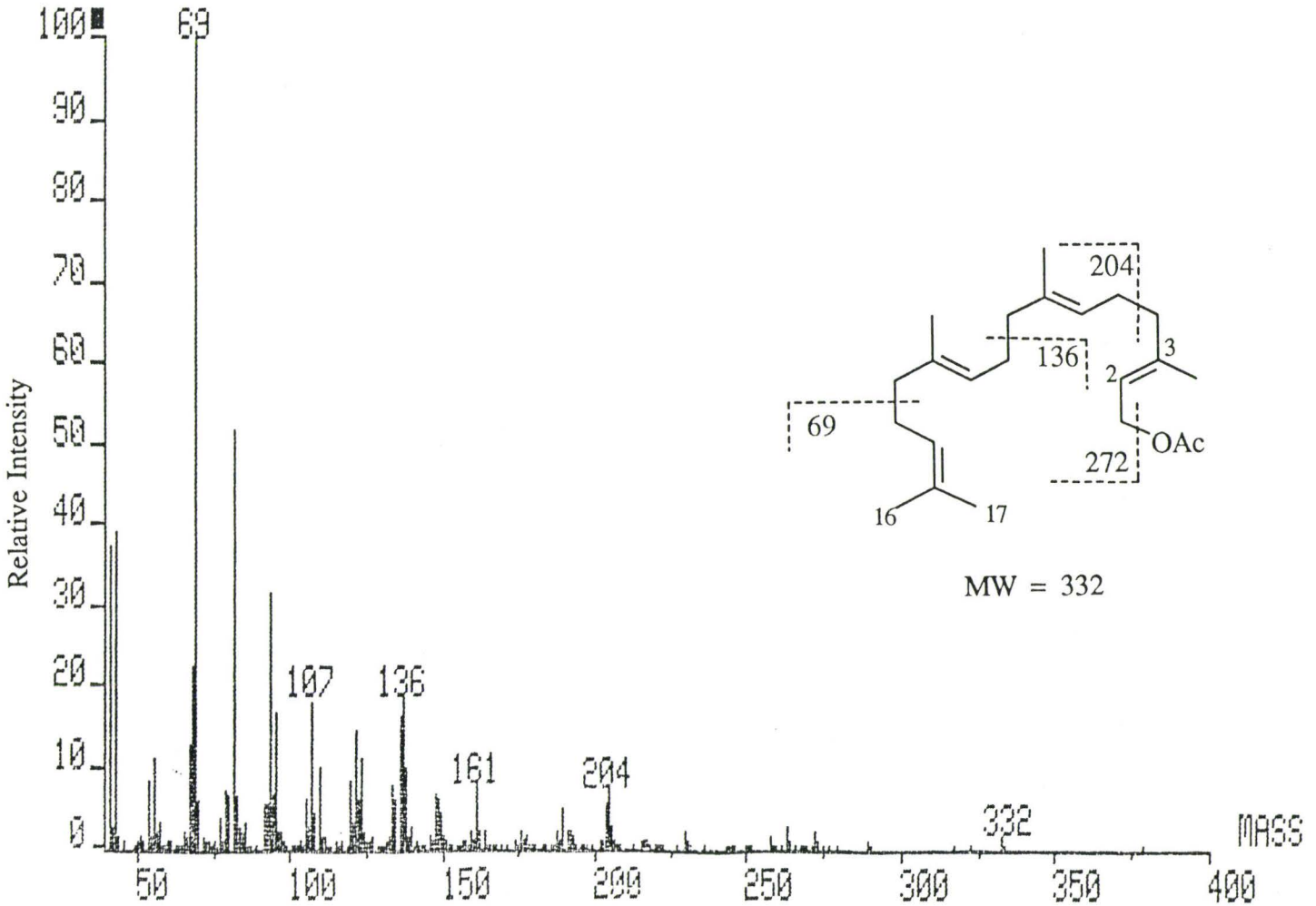

Figure 7. The EI Mass Spectrum of Geranylgeranyl Acetate (**26**)

2.0 Synthesis of 14,15-Monoepoxygeranylgeranyl Acetate (27a)

Epoxidation of geranylgeranyl acetate with *m*-chloroperbenzoic acid in methylene chloride yields a very complex mixture of epoxides. The regioselectivity of the oxidation is very low, since the product mixture consists of all three monoepoxygeranylgeranyl acetates (**27a**, **27b** and **27c**), and several more di- and triepoxides (Scheme 16). The nonconjugated, trisubstituted double bonds are approximately chemically and sterically equivalent, making selective oxidation of the terminal double bond difficult. The double bond at position C-2 and C-3 is more sterically hindered by the acetate group and less electron-rich than the others and was not epoxidized in the oxidation. By monitoring the reaction by TLC, it was shown that the monoepoxides are dominant at first, but as the reaction proceeds, the polyepoxides start to form from the monoepoxides. The reaction was performed at 0°C with the oxidizing agent added to the reaction mixture slowly in portions over the period of 3 hours to avoid over-epoxidation. The major products of the reaction are the monoepoxygeranylgeranyl acetates (67%), but this yield was not optimized. The monoepoxides were separated from the polyepoxides by flash chromatography. The TLC of the monoepoxides indicates at least two sets of compounds were present (R_f values of 0.59 and 0.69); however, it is more practical to carry over the whole mixture of monoepoxides into the next reaction, and then purify the products. The ^{1}H NMR spectrum of the mixture of monoepoxides has three vinyl proton resonances as expected: one triplet at 5.34 ppm for the proton at C-3; overlapping triplets centered at 5.12 ppm for the other two vinylic protons in each of the monoepoxides (H-6, H-10 in **27a**; H-6, H-14 in **27b**; and H-10,H-14 in **27c**); and the multiplet at 2.70 ppm for the

Scheme 16

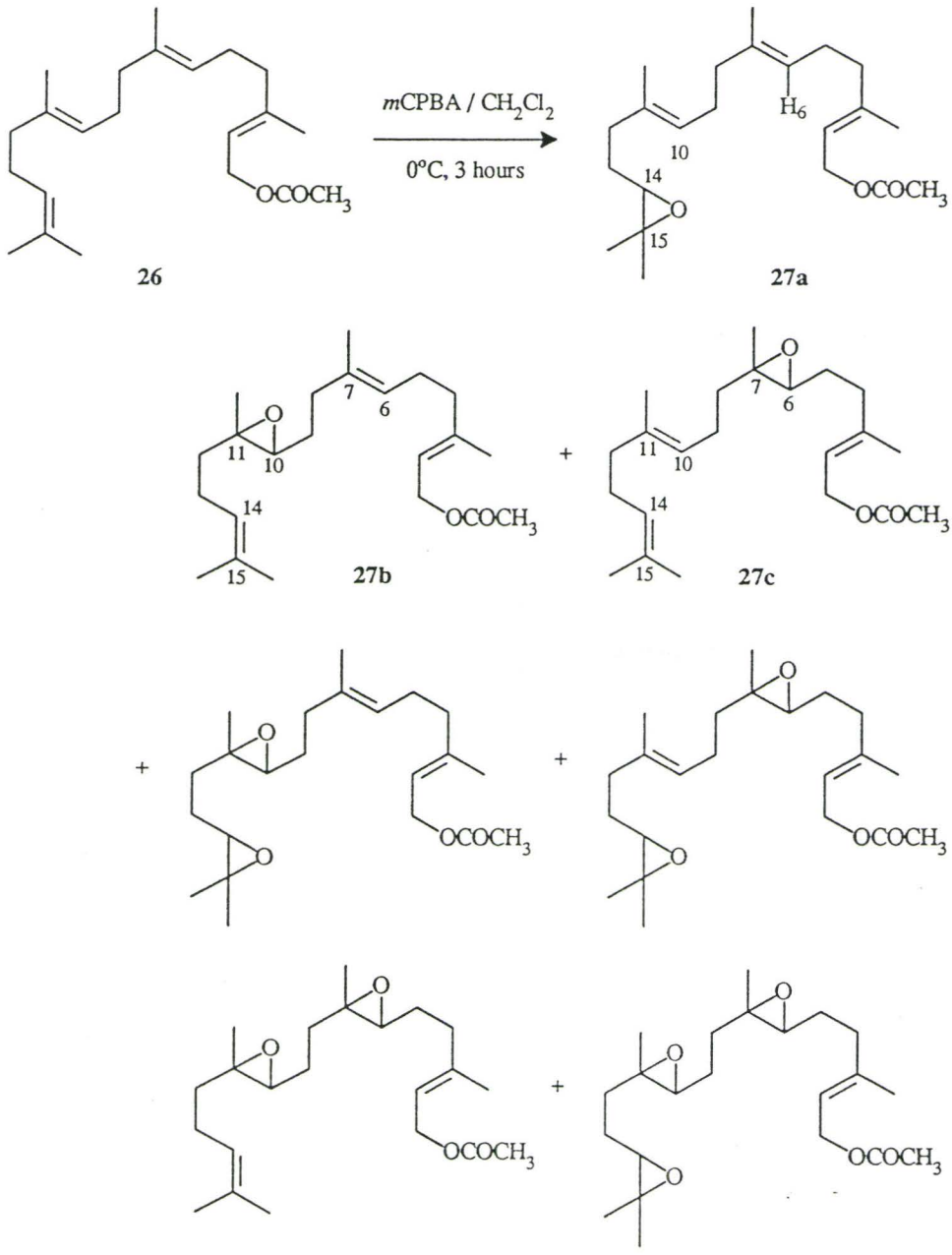

26 **27a** **27b** **27c**

epoxide rings (H-14 in **27a**, H-10 in **27b** and H-6 in **27c**). The methyl groups attached to the epoxide ring are shielded and move upfield to about 1.25 - 1.30 ppm, compared to the allylic methyl groups at 1.60 -1.70 ppm. The polyepoxides were also partially purified by flash chromatography. There are about seven or eight detectable compounds in the mixture of polyepoxides, most of which are diepoxides (regioisomers and diastereomers). The ^{1}H NMR spectrum of diepoxide(s) isolated from the chromatography has only 2 vinylic protons, a triplet at 5.39 ppm and a multiplet at 5.08 -5.15 ppm; the other two double bonds are epoxidized. One isolated product has only one vinylic proton resonance in the ^{1}H NMR spectrum, indicating that three of the double bonds had been oxidized. The polyepoxides were not used in the rest of the synthetic sequence, but they might be useful in future work, where the precursor geranylgeranyl pyrophosphate needs to be labelled at other positions in the molecule.

3.0 Synthesis of 14,15-Dihydroxygeranylgeranyl Acetate (28a)

The mixture of monoepoxides was converted to a mixture of corresponding diols by opening the epoxide ring with 3% perchloric acid (Scheme 17). The reaction was performed in THF:H_2O (1:1 ratio) at room temperature for three hours. The product mixture contained three new compounds and the starting material. The mixture of diols was separated by flash chromatography and tentatively identified as 14,15-dihydroxygera--nylgeranyl acetate (**28a**), 10,11-dihydroxygeranylgeranyl acetate (**28b**) and 6,7-dihydroxygeranylgeranyl acetate (**28c**) with R_f values of 0.47, 0.61 and 0.70 respectively.

Scheme 17

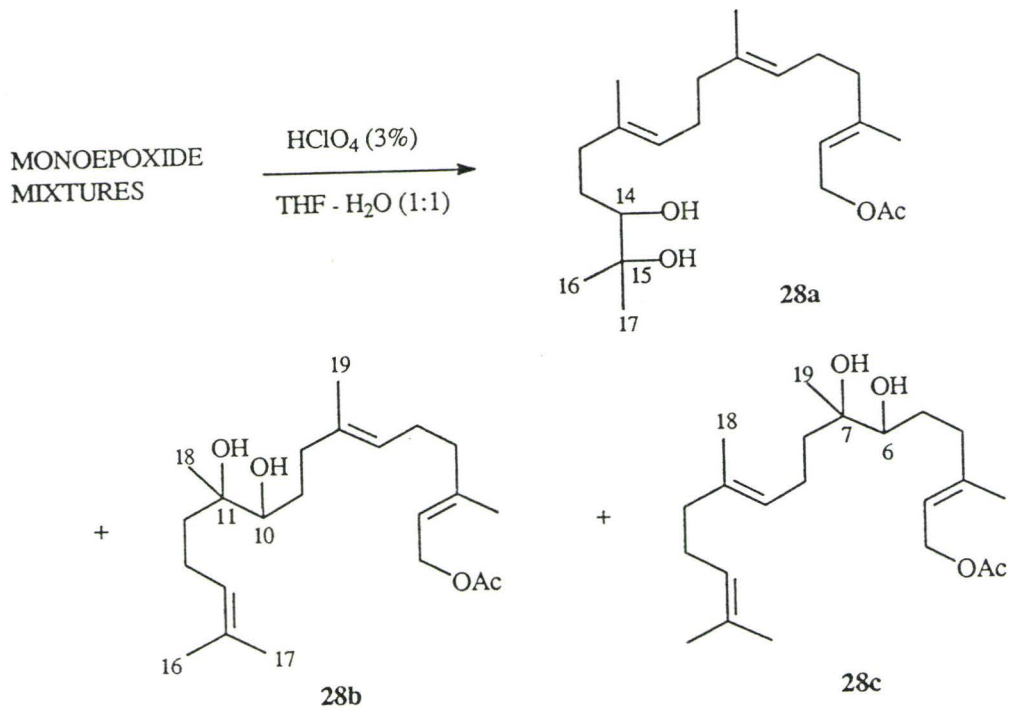

The ^{1}H NMR spectrum of 14,15-dihydroxygeranylgeranyl acetate (Figure 8) distinguishes this diol from the other two. The protons of two terminal methyl groups (C-16 and C-17) are shifted upfield to around 1.1 - 1.2 ppm due to the influence of the hydroxyl group. The protons (H-13) of the methylene group next to the diol moiety are also shifted 0.50 ppm upfield. The rest of the allylic methyl groups are unchanged and resonate at 1.60 - 1.70 ppm. The C<u>H</u>-OH proton (H-14) is shifted upfield to 3.36 ppm, while the resonances at 5.34 and 5.15 ppm are assigned to the remaining three vinyl protons as before. It was not possible to differentiate the remaining other two diol compounds (**28b** and **28c**) because both have an internal diol group. Both have very similar proton spectra, in which the protons of the methyl group bonded to the hydroxyl

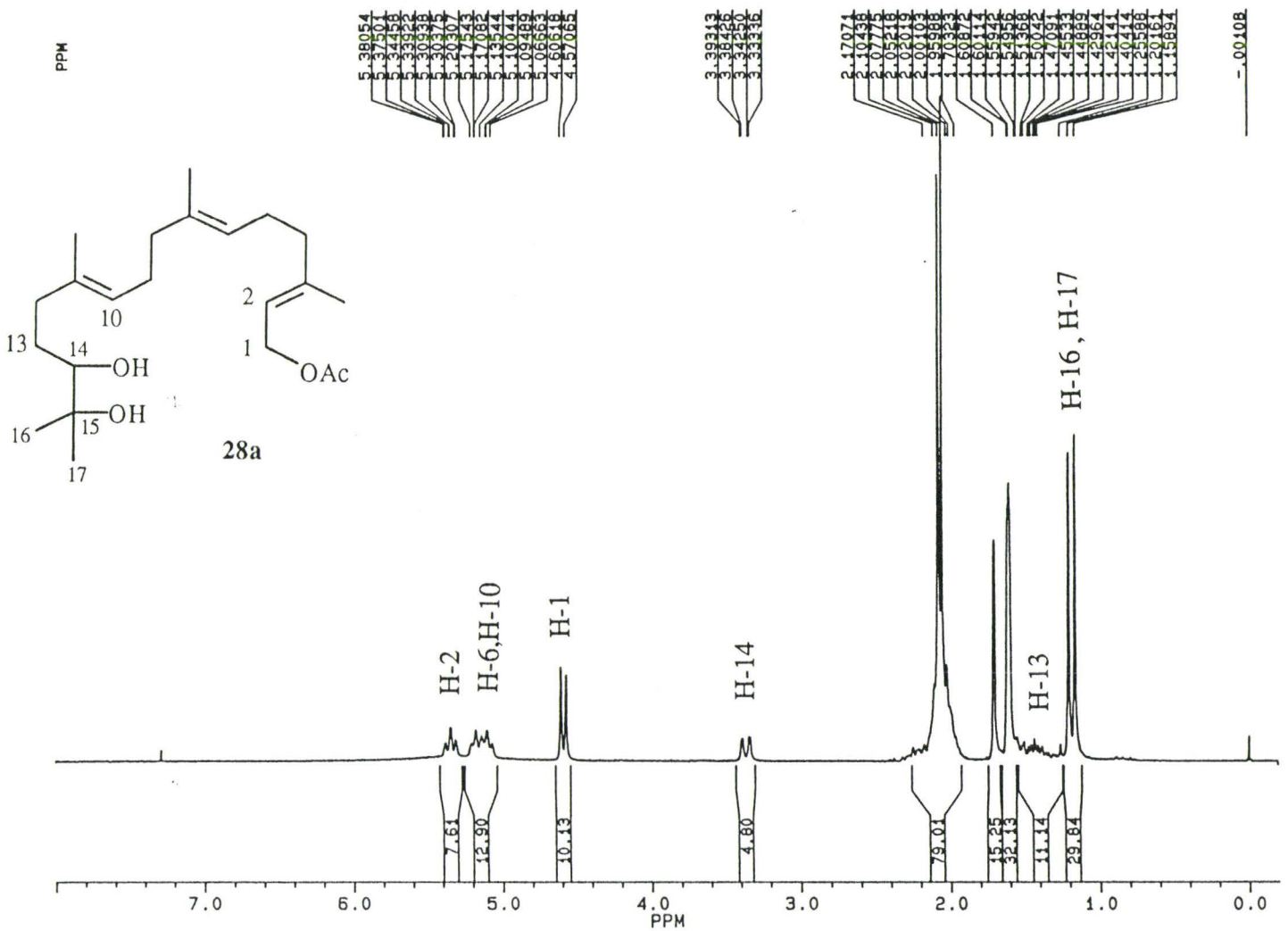

Figure 8. The ^{1}H NMR Spectrum of 14,15-Dihydroxygeranylgeranyl Acetate (**28a**)

carbon (C-18 in **28b** and C-19 in **28c**) are shifted upfield to 1.17 ppm. There are two methylene groups (one on each side of the diol moiety) in each diol which are shielded by the hydroxyl group and give rise to resonances at 1.26 -1.50 ppm.

The different mass spectra of these three diols also help in the confirmation of the identity of **28a**. The external diol of 14,15-dihydroxygeranylgeranyl acetate caused its mass spectrum (Figure 9) to differ from the other two which had internal diol groups. The base peak of the MS of **28a** is at *m/z* 44 and derives from fragmentation of the ion formed from of the allylic cleavage of the terminal isopentenyl group containing the diol as shown in Scheme 18.

Scheme 18

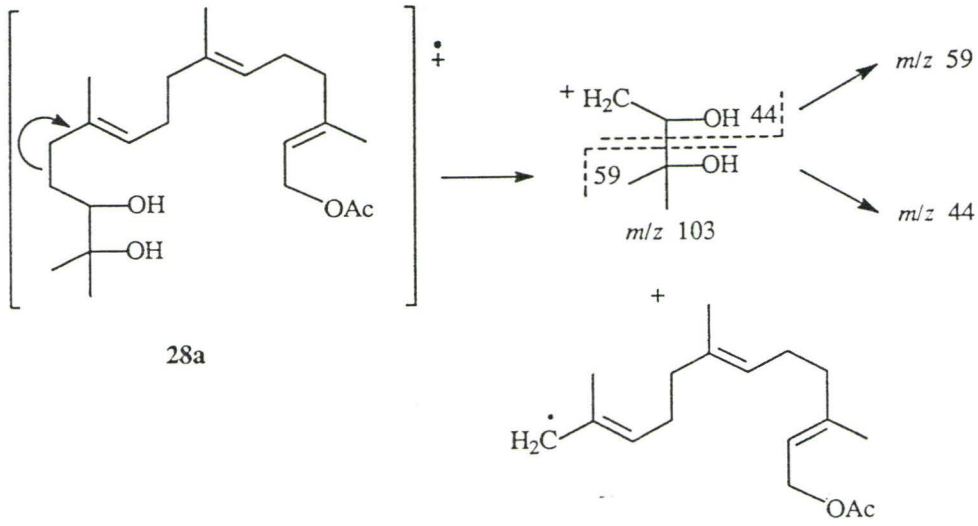

28a

This ion is not present in the mass spectra of **28b** and **28c**, both of which have an ion at *m/z* 69 (fragment of the allylic cleavage of the terminal isopentenyl unit) as base peak. The ion at *m/z* 59 is formed by α cleavage of the terminal hydroxyl group. The rest

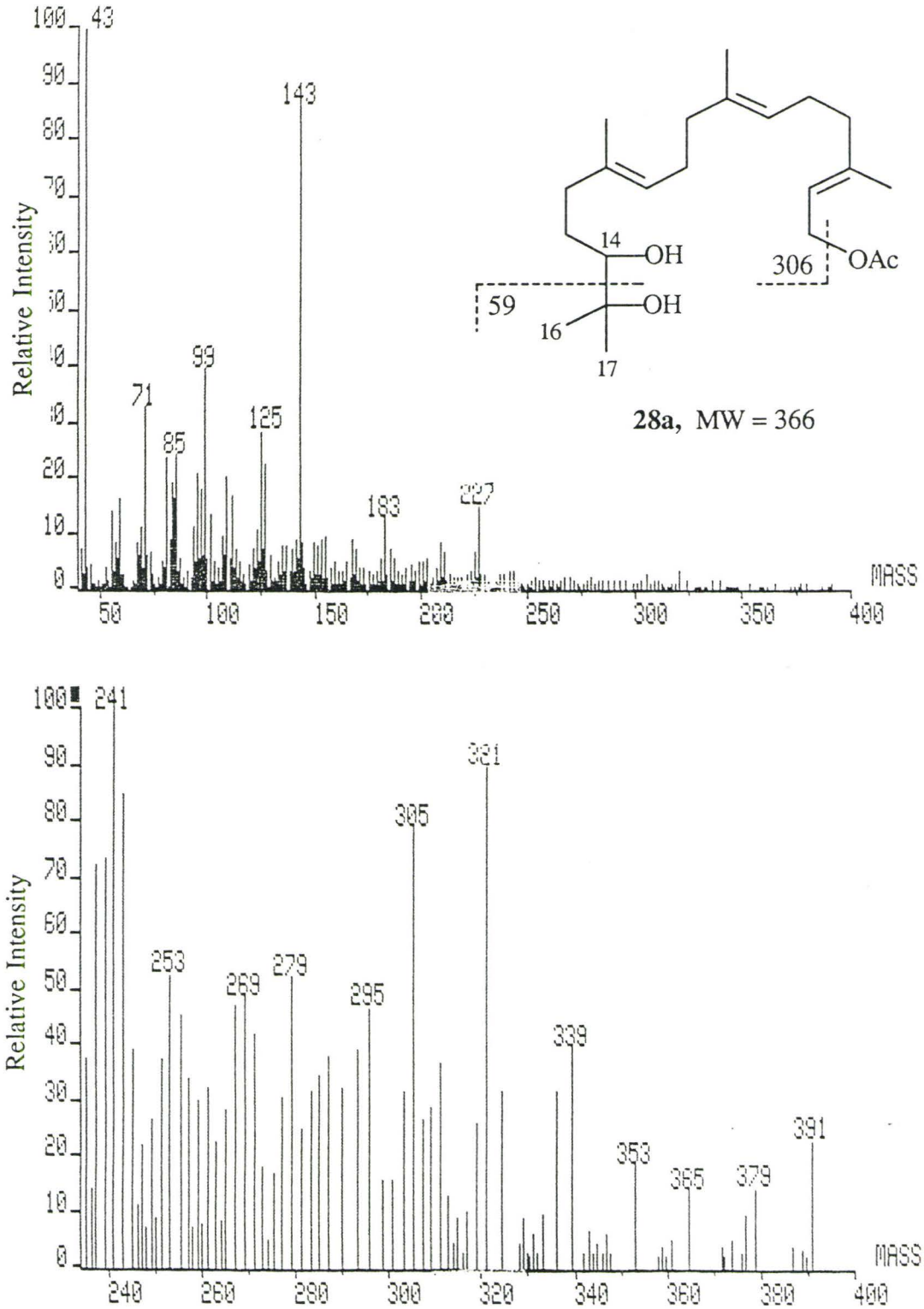

Figure 9. The EI Mass Spectrum of 14,15-Dihydroxygeranylgeranyl Acetate (**28a**)

of the mass spectrum of **28a** is similar to the spectrum of geranylgeranyl acetate (**26**). On the other hand, the mass spectra of the internal diol compounds are very different from the mass spectrum of **26**. The yield of the pure diol of interest **28a** was 43% from the monoepoxygeranylgeranyl acetate mixture.

4.0 Synthesis of Geranylgeranyl Acetate Trisnoraldehyde (29)

The identities of all three diol compounds were confirmed by cleaving the diols, thus generating the aldehyde and ketone fragments, which could be easily characterized. Diol **28a** was cleaved by selective oxidation with sodium periodate in THF-H_2O for 3 hours at room temperature, giving geranylgeranyl acetate trisnoraldehyde (**29**) in 84% yield and acetone (Scheme 19).

Scheme 19

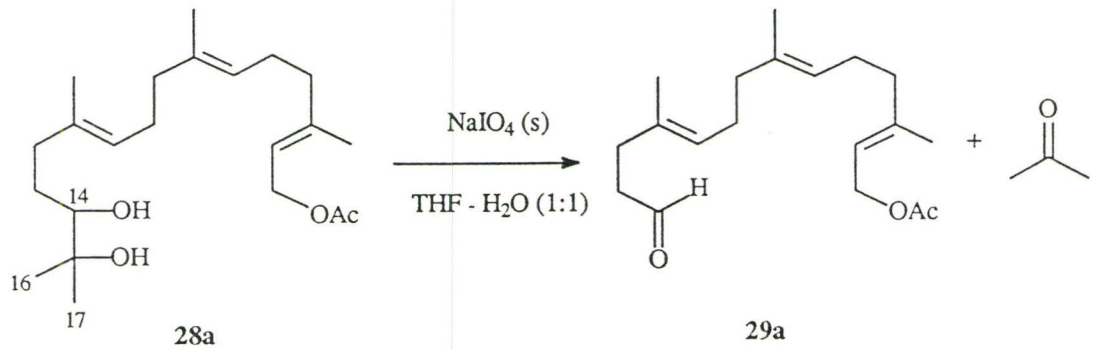

28a **29a**

The aldehyde was characterized by proton and carbon NMR, which in turn, confirmed the structure of the starting material to be 14,15-dihydroxygeranylgeranyl acetate. The ^{13}C NMR spectrum of **29** has nineteen resonances indicating that three carbons were cleaved from the molecule (Figure 10). There are six resonances at 118 to

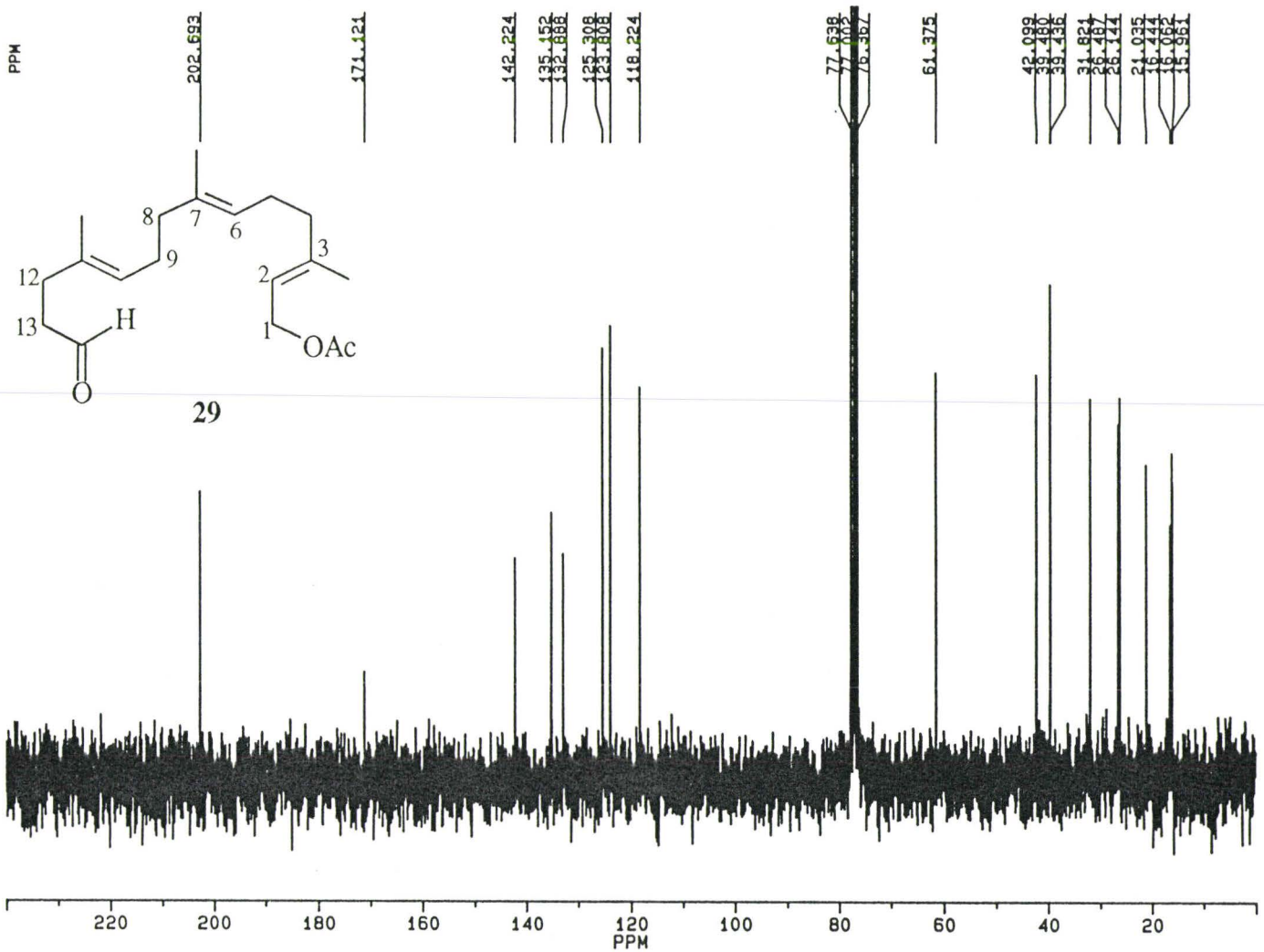

Figure 10. The ^{13}C NMR Spectrum of Geranylgeranyl Acetate Trisnoraldehyde (**29**)

142 ppm which are assigned to the six sp^2 carbons of three double bonds, and a new signal at 202.69 ppm corresponding to the aldehyde carbon. Of the three pairs of methylene groups present in **29**, one pair (C-12 and C-13) is deshielded by the aldehyde functional group from 39.6 to 42.1 ppm and from 29.7 to 31.8 ppm. The proton spectrum of **29** (Figure 11) shows signals at 1.59 - 1.71 ppm which are assigned to three allylic methyl groups. The resonances in the spectrum at 5.06 to 5.34 ppm are due to the three vinyl protons, and the signal for the aldehyde proton is at 9.75 ppm. From the chemical ionization mass spectrum of **29** (Figure 12) the ion at *m/z* 324 ($[M+NH_4]^+$) indicates that the molecular weight of the aldehyde is 306, thus providing additional evidence for the identity of **29**. The signal at *m/z* 229 ($[M-OAc-18]^+$) suggests the anomalous loss of water from the molecule along with the acetate moiety. The base peak of the MS at *m/z* 137 is the ion of two isopentenyl units formed by allylic cleavage at both ends of the molecule.

The other two diols were also oxidized with sodium periodate, using the same reaction conditions as with 14,15-dihydroxygeranylgeranyl acetate, giving the corresponding aldehyde and ketone compounds. The compound with the diol group at position 10 and 11 gave the oxidation products farnesyl acetate trisnoraldehyde (**30a**) and 6-methylhept-5-en-2-one (**30b**) (Scheme 20). The structure of the aldehyde was inferred from its proton NMR, carbon-13 NMR and mass spectra. The carbon-13 NMR spectrum indicates that the molecule has 14 carbons, four of which are vinyl carbons, one is an aldehyde carbon and one an acetate carbon. There are two pairs of methylene groups left in the molecule: one set (C-8 and C-9) is shifted downfield compared to the other (C-4

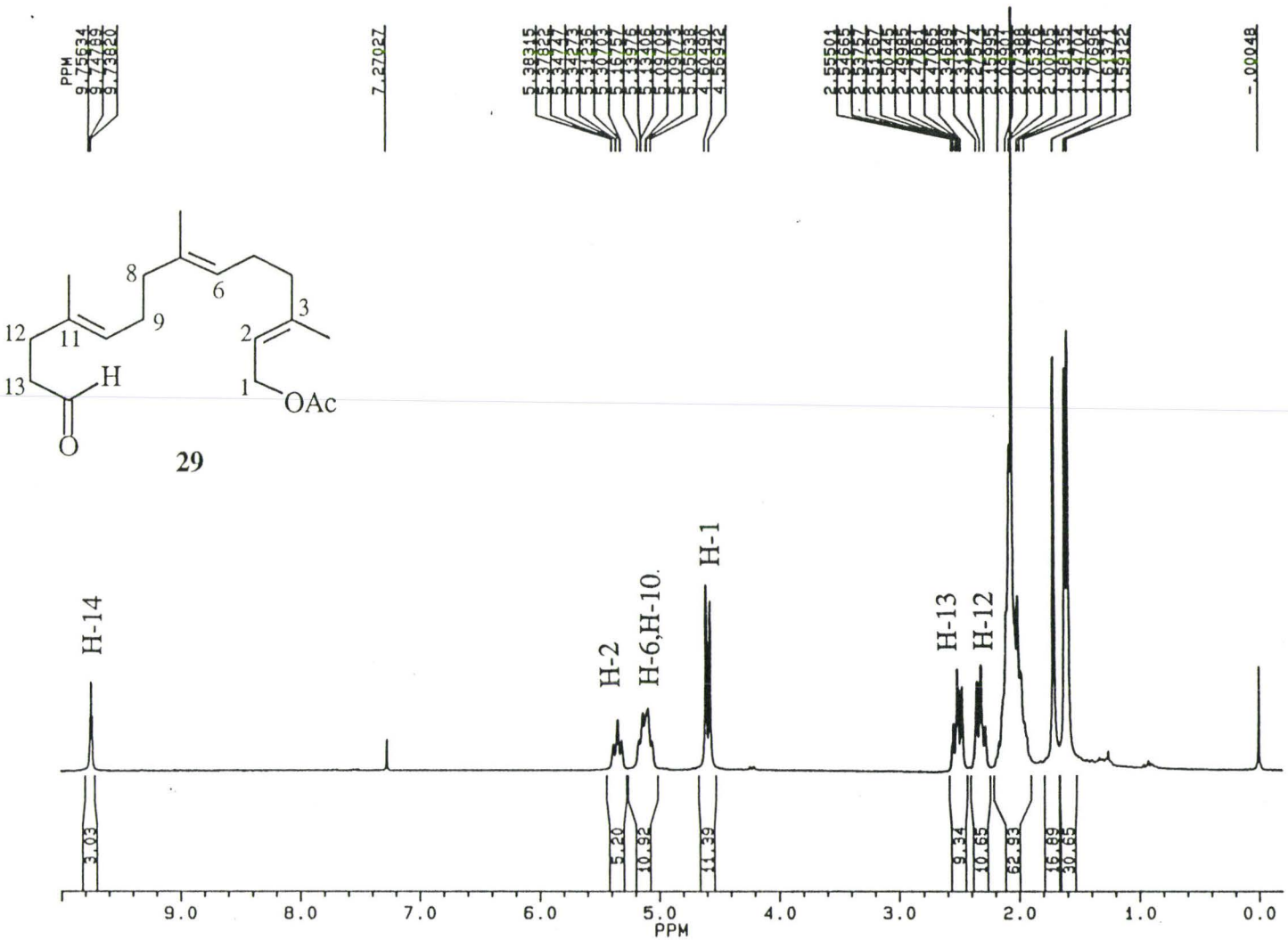

Figure 11. The ^{1}H NMR Spectrum of Geranylgeranyl Acetate Trisnoraldehyde (**29**)

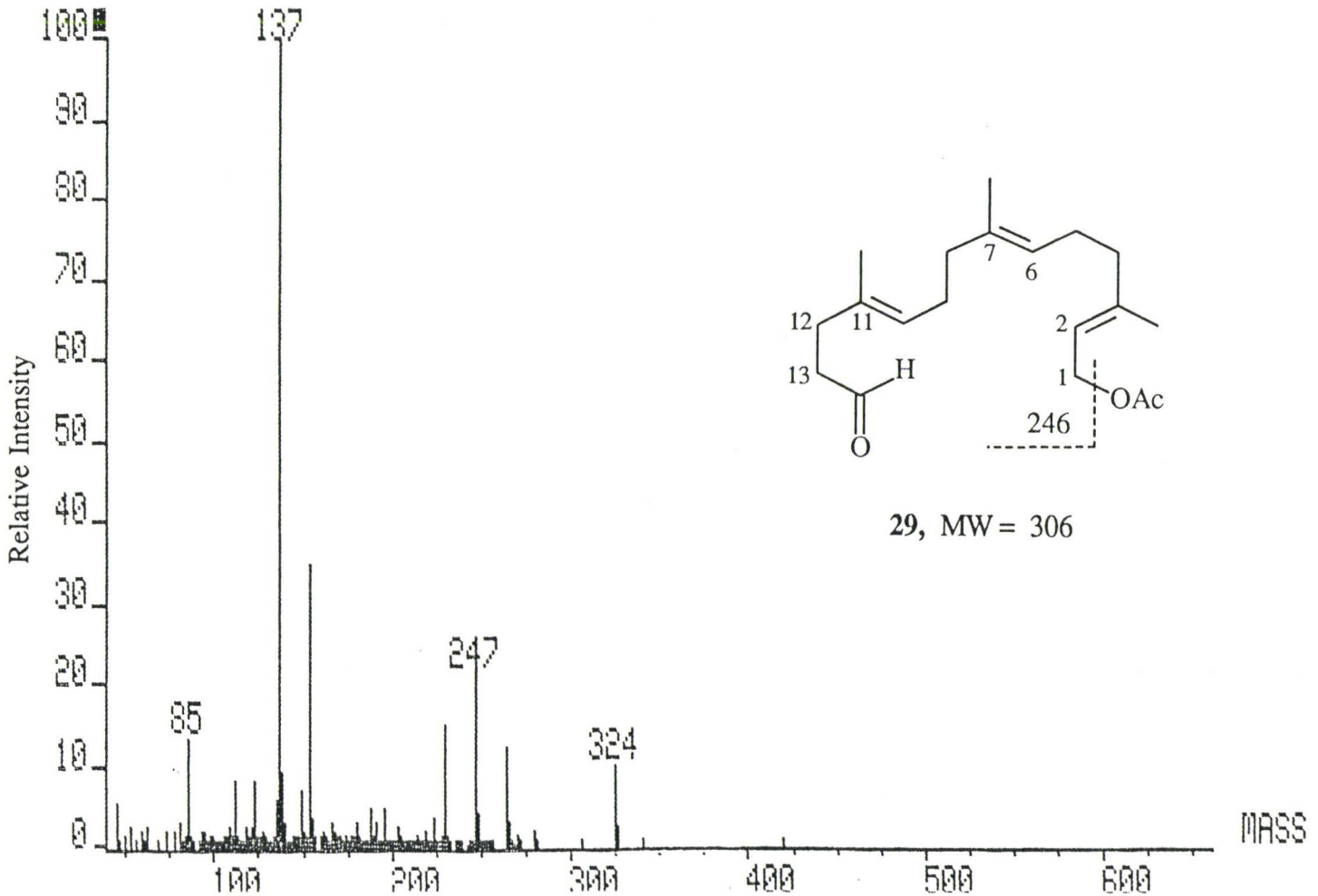

29, MW = 306

Figure 12. The NH_3 CI Mass Spectrum of Geranylgeranyl Acetate Trisnoraldehyde (**29**)

and C-5), due to the influence of the aldehyde group. Similarly, the proton spectrum supports the structure of farnesyl acetate trisnoraldehyde. The mass spectrum (NH_3 CI) has a signal at *m/z* 256 ($[M+NH_4]^+$), indicating a molecular weight of 238 for the parent ion (Figure 13). The base peak of the spectrum is the ion at *m/z* 179 formed by the loss of the acetate group. The ion at *m/z* 161 was formed by the anomalous loss of water ($[M-OAc-18]^+$) from the aldehyde molecule.

Scheme 20

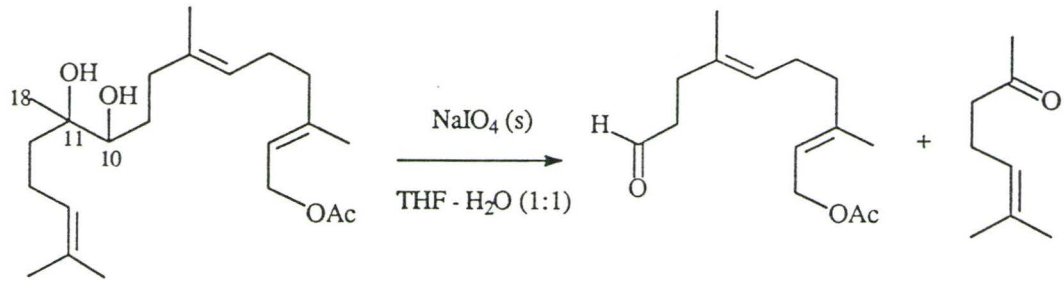

28b **30a** **30b**

The structure of ketone product (**30b**) was also determined by the spectroscopic and spectrometric data and comparison with an authentic reference sample. The ^{13}C NMR spectrum of **30b** indicates a C_8 molecule. The signals are assigned to the structure of the ketone such as the resonance for the ketonic carbon at 208.41 ppm and the two vinylic carbon signals of the only double bond in the molecule at 122.55 and 132.44 ppm (C-5 and C-6). The methylene carbon (C-3) next to the carbonyl group is shifted downfield to 43.54 ppm, while the next methylene carbon (C-4) resonates at 29.64 ppm (compared to 39 and 26 ppm in geranylgeranyl acetate). The mass spectrum (Figure 14) has the parent peak at *m/z* 126 which is the molecular weight of the ketone. The spectrum also

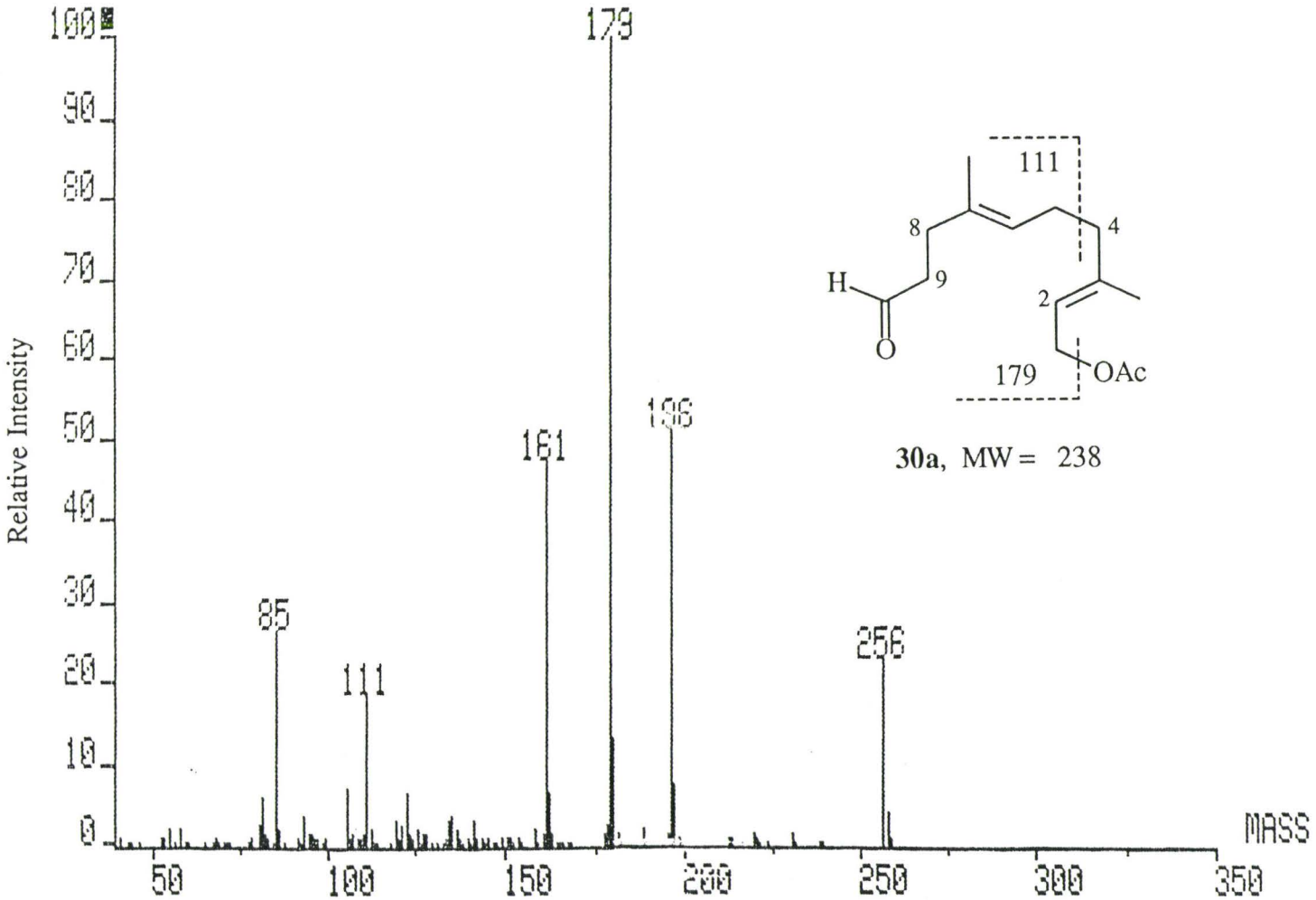

Figure 13. The NH_3 CI Mass Spectrum of Farnesyl Acetate Trisnoraldehyde (**30a**)

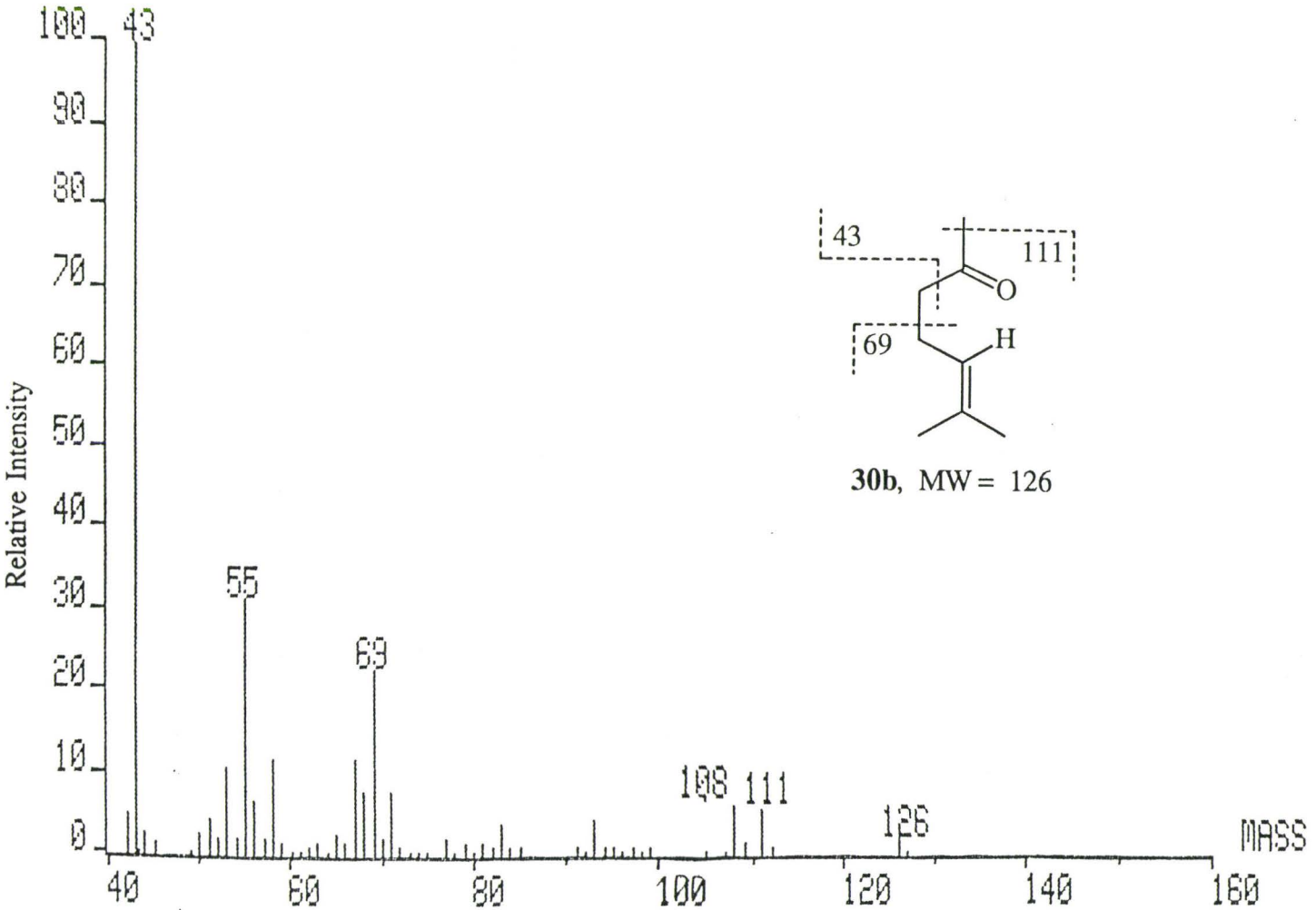

Figure 14. The EI Mass Spectrum of 6-methylhepten-2-one (**30b**)

contains the signal at *m/z* 108, due to the loss of water. The α cleavages on either sides of the ketone group resulted in the formation of the acylium ions at *m/z* 43 and *m/z* 111. The formation of ion at *m/z* 58 can be explained as shown in Scheme 21. The double bond is isomerized to a more favourable position for the γ hydrogen rearrangement, which is then followed by β cleavage.

Scheme 21

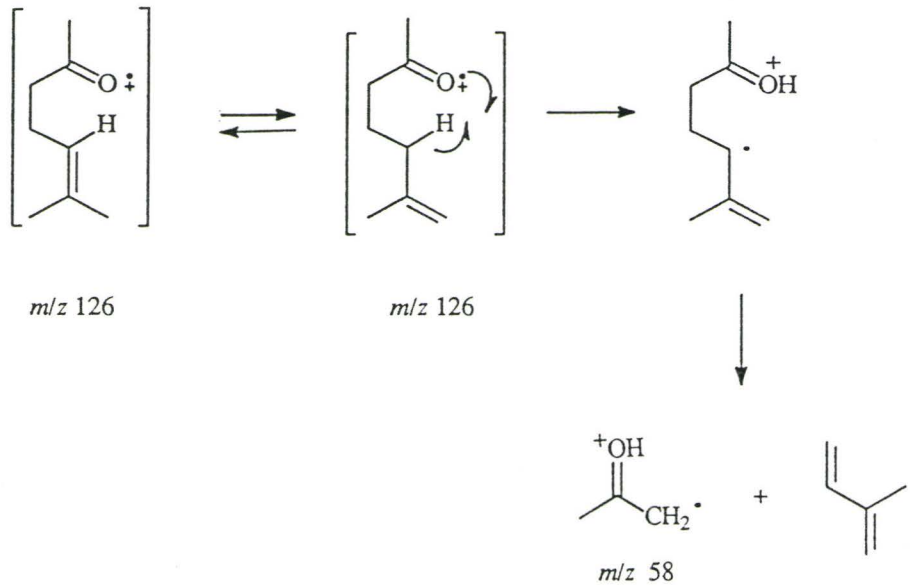

The remaining diol compound was assigned the structure of **28c** and the products from the selective oxidation with sodium periodate confirmed its identity. Geranyl acetate trisnoraldehyde (**31a**) was obtained in 55% yield (Scheme 22) along with the corresponding ketone (**31b**).

The structure of the aldehyde **31a** was verified by its proton NMR, carbon-13 NMR and mass spectra. The carbon-13 NMR spectrum has 9 signals: the signal at 201.63 ppm for the aldehyde carbon; the signal at 171.10 ppm for the ester carbon; one set of vinyl

Scheme 22

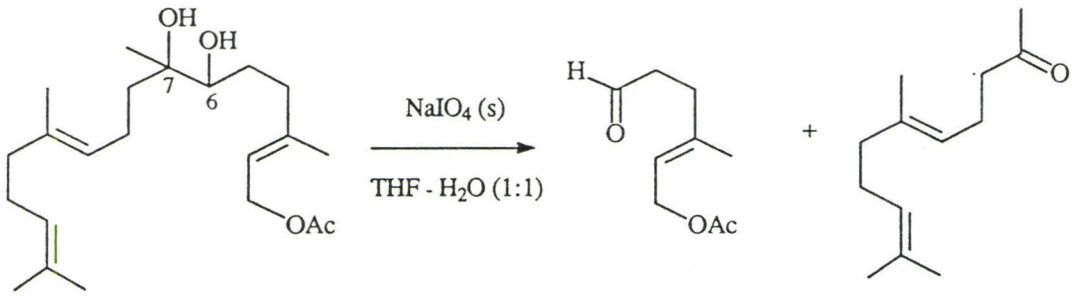

28c **31a** **31b**

carbons (C-2 and C-3) at 140.45 and 119.33 ppm ; the methylene carbon attached to the acetate group at 61.07 ppm; 2 methylene carbons at 31.42 and 41.71 ppm; the carbon of the methyl in the acetate group at 21.05 ppm and the carbon of the allylic methyl (C-7) at 16.57 ppm. The proton spectrum is much simplified compared to the others. It shows the resonances for the aldehyde proton at 9.78 ppm, the vinyl proton (H-2) at 5.37 ppm which was coupled to the methylene of C-1 at 4.58 ppm, two pairs of methylene protons which are shifted downfield to 2.38 and 2.52 ppm due to the deshielding effect of the aldehyde group, and the methyl group on the olefin at 1.72 ppm. The signal of the methyl of the acetate group occurs at the usual 2.04 ppm. The mass spectrum (NH_3 CI) gives the molecular weight of the molecule as 170 from the ion *m/z* 188 ($[M+NH_4]^+$)(Figure 15). The base peak of the spectrum was formed by the loss of the acetate group (*m/z* 111). Alpha cleavage at the carbonyl site generated the ion at *m/z* 43 (11%).

The corresponding ketone was also characterized by proton NMR spectroscopy and mass spectrometry. The ^1H NMR spectrum contains a signal at 5.04 ppm which is assigned to the two vinyl protons (H-5 and H-9) in the molecule. The resonances of the

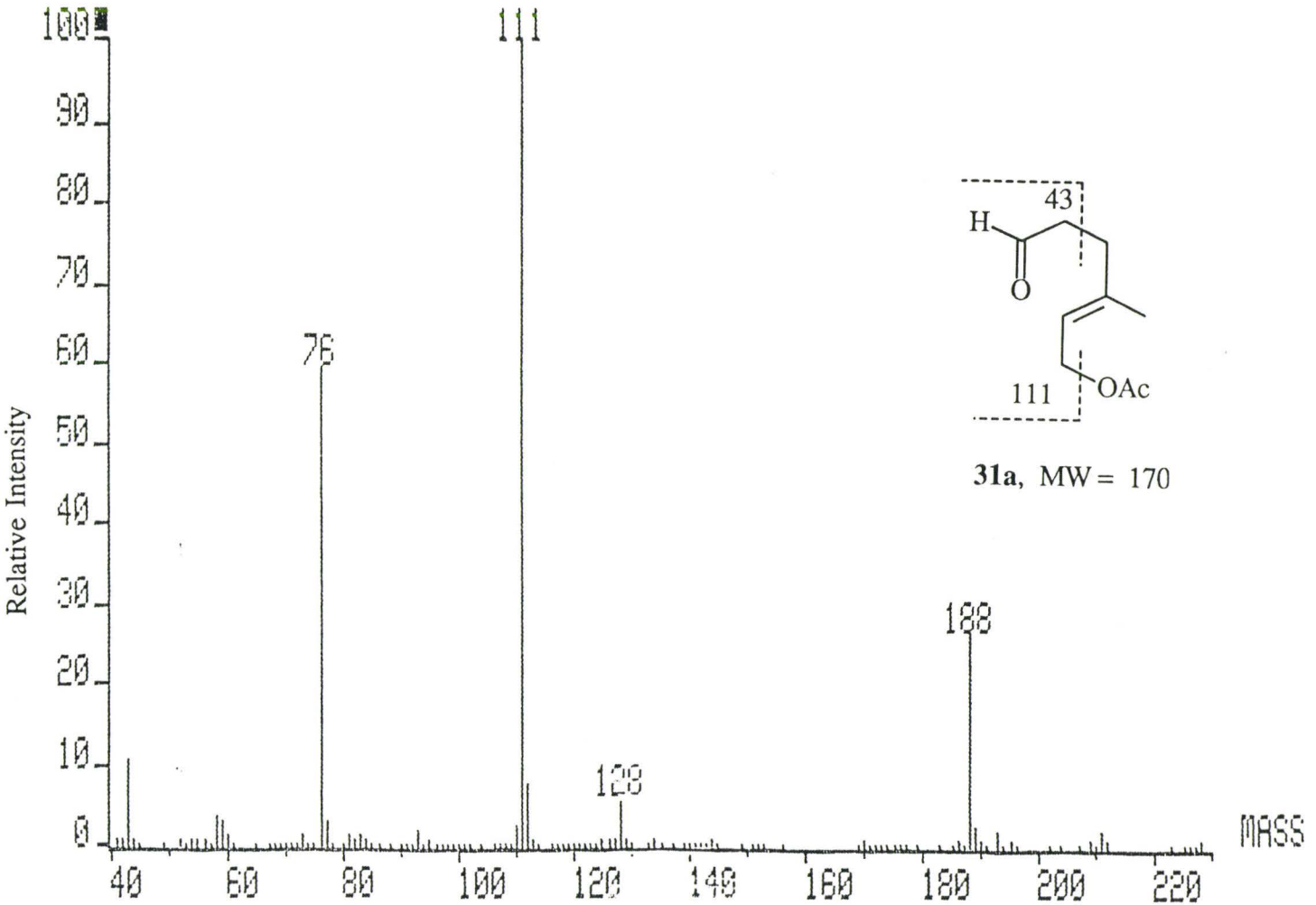

Figure 15. The NH_3 CI Mass Spectrum of Geranyl Acetate Trisnoraldehyde (**31a**)

methyl groups on the double bonds are at 1.60 -1.68 ppm, while the resonance for the methyl of the carbonyl (C-1) occurs downfield at 2.14 ppm. The protons of two methylene groups (C-3 and C-4) next to the carbonyl were shifted downfield to 2.28 and 2.46 ppm compared to the two methylene groups *cis* to the olefin at 1.98 - 2.04 ppm. The mass spectrum of **31b** was contaminated with that of phthalate giving ion at *m/z* 391 and 408. The $[M+NH_4]^+$ ion confirms the molecular weight of the ketone to be 194 (Figure 16). The base peak of the spectrum is the $[M+H]^+$ ion at *m/z* 195. The peak formed by anomalous loss of water (*m/z* 177) was also present in the mass spectrum.

5.0 Wittig Reaction

Geranylgeranyl acetate trisnoraldehyde was utilized in the Wittig reaction with ^{14}C labelled isopropyl triphenylphosphonium ylid. Ethyltriphenylphosphonium iodide was prepared by heating triphenylphosphine with ethyl iodide for 6 hours at reflux (Scheme 23a). The resulting white precipitate was filtered, dried and characterized as the phosponium salt required for the Wittig reaction. The phosphonium salt was suspended in dry THF at 0°C under anhydrous conditions and converted to the corresponding ylid with one equivalent of *n*-butyllithium (Scheme 23b). All the white precipitate reacted with the base and a yellow-orange solution was formed. The solution was allowed to stir for 30 minutes, and unlabelled methyl iodide (0.33 equivalents) was added first to the reaction flask to quench any unreacted *n*-butyllithium still present. The solution still contained the ylid since the yellow-orange colour persisted. Methyl iodide (0.33 equivalents) labelled with ^{14}C isotope dissolved in dry THF was added to the reaction

Scheme 23a

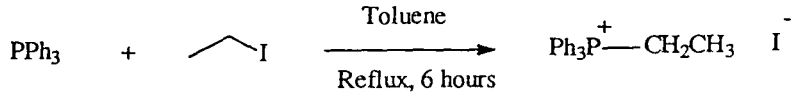

Scheme 23b

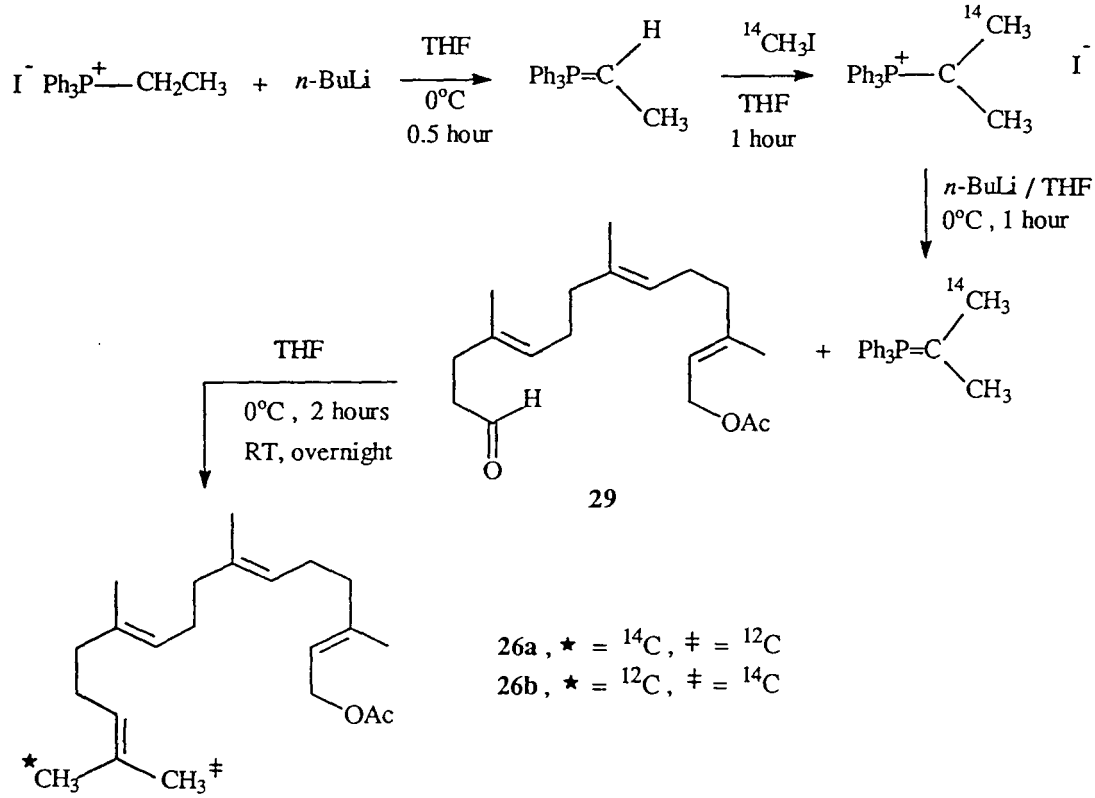

Scheme 23c

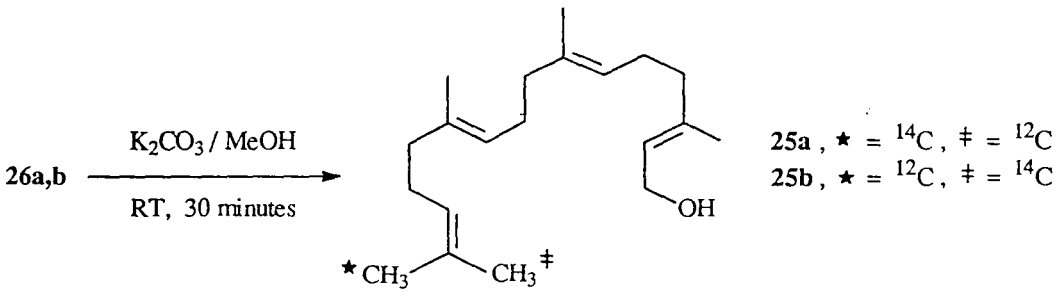

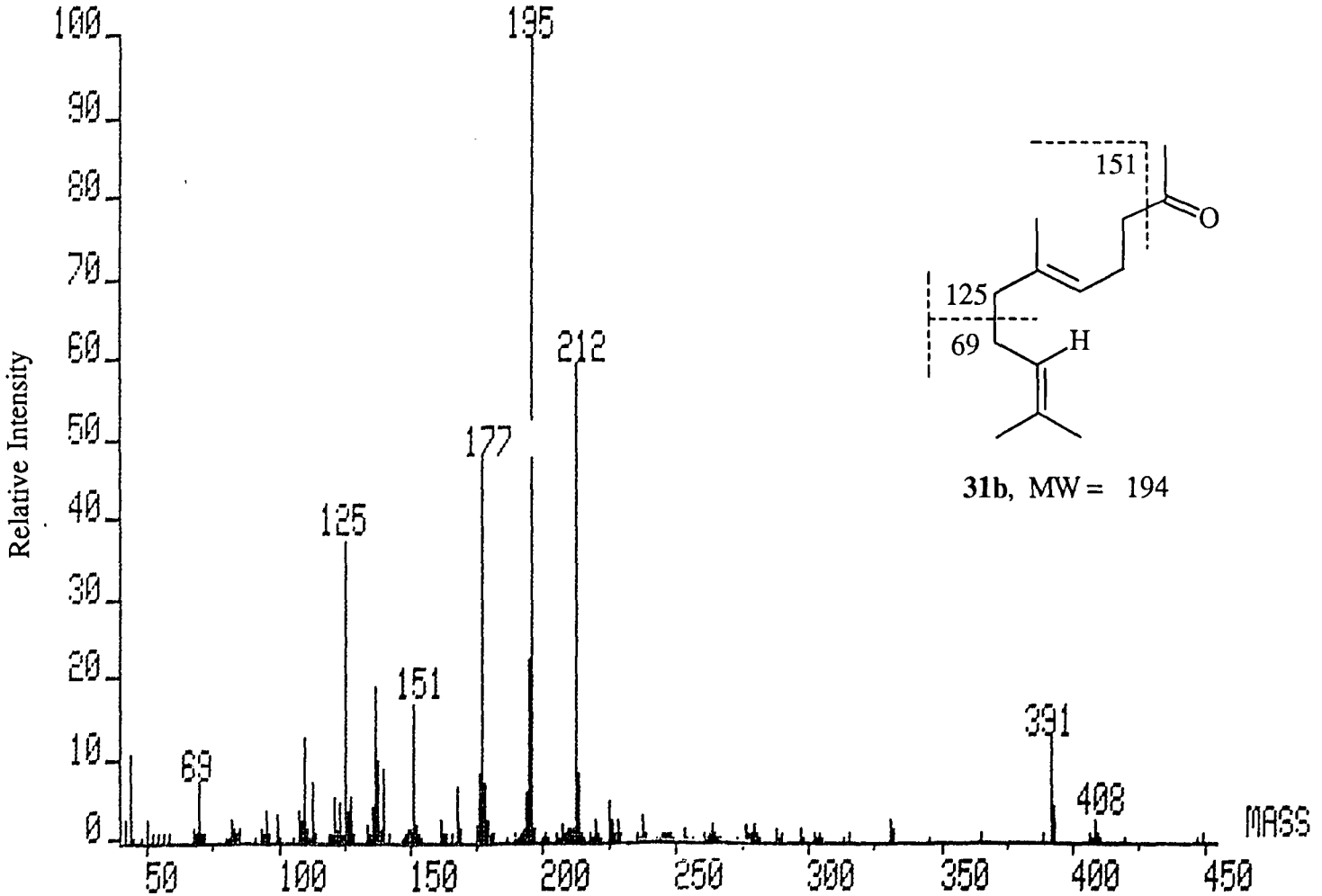

Figure 16. The NH_3 CI Mass Spectrum of 6,10-dimethylundeca-5,9-dien-2-one (**31b**)

mixture next. The solution was discoloured slightly as methyl iodide quenched the yellow-orange ylid. Next, the rest of the required amount of methyl iodide (unlabelled, 0.44 equivalents) was added to quench the rest of the ylid. The solution became colorless as the white precipitate of labelled isopropyltriphenylphosphonium iodide was formed. After one hour, *n*-butyllithium was added to the reaction mixture, turning all of the halide salt into blood-red ylid. Geranylgeranyl acetate trisnoraldehyde (**29**) dissolved in dry THF was added slowly to the reactive ylid, and the blood-red colour disappeared as the ylid reacted. The solution was stirred at 0°C for 2 hours and was allowed to warm up to room temperature overnight, thus ensuring that the betaine intermediate decomposed to the products: triphenylphosphine oxide and geranylgeranyl acetate labelled with ^{14}C isotope at either position C-16 or C-17. Labelled geranylgeranyl acetate was isolated and without any purification, was hydrolyzed to the corresponding alcohol (**25a,b**)(Scheme 23c). The alcohol was separated from *cis* and *trans* desmethyl geranylgeranyl acetate by flash chromatography using silica gel impregnated with silver nitrate (10% w/w). The labelled alcohol was determined by liquid scintillation counting to have the specific activity of 8.0 $\pm$ 0.2 x 10^6 dpm/mg and 21.6 $\pm$ 0.5 % radiochemical yield. The ^1H NMR spectrum of the product was identical to that of authentic geranylgeraniol (Figure 5).

6.0 Pyrophosphorylation Reaction

The terpene system is highly reactive and phosphate and pyrophosphate residues are superb leaving groups when they bear little or no negative charge. Both these factors render the pyrophosphorylation reaction difficult to achieve. Allylic pyrophosphates had

first been synthesized (1959) using a one-pot sequence[78,79,80] of treating the allylic alcohol with inorganic phosphate and trichloroacetonitrile. The desired product must then be isolated from a complex mixture of organic and inorganic mono-, di- and triphosphates by ion-exchange chromatography. The yields are sometimes as high as 30% but often are less. In addition, the procedure is difficult to manage if more than 50 mg of product is desired. Another procedure[81,82] was introduced for phosphorylating the allylic alcohols involving a two-step sequence, in which the labile carbon-pyrophosphate bond was introduced in the second step utilizing a salt of inorganic pyrophosphate in a direct displacement. Reagents and intermediates can be prepared in bulk and stored until needed. The labelled alcohol needs to be converted to a more reactive intermediate which is capable of undergoing a displacement reaction to form the corresponding pyrophosphate.

Therefore **25** was transformed into its chloride derivative[83] by heating at reflux with carbon tetrachloride and triphenylphosphine for 6 hours at 84°C (Scheme 24). The darkened reaction solution was diluted with pentane to precipitate triphenylphosphine oxide out of the solution, which was removed by filtration. Traces of triphenylphosphine oxide were still present in the products as can be seen from the proton NMR spectrum of [16,17-^{14}C]geranylgeranyl chloride (Figure 17).

The proton NMR of **32** is similar to the spectrum of the corresponding alcohol (Figure 5), except that the chloride has shifted the resonance of the protons of the C-1 methylene group upfield by 0.06 ppm. The mass spectrum of geranylgeranyl chloride (Figure 18) shows the parent peak for the molecule at *m/z* 308 and *m/z* 310 where the

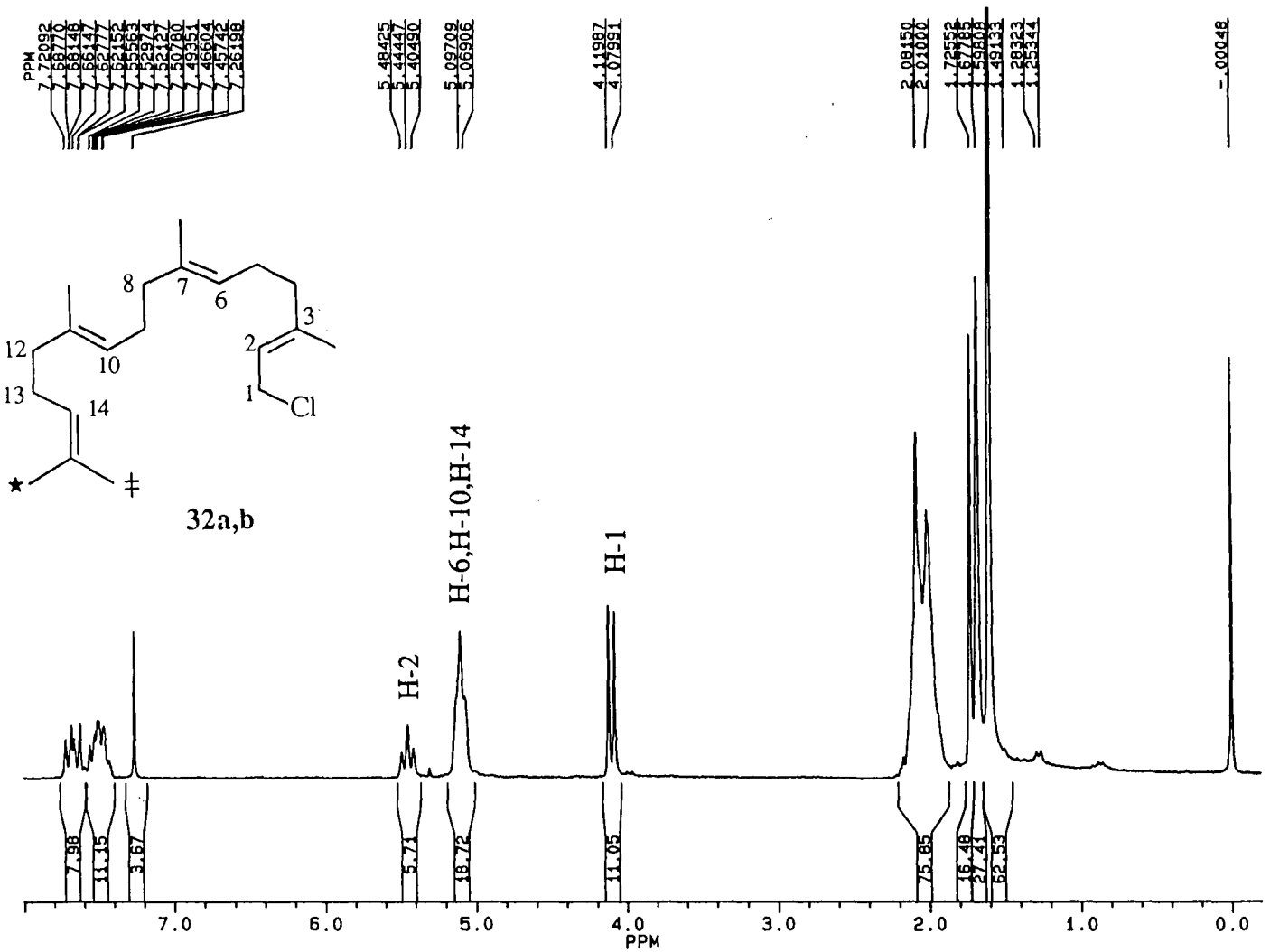

Figure 17. The ^{1}H NMR Spectrum of [16,17-^{14}C]Geranylgeranyl Chloride (**32a,b**)

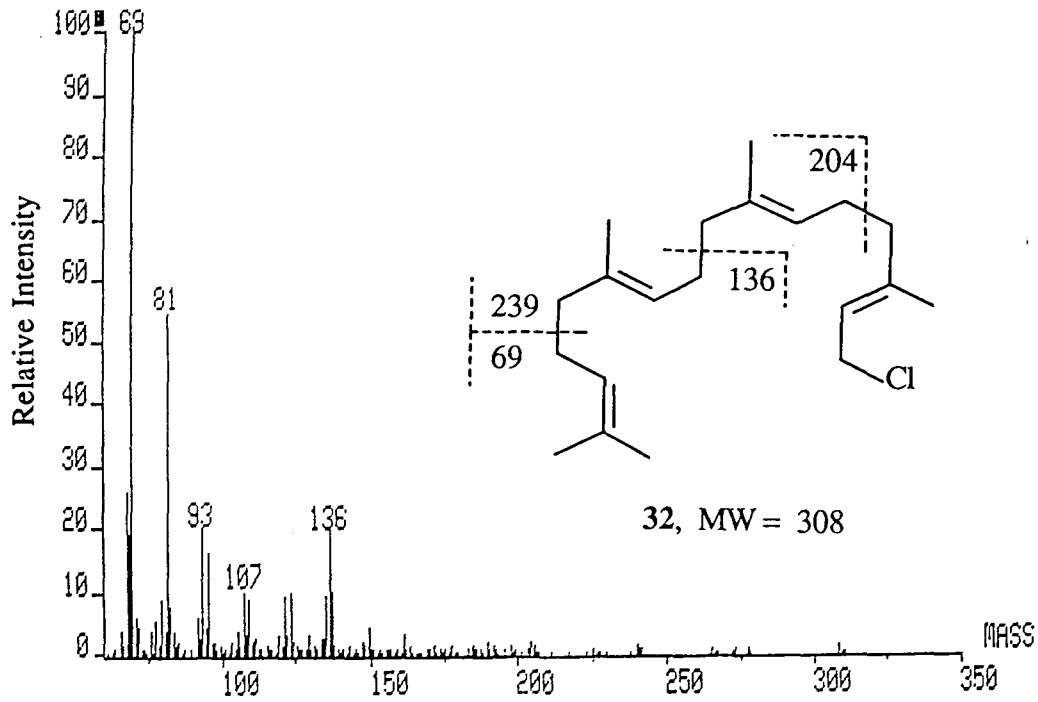

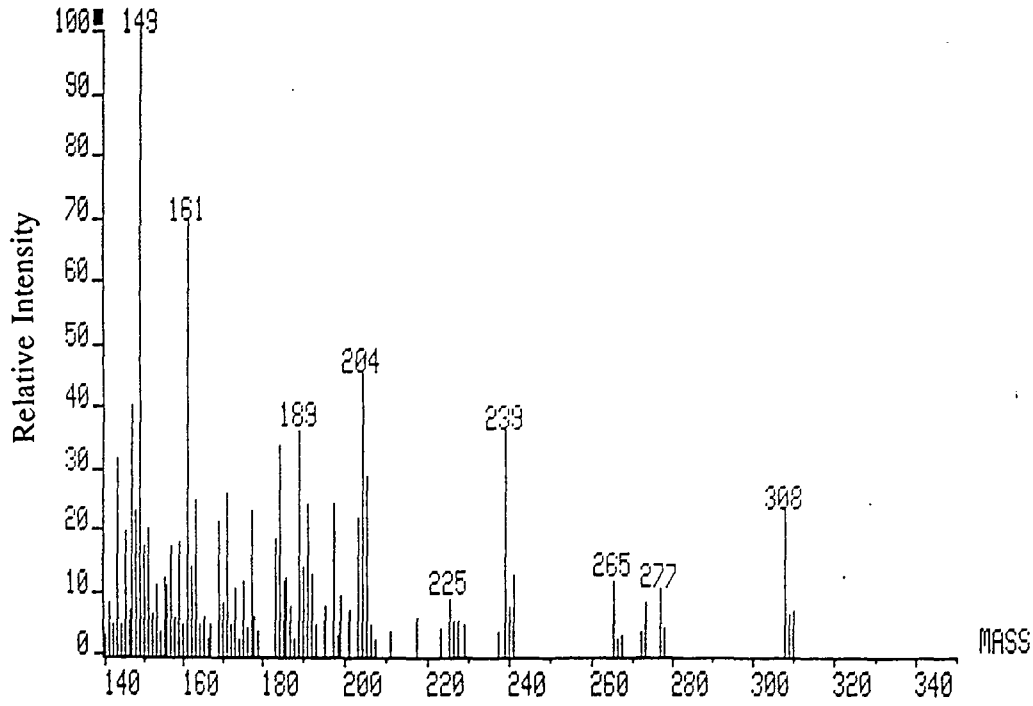

Figure 18. The EI Mass Spectrum of [16,17-^{14}C]Geranylgeranyl Chloride (**32a,b**)

Scheme 24

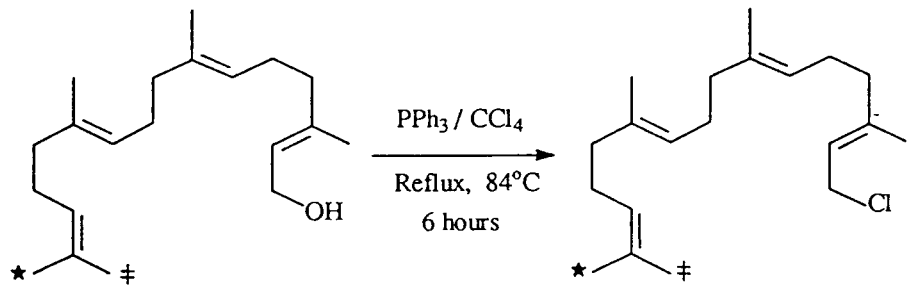

[16,17-^{14}C]Geranylgeraniol

25a, ★ = ^{14}C, ‡ = ^{12}C
25b, ★ = ^{12}C, ‡ = ^{14}C

32a, ★ = ^{14}C, ‡ = ^{12}C
32b, ★ = ^{12}C, ‡ = ^{14}C

latter is the signal for the ion containing ^{37}Cl atom and appears at 1/3 the intensity of the ion containing the ^{35}Cl atom. The MS has a base peak at *m/z* 69 which is indicative of the isopentenyl skeleton. The ion formed from the loss of the chlorine atom was not observed, but an ion at *m/z* 204, which was due to the loss of a chlorine atom and an isopentenyl unit, was present in the spectrum. Other major signals from the spectrum were formed from the ion at *m/z* 204: for example, the ion at *m/z* 136 was formed by the loss of an isopentenyl unit from *m/z* 204 ion. The chemical ionization mass spectrum of **32** has the ion formed from the loss of a chlorine atom (*m/z* 273) as its base peak. The molecular weight of the chloride derivative was also confirmed by its $[M+NH_4^+]^+$ ion at *m/z* 326 and its $[M+H]^+$ ion at *m/z* 309. This activated chloride (**32**) is prone to decomposition via carbocation formation, so the chloride derivative was used immediately in the pyrophosphorylation process without purification after it was checked by IR and ^{1}H NMR spectroscopy.

The phosphorylating agent used is tris(tetra-*n*-butylammonium) hydrogen pyro--phosphate[81,82] (**33**). A column was packed with a slurry of Dowex AG 50W-X8 exchange resin (H^+ form) in deionized water, and was washed with 3 column volumes of deionized water. A solution of disodium dihydrogen pyrophosphate was applied to the column, and the pyrophosphoric acid formed was eluted with deionized water (Scheme 25a). The pH of the eluent was monitored and the eluent was collected when the pH was acidic. The collection was stopped when the pH returned to the pH of deionized water. The solution of pyrophosphoric acid was immediately titrated to pH 7.3 with aqueous tetra-*n*-butyl ammonium hydroxide. The water was removed by lyophilization, giving a hygroscopic, white solid. The inorganic salt was stored over phosphorus pentoxide until needed.

Scheme 25

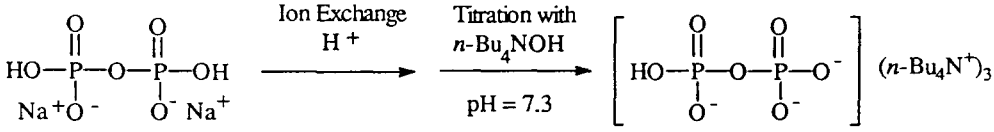

Disodium dihydrogen pyrophosphate

33

In the final step, geranylgeranyl chloride and tris(tetra-*n*-butylammonium) hydrogen pyrophosphate were stirred in anhydrous acetonitrile for 6 hours (Scheme 26). The solvent was removed *in vacuo* and the product mixture was dissolved in 0.05 M triethylammonium bicarbonate (pH 8.00) (Et_3NH^+ HCO_3^-), and extracted with ether to remove any unreacted organic material. The aqueous layer was then subjected to chromatography on a column of DEAE Sephadex A-25 at 4°C. The column was eluted

Scheme 26

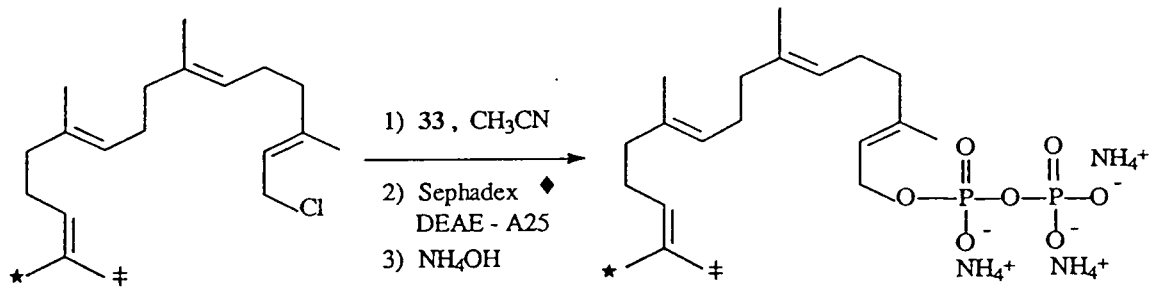

♦ Buffer = $Et_3NH.HCO_3$

32a, ★ = ^{14}C, ‡ = ^{12}C
32b, ★ = ^{12}C, ‡ = ^{14}C

8a, ★ = ^{14}C, ‡ = ^{12}C
8b, ★ = ^{12}C, ‡ = ^{14}C

with a linear gradient from 0.05 M to 1 M Et_3NH^+ HCO_3^-, pH 8.00. The fractions collected were checked by scintillation counting and fractions that contained [16,17-^{14}C]geranylgeranyl pyrophosphate were pooled together and lyophilized. The lyophilization process was repeated once more as ammonium hydroxide was added to displace triethylammonium as the counter cation. The product (**8a,b**, 3.0 ± 0.2 x 10^5 dpm ^{14}C) was obtained in 24 ± 1 % yield from [16,17-^{14}C]geranylgeraniol.

7.0 Future Work

The biosynthesis of taxol (**1**) via the enzymatic transformations of [1-^{3}H]-geranylgeranyl pyrophosphate[73] and [16,17-^{14}C]geranylgeranyl pyrophosphate will be investigated. Cell-free extracts from yew needles from *Taxus x media* densiformis will be prepared and used to incubate the labelled pyrophosphate(s). The hydrocarbon intermediates from the incubation will be isolated, and then analyzed by scintillation counting and radioactive gas chromatography. If the intermediates isolated are found to be labelled, this will indicate that geranylgeranyl pyrophosphate is indeed the precursor for these diterpene(s) and hence taxol as the hypothesis predicted. The next step is to determine what the intermediates are, and then which enzymes are responsible for the transformation of GGPP to taxol or to its intermediates. Isolation, purification, and identification of these enzymes would enable the biosynthesis of taxol intermediates. Similarly, the hydrocarbon intermediates would serve as precursors in the synthesis of taxol.

III. CONCLUSION

In order to study the biosynthesis of taxol, a diterpene compound found to exhibit excellent activity against advanced and refractory ovarian and breast cancers, the diterpene precursor was synthesized. The compound [16,17-^{14}C]geranylgeranyl pyrophosphate was synthesized from geranylgeraniol (available commercially) in 8 steps. The synthesis requires the cleavage of the terminal double bond (C-14 and C-15) of the C_{20} acyclic isoprenoid chain and by using the Wittig reaction, reattachment of the labelled isopropyl group onto the molecule.

EXPERIMENTAL

General

All reactions requiring non-aqueous conditions were performed in oven-dried glassware under a positive pressure of nitrogen. The solvents used were of HPLC grade or distilled (hexane, ethyl acetate, tetrahydrofuran distilled from potassium and acetonitrile distilled from phosphorus pentoxide). All reagents were reagent grade or better. All buffers were prepared with deionized water obtained from a Millipore Water Purification System. The term concentrated *in vacuo* refers to the removal of solvent on a rotary evaporator followed by evacuation to constant weight (< 0.5 mm Hg). All reactions were followed by thin layer chromatography (TLC) using either UV fluorescence, staining with iodine or *p*-anisaldehyde for visualisation. The latter reagent was prepared by adding 1 mL of concentrated sulfuric acid and 0.5 mL of *p*-anisaldehyde to 50 mL of 95% ethanol. Commercial TLC plates used were Kieselgel Merck 60F-254. Flash chromatography was performed according to the method of Still *et al.*[85] on Merck Type 60 silica gel, 230-420 mesh.

Proton nuclear magnetic resonance (^{1}H NMR) spectra were recorded on the Varian EM390 (90MHz) or the Bruker AC-200 (200.132 MHz) spectrometers. Carbon nuclear magnetic resonance (^{13}C NMR) spectra were recorded on the Bruker AC-200 (50.323 MHz) spectrometer. All spectra were recorded at ambient temperature in deuterated solvent ($CDCl_3$ or D_2O). All spectra are reported as parts per million, using

tetramethylsilane (TMS, δ 0) as internal standard for ^{1}H spectra and $CDCl_3$ (δ 77.0) as internal standard for ^{13}C spectra. The abbreviations for the multiplicities are s = singlet, d = doublet, t = triplet, q = quartet, m = multiplet and br = broad. Infrared spectra were recorded on the Bio-rad FTS40 spectrometer. Mass spectra were recorded on the ZAB-E mass spectrometer using electron ionization (EI) or chemical ionization with ammonia (NH_3 CI). The pH measurements were recorded on the Orion SA200 pH meter. Melting points were recorded on the Canlab Gallenkamp melting point apparatus. Liquid scintillation spectrometry was performed on the Beckman LS 5801 scintillation counter, using Beckman Ready Safe Liquid Scintillation cocktail, in Fisherbrand 20 mL plastic scintillation screwtop vials. The raw count data were reported in cpm and with the error of 2sigma (95.5% confidence). The data were calibrated to dpm values using ^{14}C toluene standard (4.02×10^8 dpm/ml).

Preparation of Geranylgeranyl Acetate (26).[75]

A mixture of geranylgeraniol (1.0789 g, 3.714 mmol) and acetic anhydride (10.0 mL) in pyridine (10.0 mL) was stirred overnight at room temperature. The solution was poured into 20 mL of ice cold water, and the aqueous layer was extracted with ether (3 x 20 mL). The combined ethereal extracts were washed with 50 mL each of 5% sulfuric acid (H_2SO_4), cold water, saturated potassium bicarbonate ($KHCO_3$), and saturated sodium chloride (NaCl) successively, and then dried with anhydrous magnesium sulfate ($MgSO_4$). The filtrate was concentrated *in vacuo* to yield 0.9717 g (79%) of geranylgeranyl acetate (TLC: hexane-ethyl acetate, 5:1; R_f 0.68). TLC and NMR showed the product was pure:

^{1}H NMR ($CDCl_3$, 200 MHz) δ 1.60 (s, 9H, 3 C$\underline{H}_3$), 1.68 (s, 3H, C$\underline{H}_3$), 1.71 (s, 3H, C$\underline{H}_3$), 2.05 (s, 3H, C$\underline{H}_3$CO), 1.95 - 2.17 (br m, 12H, 6 C$\underline{H}_2$), 4.59 (d, J = 7.1 Hz, 2H, C$\underline{H}_2$OAc), 5.07 - 5.10 (overlapping t, 3H, vinyl $\underline{H}$), 5.34 (t of d, J = 1.0, 7.2 Hz, 1H, vinyl $\underline{H}$ at C-2); ^{13}C NMR ($CDCl_3$) δ 170.90 ($CH_3\underline{C}OOR$), 142.04, 135.30, 134.77, 131.04 (4 CH=$\underline{C}CH_3$), 124.28, 124.06, 123.51, 118.20 (4 $\underline{C}H=CCH_3$), 61.24 ($\underline{C}H_2OAc$), 39.61, 39.57, 39.42 (3 $\underline{C}H_2$-C(CH_3)=CH), 26.64, 26.49, 26.08 (3 $\underline{C}H_2$-CH=C(CH_3)), 25.56, 20.86, 17.54, 16.31, 15.87 (5 $\underline{C}H_3$); IR ν_{max} ($CHCl_3$) 1748 (acetate) cm^{-1}; MS (EI) *m/z* (relative intensity) 332 (M^+, 1), 272 ([M-OAc]$^+$, 3), 263 ([M-69]$^+$, 3), 204 ([*m/z* 272-68]$^+$, 11), 189 ([*m/z* 204-CH_3]$^+$, 6), 161 ([*m/z* 204-C_3H_7]$^+$, 10), 136 ([*m/z* 204-69]$^+$, 20), 121 ([*m/z* 136-CH_3]$^+$, 15), 107 ([*m/z* 136-C_2H_5]$^+$, 20), 93 ([*m/z* 136-C_3H_7]$^+$, 30), 81 ([*m/z* 136-C_4H_7]$^+$, 52) and 69 (100).

Preparation of 14,15-Epoxygeranylgeranyl Acetate (27a).

Geranylgeranyl acetate (0.9717 g, 2.922 mmol) was dissolved in 10 mL of methylene chloride at 0°C and the oxidizing agent *m*-chloroperbenzoic acid (50 %, 0.7832 g, 2.269 mmol, 0.75 equivalents) was added in portions over 3 hours as the reaction mixture was stirred. The excess oxidizing agent was destroyed at the end of the reaction by the addition of 10 mL of 10% sodium sulfite (Na_2SO_3). The aqueous layer was extracted with ether (3 x 10 mL). The combined organic extracts were washed successively with 40 mL each of saturated sodium sulfite, saturated potassium bicarbonate and saturated sodium chloride, then dried with anhydrous magnesium sulfate and concentrated *in vacuo*. The crude epoxide mixture was purified by flash chromatography.

The column was eluted with hexane, and then with mixtures of ether-hexane containing 2%, 5%, 10%, 25% and 50% of ether, to yield 0.5260 g (67%) of monoepoxygeranyl--geranyl acetate mixture (R_f 0.69 and 0.59, TLC solvent: 50% ether-hexane), 0.0397 g (4%) of unreacted geranylgeranyl acetate (R_f 0.75), 0.1507 g (18%) of diepoxygeranyl--geranyl acetate (R_f 0.38) and 0.0465 g (5%) of triepoxygeranylgeranyl acetate (R_f 0.18). The mixture of three monoepoxygeranylgeranyl acetates was not separated at this point. The separation was difficult and unnecessary because the whole mixture could be converted to the corresponding mixture of diols where the purification was easier.

Monoepoxygeranylgeranyl acetate mixture: ^{1}H NMR ($CDCl_3$, 200 MHz) δ 1.25, 1.26, 1.30 (s, C$\underline{H}_3$ bonded to the epoxide rings), 1.60, 1.62, 1.65 - 1.70 (s, C$\underline{H}_3$ bonded to the double bonds)(total 15 H), 1.65 - 1.70 (m, 4H, 2 C$\underline{H}_2$ bonded to the epoxide rings), 2.05 (s, 3H, C$\underline{H}_3$CO), 2.02 - 2.20 (br m, 8H, 4 C$\underline{H}_2$ bonded to the double bonds), 2.70 (t, J = 6.2 Hz, 1H, epoxide $\underline{H}$), 4.59 (d, J = 7.1 Hz, 2H, C$\underline{H}_2$OAc), 5.08 - 5.16 (overlapping t, 2H, vinyl $\underline{H}$), 5.34 (t, J = 7.0 Hz, 1 H, vinyl $\underline{H}$ at C-2); IR ν_{max} ($CHCl_3$) 1721 (acetate) cm^{-1}.

Diepoxygeranylgeranyl acetates: ^{1}H NMR ($CDCl_3$, 200 MHz) δ 1.24 (m, 9H, 3 C$\underline{H}_3$ bonded to the epoxide rings), 1.48 - 1.69 (m, 6H, 2 C$\underline{H}_3$ bonded to the double bonds), 1.48 - 1.69 (m, 6H, 3 C$\underline{H}_2$ bonded to the epoxide rings), 2.01 (s, 3H, C$\underline{H}_3$CO), 2.01 - 2.20 (br m, 8H, 4 C$\underline{H}_2$ bonded to the double bonds), 2.70 (t of d , J = 1.5, 6.1 Hz, 2H, 2 epoxide $\underline{H}$), 4.59 (d, J = 7.0 Hz, 2H, C$\underline{H}_2$OAc), 5.08 - 5.15 (overlapping t, 1H, vinyl $\underline{H}$), 5.39 (t of d, J = 1.2, 6.0 Hz, 1H, vinyl $\underline{H}$ at C-2); IR ν_{max} ($CHCl_3$) 1730 (acetate) cm^{-1}.

Preparation of 14,15-Dihydroxygeranylgeranyl Acetate (28a).

The mixture of monoepoxygeranylgeranyl acetates (0.4948 g, 1.420 mmol) was dissolved in 20 mL of THF-H_2O (1:1), and perchloric acid (3%, 1.50 mL) was added. The solution was stirred for 3 hours at room temperature, after which solid sodium chloride (1.0 g) was added to separate the phases of the solution. The aqueous phase was extracted with ether (3 x 20 mL). The combined organic extracts were washed with 50 mL each of saturated potassium bicarbonate and saturated sodium chloride, then dried with anhydrous magnesium sulfate and concentrated. The crude diol was purified by flash chromatography. The column was eluted with mixtures of ether-hexane containing 10%, 25%, 50% of ether, then mixtures of methylene chloride-ether containing 5%, 10% and 50% of ether, to give 0.2240 g (43%) of the desired 14,15-dihydroxygeranylgeranyl acetate (R_f 0.47, TLC solvent 50% ether-methylene chloride). The other dihydroxygeranylgeranyl acetates were also isolated from the purification process: 0.0486 g (9%) of 6,7-dihydroxygeranylgeranyl acetate (R_f 0.61), and 0.1582 g (30%) of 10,11-dihydroxygeranylgeranyl acetate (R_f 0.70).

14,15-Dihydroxygeranylgeranyl acetate (**28a**): ^{1}H NMR ($CDCl_3$, 200 MHz) δ 1.16, 1.20 (s, 6H, 2 diol C$\underline{H}_3$), 1.26 - 1.56 (m, 2H, C$\underline{H}_2$-CH(OH)), 1.60, 1.61 (s, 6H, 2 C$\underline{H}_3$ bonded to the double bonds), 1.70 (s, 3H, C$\underline{H}_3$ bonded to the double bond), 2.05 (s, 3H, C$\underline{H}_3$CO), 1.95 - 2.17 (br m, 10H, 5 C$\underline{H}_2$), 1.95 - 2.17 (br m, 2H, 2O$\underline{H}$), 3.36 (d of d, J = 1.8, 10.2 Hz, 1H, C$\underline{H}$-OH), 4.59 (d, J = 7.1 Hz, 2H, C$\underline{H}_2$OAc), 5.07 - 5.20 (overlapping t, 2H, 2 vinyl $\underline{H}$), 5.34 (t of d, J = 1.1, 7.1 Hz, 1H, vinyl $\underline{H}$ at C-2); ^{13}C NMR ($CDCl_3$) δ 171.29 ($CH_3\underline{C}OOR$), 142.21, 135.27, 134.77 (C-3, C-7, C-11), 124.84, 123.68, 118.20

(C-2, C-6, C-10), 78.21, 73.23 (C-14, C-15), 61.41 ($\underline{C}H_2OAc$), 39.53, 39.44 (C-4, C-8), 36.71 (C-12), 29.70 (C-13), 26.48, 26.23 (C-5, C-9), 26.09, 23.12, 20.96, 16.37, 15.91, 15.83 (5 $\underline{C}H_3$ and $\underline{C}H_3CO$); IR ν_{max} ($CHCl_3$) 1732 (acetate), 3467 (hydroxyl) cm^{-1}; MS (EI) *m/z* (relative intensity) 365 ($[M-H]^+$, 1), 321 (4), 305 (3), 241 (5), 227 (16), 183 (13), 143 (85), 125 (28), 99 (40), 85 (24), 71 (32), 59 (17) and 44 (100).

10,11-Dihydroxygeranylgeranyl acetate (**28b**): ($CDCl_3$, 200 MHz) δ 1.17 (s, 3H, $C\underline{H}_3$-CH(OH)), 1.26 - 1.58 (m, 4H, $C\underline{H}_2$-C-OH), 1.62, 1.63 (s, 6H, 2 $C\underline{H}_3$ bonded to the double bonds), 1.70 (s, 6H, 2 $C\underline{H}_3$ bonded to the double bonds), 2.06 (s, 3H, $C\underline{H}_3CO$), 2.00 - 2.24 (br m, 8H, 4 $C\underline{H}_2$), 2.00 - 2.24 (br m, 2H, 2 O$\underline{H}$), 3.36 (d of d, J= 1.5, 10.2 Hz, 1H, C$\underline{H}$-OH), 4.59 (d, J = 7.0 Hz, 2H, $C\underline{H}_2OAc$), 5.10 - 5.17 (overlapping t, 2H, 2 vinyl $\underline{H}$), 5.34 (t, J = 7.3 Hz, 1H, vinyl $\underline{H}$ at C-2); ^{13}C NMR ($CDCl_3$) δ 171.16 ($CH_3\underline{C}OOR$), 141.92, 135.36, 131.82 (C-3, C-7, C-15), 124.69, 124.34, 118.49 (C-2, C-6, C-14), 78.12, 74.61 (C-10, C-11), 61.40 ($\underline{C}H_2OAc$), 39.37 (C-4), 36.77, 35.87 (C-12, C-8), 29.00 (C-9), 26.01, 25.66 (C-5, C-13), 23.36, 22.05, 21.00, 17.63, 16.36, 15.89 (5 $\underline{C}H_3$ and $\underline{C}H_3CO$); IR ν_{max} ($CHCl_3$) 1732 (acetate), 3452 (hydroxyl) cm^{-1}; MS (EI) *m/z* (relative intensity) 366 (M^+, 1), 306 ($[M-OAc]^+$, 2), 289 ($[M-OAc-H_2O]^+$, 8), 271 ($[m/z\ 289-H_2O]^+$, 3), 161 (10), 127 (31), 109 (90), 93 (38), 81 (56) and 69 (100); MS (NH_3 CI) 384 ($[M+NH_4]^+$, 6), 349 ($[M-OH]^+$, 5), 307 ($[M-OAc]^+$, 11), 289 ($[M-OAc-H_2O]^+$, 100), 271 ($[m/z\ 289-H_2O]^+$, 18), 221 ($[m/z\ 289-69]^+$, 6) and 127 (6).

6,7-Dihydroxygeranylgeranyl acetate (**28c**): ($CDCl_3$, 200 MHz) δ 1.18 (s, 3H, $C\underline{H}_3$-CH(OH)), 1.26 - 1.54 (m, 4H, $C\underline{H}_2$-CH(OH)), 1.61, 1.62 (s, 6H, 2 $C\underline{H}_3$ bonded to the double bonds), 1.68, 1.72 (s, 6H, 2 $C\underline{H}_3$ bonded to the double bonds), 2.09 (s, 3H,

$C\underline{H}_3CO$), 1.95 - 2.18 (br m, 8H, 4 $C\underline{H}_2$ bonded to the double bonds), 1.95 - 2.18 (br m, 2H, 2 O$\underline{H}$), 3.37 (d of d, J= 1.8, 10.1 Hz, 1H, $C\underline{H}$-OH), 4.59 (d, J = 7.1 Hz, 2H, $C\underline{H}_2OAc$), 5.05 - 5.18 (overlapping t, 2H, 2 vinyl $\underline{H}$), 5.39 (t of d, J = 1.2, 7.1 Hz, 1H, vinyl $\underline{H}$ at C-2); ^{13}C NMR ($CDCl_3$) δ 171.16 ($CH_3\underline{C}OOR$), 142.10, 135.58, 131.41 (C-3, C-11, C-15), 124.33, 124.17, 118.64 (C-2, C-10, C-14), 78.04, 74.70 (C-6, C-7), 61.31 ($\underline{C}H_2OAc$), 39.64 (C-12), 36.66, 35.71 (C-4 and C-8), 29.05 (C-5), 26.60, 25.65 (C-9, C-13), 23.39, 21.93, 21.00, 17.64, 16.44, 15.98 (5 $\underline{C}H_3$ and $\underline{C}H_3CO$); IR ν_{max} ($CHCl_3$) 1732 (acetate), 3452 (hydroxyl) cm^{-1}; MS (EI) *m/z* (relative intensity) 349 ($[M\text{-}OH]^+$, 0.5), 307 ($[M\text{-}HOAc]^+$, 1), 289 ($[M\text{-}OAc\text{-}H_2O]^+$, 4), 271 ($[m/z\ 289\text{-}H_2O]^+$, 2), 195 (10), 177 ($[m/z\ 195\text{-}H_2O]^+$, 18), 138 (17), 109 (32), 93 (20), 81 (49) and 69 (100); MS (NH_3 CI) 383 ($[M+NH_3]^+$, 8), 365 ($[M\text{-}H]^+$, 23), 307 ($[M\text{-}OAc]^+$, 56), 289 ($[M\text{-}OAc\text{-}H_2O]^+$, 100), 271 ($[m/z\ 289\text{-}H_2O]^+$, 12), 221 (18), 195 (21), 177 ($[m/z\ 195\text{-}H_2O]^+$, 18), 151 (21), 109 (11) and 85 (8).

Preparation of Geranylgeranyl Acetate Trisnoraldehyde (29).

A solution of 14,15-dihydroxygeranylgeranyl acetate (42.55 mg, 116.1 μmol) in 5 mL of THF-H_2O (1:1) was stirred for 3 hours at room temperature with solid sodium periodate (52.45 mg, 245.2 μmol, 2.11 equivalents) which was added in portions. Solid sodium chloride (1.0 g) was added to separate the phases at the end of the reaction, and the reaction mixture was extracted with ether (3 x 10 mL). The combined organic extracts were washed with 30 mL of water and 30 mL of saturated sodium chloride, dried with anhydrous magnesium sulfate and concentrated *in vacuo*. The crude aldehyde product

was purified by flash chromatography. The column was eluted with hexane, then mixtures of ethyl acetate-hexane containing 5%, 10%, 20% of ethyl acetate, to yield 29.70 mg (84%) of geranylgeranyl acetate trisnoraldehyde (R_f 0.46, TLC solvent: hexane-ethyl acetate, 4:1). ^{1}H NMR ($CDCl_3$, 200 MHz) δ 1.59, 1.61 (s, 6H, 2 $C\underline{H}_3$), 1.71 (s, 3H, $C\underline{H}_3$), 2.06 (s, 3H, $C\underline{H}_3CO$), 1.95 - 2.15 (br m, 8H, 4 $C\underline{H}_2$), 2.31 (t, J = 7.1 Hz, 2H, $C\underline{H}_2$-CH_2-CHO), 2.50 (t of t, J = 1.7, 7.2 Hz, 2H, $C\underline{H}_2$-CHO), 4.59 (d, J = 7.1 Hz, 2H, $C\underline{H}_2OAc$), 5.06 - 5.17 (overlapping t, 2H, 2 vinyl $\underline{H}$), 5.34 (t of d, J = 1.0, 7.0 Hz, 1H, vinyl $\underline{H}$ at C-2), 9.75 (t, J = 1.8 Hz, 1H, $C\underline{H}O$); ^{13}C NMR ($CDCl_3$) δ 202.69 ($\underline{C}HO$), 171.12 ($CH_3\underline{C}OOR$), 142.22, 135.15, 132.89 (C-3, C-7, C-11), 125.31, 123.81, 118.22 (C-2, C-6, C-10), 61.38 ($\underline{C}H_2OAc$), 42.10 (C-12), 39.48, 39.44 (C-4, C-8), 31.82 (C-13), 26.49, 26.14 (C-5, C-9), 21.04, 16.44, 16.06, 15.96 (3 $\underline{C}H_3$ and $\underline{C}H_3CO$); IR ν_{max} ($CHCl_3$) 1732 (acetate), 1743 (aldehyde) cm^{-1}; MS (NH_3 CI) *m/z* (relative intensity) 324 ($[M+NH_4]^+$, 11), 262 (14), 247 ($[M-OAc]^+$, 22), 229 ($[M-OAc-H_2O]^+$, 16), 152 (35), 137 (100) and 85 (13).

Preparation of Farnesyl Acetate Trisnoraldehyde (30a).

Solid sodium periodate (168.7 mg, 788.7 μmol, 5.5 equivalents) was added in portions to a solution of 10,11-dihydroxygeranylgeranyl acetate (52.50 mg, 143.2 μmol) in 10 mL of THF-H_2O (1:1). The solution was stirred for 3 hours at room temperature. Solid sodium chloride (1.0 g) was added to the mixture to separate the phases and the aqueous layer was extracted with ether (3 x 10 mL). The combined organic extracts were washed with 30 mL of water and 30 mL of saturated sodium chloride, dried with anhydrous magnesium sulfate and concentrated *in vacuo*. The crude product was purified

by flash chromatography, eluting with hexane, then mixtures of ethyl acetate-hexane containing 5%, 10%, 20% of ethyl acetate, and yielding 22.05 mg (65%) of farnesyl acetate trisnoraldehyde (R_f 0.48, TLC solvent 20% ethyl acetate-hexane), 20.55 mg (39%) of unreacted 10,11-dihydroxygeranylgeranyl acetate (R_f 0.21) and 8.450 mg of 6-methylhept-5-en-2-one (**30b**) (R_f 0.57).

Farnesyl acetate trisnoraldehyde (**30a**): ^{1}H NMR ($CDCl_3$, 200 MHz) δ 1.62, 1.70 (s, 6H, 2 C$\underline{H}_3$), 2.06 (s, 3H, C$\underline{H}_3$CO), 2.02 - 2.14 (br m, 4H, 2 C$\underline{H}_2$), 2.32 (t, J = 7.1 Hz, 2H, C$\underline{H}_2$-CH_2-CHO), 2.52 (t of t, J = 1.7, 7.4 Hz, 2H, C$\underline{H}_2$-CHO), 4.59 (d, J = 7.1 Hz, 2H, C$\underline{H}_2$OAc), 5.13 (t, 1H, vinyl $\underline{H}$), 5.29 (t of d, J = 1.1, 7.1 Hz, 1H, vinyl $\underline{H}$ at C-2), 9.75 (t, J = 1.8 Hz, 1H, C$\underline{H}$O); ^{13}C NMR ($CDCl_3$) δ 202.55 (C$\underline{H}$O), 171.10 ($CH_3\underline{C}$OOR), 141.88, 133.45 (C-3, C-7), 124.75, 118.52 (C-2, C-6), 61.35 ($\underline{C}H_2$OAc), 42.10 (C-8), 39.48 (C-4), 31.80 (C-9), 26.03 (C-5), 21.05, 16.41, 16.11 (2 $\underline{C}H_3$ and $\underline{C}H_3$CO); IR ν_{max} ($CHCl_3$) 1732 (acetate), 1744 (aldehyde) cm^{-1}; MS (NH_3 CI) *m/z* (relative intensity) 256 ($[M+NH_4]^+$, 24), 196 (50), 179 ($[M-OAc]^+$, 100), 161 ($[M-OAc-H_2O]^+$, 47), 111 ([*m/z* 179-69]$^+$, 18) and 85 (27).

6-Methylhept-5-en-2-one (**30b**): ^{1}H NMR ($CDCl_3$, 200 MHz): δ 1.62 (s, 3H, C$\underline{H}_3$), 1.68 (s, 3H, C$\underline{H}_3$), 2.13 (s, 3H, C$\underline{H}_3$CO), 2.25 (q, J = 7.0, 14 Hz, 2H, C$\underline{H}_2$-CH=C), 2.46 (t, J = 7.2 Hz, 2H, C$\underline{H}_2$-$COCH_3$), 5.06 (t, 1H, vinyl $\underline{H}$); ^{13}C NMR ($CDCl_3$) δ 208.41 ($\underline{C}OCH_3$), 132.44 (C-6), 122.55 (C-5), 43.54 (C-3), 29.64 (C-4), 25.44 ($\underline{C}H_3$-*trans*), 22.37 (C-1), 17.42 ($\underline{C}H_3$-*cis*); MS (EI) *m/z* (relative intensity) 126 (M^+, 2), 111($[M-CH_3]^+$, 4), 108 ($[M-H_2O]^+$, 6), 93 (3), 77 (11), 69 (24), 55 (30), 43 (100); MS (NH_3 CI) *m/z* (relative intensity) 143 ($[M+NH_3]^+$, 41), 127 ($[M+H]^+$, 100), 125 ($[M-H]^+$, 63), 118 (33), 109 (12),

98 (13), 77 (15), 58 (31), 44 (36).

Preparation of Geranyl Acetate Trisnoraldehyde (31a) .

Solid sodium periodate (39.65 mg, 185.4 μmol, 1.32 equivalents) was added in portions to a solution of 6,7-dihydroxygeranylgeranyl acetate (51.55 mg, 140.6 μmol) in 10 mL of THF-H_2O (1:1). The solution was stirred for 3 hours at room temperature. Solid sodium chloride (1.0 g) was added to the mixture to separate the phases and the aqueous layer was extracted with ether (3 x 10 mL). The combined organic extracts were washed with 30 mL of water and 30 mL of saturated sodium chloride, dried over anhydrous magnesium sulfate, filtered and concentrated *in vacuo*. The crude product was purified by flash chromatography, eluting with hexane, then mixtures of ethyl acetate-hexane containing 5%, 10%, 20% of ethyl acetate, and yielding 13.10 mg (55%) of geranyl acetate trisnoraldehyde (R_f 0.49, TLC solvent 20% ethyl acetate-hexane), 21.20 mg (39%) of unreacted 6,7-dihydroxygeranylgeranyl acetate (R_f 0.27) and 10.40 mg of 6,10-dimethylundeca-5,9-dien-2-one, (R_f 0.61).

Geranyl acetate trisnoraldehyde (**31a**): ^{1}H NMR ($CDCl_3$, 200 MHz) δ 1.72 (d, 3H, C$\underline{H}_3$), 2.04 (s, 3H, C$\underline{H}_3$CO), 2.38 (t, J = 7.1 Hz, 2H, C$\underline{H}_2$-CH_2-CHO), 2.52 (t, J = 6.8 Hz, 2H, CH_2-C$\underline{H}$O), 4.58 (d, J = 7.1 Hz, 2H, C$\underline{H}_2$OAc), 5.37 (t, J = 7.0 Hz, 1H, vinyl $\underline{H}$ at C-2), 9.78 (t, J = 13.1 Hz, 1H, C$\underline{H}$O); ^{13}C NMR ($CDCl_3$) δ 201.63 ($\underline{C}$HO), 171.10 ($CH_3\underline{C}$OOR), 140.45 (C-3), 119.33 (C-2), 61.07 ($\underline{C}H_2$OAc), 41.71 (C-4), 31.42 (C-5), 21.05 ($\underline{C}H_3$CO), 16.57($\underline{C}H_3$); IR ν_{max} ($CHCl_3$) 1732 (acetate), 1743 (aldehyde) cm^{-1}; MS (NH_3 CI) *m/z* (relative intensity) 188 ([M+NH_4]$^+$, 26), 128 (7), 111 ([M-OAc]$^+$, 100), 76

(59) and 43 (11).

6,10-Dimethylundeca-5,9-dien-2-one (**31b**): ^{1}H NMR ($CDCl_3$, 200 MHz) δ 1.60, 1.68 (s, 9H, 3C$\underline{H}_3$), 1.98 - 2.04 (br m, 4H, 2C$\underline{H}_2$), 2.14 (s, 3H, C$\underline{H}_3$CO), 2.28 (t, J = 6.0 Hz, 2H, C$\underline{H}_2$-CH_2-$COCH_3$), 2.46 (t, J = 7.1 Hz, 2H, C$\underline{H}_2$-$COCH_3$), 5.04 (t, J = 6.7 Hz, 2H, vinyl $\underline{H}$); IR ν_{max} ($CHCl_3$) 1732 (acetate) cm^{-1}; MS (NH_3 CI) *m/z* (relative intensity) 212 ($[M+NH_4]^+$, 59), 195 ($[M+H]^+$, 100), 177 ($[M-17]^+$, 48), 151 ($[M-43]^+$, 18), 136 ($[M-58]^+$, 19), 125 ($[M-69]^+$, 38), 110 (12) and 69 (8); High Resolution MS Calcd for $C_{13}H_{22}O_1$ (M^+) *m/z*: 194.1670, found *m/z*: 194.1885.

Wittig Reaction

Preparation of Ethyltriphenylphosphonium Iodide.

A solution of triphenylphosphine (1.997 g, 7.61 mmol) and ethyl iodide (0.5 mL, 6.25 mmol, 0.82 equivalents) in toluene (10 mL) was heated at reflux at 100°C for 6 hours. The white precipitate of the salt which formed was collected by filtration, washed with toluene and dried, giving 2.4105 g (92%) of ethyltriphenylphosphonium iodide. ^{1}H NMR ($CDCl_3$, 90 MHz) δ 1.40 (d of t, J = 7.5, 21.0 Hz, 3H, C$\underline{H}_3$), 3.75 (s, 3H, C$\underline{H}_2$), 7.80 (br m, 15H, aromatic $\underline{H}$); MS (EI) *m/z* (relative intensity) 277 (26), 203 (8), 201 (8), 152 (4), 91 (100), 77 (22) and 45 (75) ; MS (NH_3 CI) *m/z* (relative intensity) 291 ($[M-I]^+$, 6, 279 (5), 263 (100), 215 (18), 186 (59), 184 (20), 130 (11), 129 (10) and 72 (9); melting point: 158 - 161°C.

Preparation of [16,17-^{14}C]-Geranylgeraniol (25a,b).

The solution of *n*-butyllithium in hexane (standardized by titration with 2,5-dimethoxybenzyl alcohol, 1.376 M, 54 μL, 74 μmol) was added slowly to the solution of ethyltriphenylphosphonium iodide (30.75 mg, 73.5 μmol) in 2.0 mL of dry THF at 0°C under nitrogen. The yellow-orange solution was stirred for 30 minutes. Unlabelled methyl iodide (1.5 μL, 24 μmol, 0.33 equivalents, dried over calcium chloride and freshly distilled) was added first to the ylid solution to quench any unreacted base. Next, a solution of [^{14}C]methyl iodide (250 μCi, specific activity 15 μCi/μmol, 16.66 μmol, 0.23 equivalents) in 1.0 mL of THF was added to the ylid solution, and the mixture was stirred for 30 minutes. Then unlabelled methyl iodide (2.0 μL, 32 μmol, 0.44 equivalents) was added, giving a white precipitate in a colorless solution. The solution was stirred for an additional 30 minutes. Next, *n*-butyllithium (1.376 M in hexane, 54 μL, 74 μmol) was added, and the blood-red ylid solution was stirred for 1 hour at 0°C. Geranylgeranyl acetate trisnoraldehyde (**29**)(22.3 mg, 73.0 μmol) in 2.0 mL of THF was added to the reaction mixture, and the slightly yellow solution was stirred at 0°C for 2 hours, and then was allowed to warm up to room temperature overnight. The solution was quenched with 10 mL of solution of 40% methanol in half saturated ammonium chloride. The aqueous layer was extracted with 3 x 10 mL of hexane. The combined organic extracts were washed with 30 mL of 40% methanol in half saturated ammonium chloride, water and saturated sodium chloride successively, dried over anhydrous magnesium sulfate, filtered and concentrated *in vacuo*. The crude [16,17-^{14}C]geranylgeranyl acetate (**26a,b**) (29.95 mg) was hydrolyzed to the corresponding alcohol by stirring with anhydrous potassium

carbonate (K_2CO_3)(17.65 mg, 127.7 μmol) in 0.4 mL of methanol at room temperature for 30 minutes. Saturated sodium chloride solution (5 mL) was added to separate the phases of the reaction mixture, and the aqueous layer was extracted with hexane (3 x 10 mL). The combined organic extracts were washed with 30 mL of water and saturated sodium chloride, dried with anhydrous magnesium sulfate and concentrated. The crude alcohol was purified by flash chromatography on 10% silver nitrate impregnated silica gel (Aldrich). The column was eluted with hexane, then with mixtures of ethyl acetate-hexane containing 5%, 10%, 20%, 30% and 50% ethyl acetate, to give 8.95 mg (42%) of [16,17-^{14}C]geranylgeraniol, which was diluted with 6.0 mg of unlabelled geranylgeraniol (total activity: 1.20 ± 0.03 x 10^8 dpm, or 8.0 ± 0.2 x 10^6 dpm/mg, 21.6 ± 0.5 % radiochemical yield). The ^{1}H NMR of the product was identical to that reported for authentic geranylgeraniol: ($CDCl_3$, 200 MHz) δ 1.60 (s, 9H, 3 C$\underline{H}_3$), 1.68 (s, 6H, 2 C$\underline{H}_3$), 2.00 - 2.12 (br m, 12H, 6 C$\underline{H}_2$), 2.00 - 2.12 (br m, 1H, O$\underline{H}$), 4.16 (d, J = 6.9 Hz, 2H, C$\underline{H}$-OH), 5.08 - 5.11 (overlapping t, 3H, vinyl $\underline{H}$), 5.42 (t of q, J = 6.7 Hz, 1H, vinyl $\underline{H}$ at C-2).

Preparation of [16,17-^{14}C]Geranylgeranyl Chloride (32a,b).[83]

A solution of geranylgeraniol (20.40 mg, 70.22 μmol) and [16,17-^{14}C]geranylgeraniol (0.1545 mg, 1.239 x 10^6 dpm), triphenylphosphine (37.25 mg, 142.0 μmol, 2.0 equivalents) in 235 μL of carbon tetrachloride (freshly distilled) was heated at refluxed at 84°C for 6 hours. The solution was cooled, diluted with pentane (5 mL), and the triphenylphosphine oxide which precipitated out of the solution was removed by

filtration through celite. The filtrate was concentrated *in vacuo* at 0°C to give 19.95 mg (63.12 μmol, 90.0%) of [16,17-^{14}C]geranylgeranyl chloride. The product still contained traces of triphenylphosphine oxide, and had a the total activity of 7.6 ± 0.2 x 10^5 dpm (61 ± 3 % radiochemical yield). ^{1}H NMR ($CDCl_3$, 200 MHz) δ 1.60 (s, 9H, 3 C$\underline{H}_3$), 1.68 (s, 3H, C$\underline{H}_3$), 1.73 (s, 3H, C$\underline{H}_3$), 2.01 - 2.08 (br m, 12H, 6 C$\underline{H}_2$), 4.10 (d, J = 8.0 Hz, 2H, C$\underline{H}_2$-Cl), 5.07 - 5.10 (overlapping t, 3H, vinyl $\underline{H}$), 5.44 (t, J = 7.9 Hz, 1H, vinyl $\underline{H}$ at C-2); ^{13}C NMR ($CDCl_3$) δ 142.73, 135.58, 134.93, 131.22 (4 CH=$\underline{C}$(CH_3)), 124.34, 124.13, 123.41, 120.26 (4 $\underline{C}$H=C(CH_3)), 41.10 ($\underline{C}H_2$-Cl), 39.62, 39.49, 39.35 (3 $\underline{C}H_2$-C(CH_3)=CH) 26.73, 26.57, 26.09 (3 $\underline{C}H_2$-CH=C(CH_3)), 25.64, 17.64, 17.58, 16.01, 15.92 (5 $\underline{C}H_3$); IR ν_{max} ($CHCl_3$) 1748 (acetate) cm^{-1}; MS (EI) *m/z* (relative intensity) 308/310 (M^+, 1/0.3), 239/241 ([M-69]$^+$, 2/0.6), 225 ([M-83]$^+$, 0.5), 204 ([M-69-Cl]$^+$, 2.5), 161 ([*m/z* 204-43]$^+$, 3.5), 149 ([*m/z* 204-55]$^+$, 5), 136 ([*m/z* 204-69]$^+$, 20), 107 (12), 93 (21), 81 (55) and 69 (100); MS (NH_3 CI) *m/z* (relative intensity) 326 ([M+NH_4]$^+$, 38), 309 ([M+H]$^+$, 22), 273 ([M-Cl]$^+$, 100), 204 ([*m/z* 273-69]$^+$, 29), 191 (31), 143 (56), 118 (62), 95 (33) and 81 (35).

Pyrophosphorylation reaction

Preparation of Tris(tetra-*n*-butylammonium) Hydrogen Pyrophosphate (33).[81,82]

Disodium dihydrogen pyrophosphate (1.1505 g, 5.18 mmol) was dissolved in 9 mL of 4% (v/v) aqueous ammonium hydroxide. The clear solution was loaded onto a 1 x 10-cm column of Dowex AG 50W-X8 cation exchange resin (20 - 50 mesh, H^+ form) which had been prewashed with deionized water. The free acid was eluted with 50 mL of

deionized water, and the eluant (pH 1.23) was immediately titrated to pH 7.3 with 40% (w/w) aqueous tetra-*n*-butyl ammonium hydroxide (15 mL). The resulting solution (approximately 70 mL total volume) was dried by freezing the solution in a dry ice-isopropanol bath and lyophilizing for approximately 2 days, to yield a hygroscopic white solid (4.331 g, 92%) which was stored over phosphorus pentoxide until required. ^{1}H NMR (D_2O, 200 MHz) δ 0.83 (t, J = 7.2 Hz, 36H, 12 C$\underline{H}_3$), 1.25 (q, J = 7.0, 14.3 Hz, 24H, 12 C$\underline{H}_2$CH$_3$), 1.54 (m, 24H, 12 C$\underline{H}_2$CH$_2$CH$_3$), 3.09 (t, J = 8.3 Hz, 24H, 12 C$\underline{H}_2$-N).

Preparation of [16,17-^{14}C]Geranylgeranyl Pyrophosphate (8a,b).[83]

A mixture of [16,17-^{14}C]geranylgeranyl chloride (19.95 mg, 63.12 μmol), tris-(tetra-*n*-butylammonium) hydrogen pyrophosphate (0.1384 g, 153.3 μmol, 2.42 equivalents) and acetonitrile (0.5 mL) was stirred at room temperature for 6 hours. The solvent was removed *in vacuo* at the end of the reaction to give a yellow oil, which was dissolved in 0.05 M triethylammonium bicarbonate ($Et_3NH^+HCO_3^-$), pH 8.00 (3 mL), and the aqueous phase was extracted with ether (2 x 4 mL) and collected.

A column (1 x 25-cm) of cation exchange DEAE Sephadex A-25 (Aldrich, ion-exchange resin, 40 -120 μ) was prepared at 4°C to purify the product. The column was equilibrated to the bicarbonate form by swelling and washing (5x) first with 1 M triethylammonium bicarbonate, pH 8.00, then with 0.05 M triethylammonium bicarbonate, pH 8.00 (5x). Finally, the packed column was washed with 5 column volumes of 0.05 M triethylammonium bicarbonate, pH 8.00, and the aqueous phase from the reaction was loaded onto the column. The column was developed with a linear gradient (400 mL, 0.5

mL/minute) from 0.05 M triethylammonium bicarbonate, pH 8.00, to 1 M triethylammonium bicarbonate, pH 8.00. The fractions containing geranylgeranyl pyrophosphate (fractions 38 - 61 out of 80) as determined by liquid scintillation counting, were collected and lyophilized until all traces of triethylamonium bicarbonate (white solid) dissappeared. Excess ammonium hydroxide (NH_4OH) was added to the flask and the solution lyophilized once more to give [16,17-^{14}C]geranylgeranyl pyrophosphate: 3.0 $\pm$ 0.2 x 10^5 dpm ^{14}C, 24 $\pm$ 1 % from [16,17-^{14}C]geranylgeraniol.

REFERENCES

1. Wani, M.C.; Taylor, H.L.; Wall, M.E.; Caggon, P.; McPhail, A.T. *J. Am. Chem. Soc.***1971**, *93*, 2325 - 2327.
2. National Cancer Institute *Clinical Brochure: Taxol (NSC 125973)* **1982.**
3. Schiff, P.B.; Fant, J.; Horwitz, S.B. *Nature* **1979**, *22*, 665 - 667.
4. Crossin, K.L; Carney, D.H. *Cell* **1981**, *37*, 341-350.
5. Manfredi, J.J.; Horwitz, S.B. *Pharmacol. Ther.* **1984**, *25*, 83 - 125.
6. Schiff, P.B.; Fant, J.; Auster, L.A.; Horwitz, S.B. *J. Supramolec. Struct.* **1978**, *8*, *Suppl. 2*, 328 - 330.
7. Schiff, P.B.; Horwitz, S.B. *Proc. Natl. Acad. Sci. USA* **1980**, *77*, 1561 - 1565.
8. Rowinsky, E.K.; Cazenave, L.A.; Donehower, R.C. *J of Natl. Cancer Inst.* **1990**, *82*, 1247 - 1259.
9. Schiff, P.B.; Horwitz, S.B. *Biochemistry* **1981**, *20*, 3247 - 3252.
10. Kumar, N. *J. Biol. Chem.* **1981**, *256*, 10435 - 10441.
11. Weiss, R.B.; Donehower, R.C.; Wiernik, P.H.; Ohnuma, T.; Gralla, R.J.; Trump, D.L.; Baker, J.R. Jr; Van Ech, D.A.; Von HOff, D.D.; Leyland-Jones, B. *J. Clin. Onc.* **1990**, *8*, 1263 - 1268.
12. Lassus, M.; Scott, D.; Leyland-Jones, B. *Proc. Amer. Soc. Clin. Oncol.* **1985**, *4*, 1042.
13. Lorentz, W.; Reimann, H.-J.; Schmal, A.; Dormann, P.; Schwarz, B.; Neugebauer, E. *Agent Action* **1977**, *7*, 63 - 68.

14. National Cancer Institute *Clinical Brochure: Taxol (NSC 125973)* **1983**, 6 - 12.

15. Donehower, R.C.; Rowinsky, E.K.; Grochow, L.B.; Longnecker, S.M.; Ettinger, D.S. *Cancer Treat. Rep.* **1987**, *71*, 1171 - 1177.

16. Wiernir, P.H.; Schwartz, E.L.; Strauman, J.J.; Dutcher, J.P.; Lipton, R.B.; Paietta, E. *Cancer Res.* **1987**, *47*, 2486 - 2493.

17. Kris, M.G.; O'Connell, J.P.; Gralla, R.J.; Wertheim, M.S.; Parente, R.M.; Schiff, P.B.; Young, C.W. *Cancer Treat. Rep.* **1986**, *70*, 605 - 607.

18. Lipton, R.B.; Apfel, S.C.; Dutcher, J.B.; Rosenberg, R.; Kaplan, J.; Berger, A.; Einzig, A.I.; Wiernik, P.; Schaumburg, H.H. *Neurology* **1989**, *39*, 368 - 373.

19. Rowinsky, E.K.; Burke, P.J.; Karp, J.E. *Cancer Res.* **1989**, *49*, 4640 - 4647.

20. Koeller, J.; Brown, T.; Havlin, K. *Proc. Amer. Soc. Clin. Oncol.* **1989**, *8*, 82.

21. Wiernir, P.H.; Schwartz, E.L.; Einzig, E.; Strauman, J.J.; Lipton, R.B.; Dutcher, J.B. *J. Clin. Oncol.* **1987**, *5*, 1232 - 1239.

22. Legha, S.S.; Tenney, D.M.; Krakoff, I.R. *J. Clin. Oncol.* **1986**, *4*, 762 - 766.

23. Grem, J.L.; Tutsch, K.D.; Simon, K.J.; Alberti, D.B.; Willson, J.K.V.; Tormey, D.C.; Swaminathan, S.; Trump, D.L. *Cancer Treat. Rep.* **1987**, *71*, 1179 - 1184.

24. Ohnuma, T.; Zimet, A.S.; Coffey, V.A.; Holland, J.F.; Greenspan, E.M. *Proc. Am. Assoc. Cancer Res.* **1985**, *26*, 662.

25. McGuire, W.P.; Rowinsky, E.K.; Rosenshein, N.B.; Grumbine, F.C.; Ettinger, D.S.; Armstrong, D.K.; Donehower, R.C. *Ann. Intern. Med.* **1989**, *111*, 273 - 279.

26. Einzig, A.I.; Gorowski, E.; Sasloff, J.; Wiernik, P.H. *Proc. Am. Assoc. Cancer Res.* **1988**, *29*, 884.

27. Einzig, A.I.; Trump, D.L.; Sasloff, J. *Proc. Amer. Soc. Clin. Oncol.* **1988**, *7*, 963.

28. Legha, S.S.; Ring, S.; Papadopoulos, N.; Raber, M.; Benjamin, R.S. *Cancer* **1990**, *65*, 2478 - 2481.

29. Einzig, A.I.; Weirnik, P.H.; Sasloff, J.; Garl, S.; Runowicz, C.; O'Hanlan, K.A.; Goldberg, G. *Proc. Am. Assoc. Cancer Res.* **1990**, *31*, 1114.

30. Thigpen, T.; Blessing, J.; Ball, H. *Proc. Amer. Soc. Clin. Oncol.* **1990**, *9*, 604.

31. Holmes, R.A.; Walters, R.S.; Theriault, R.L.; Forman, A.D.; Newton, L.K.; Raber, M.N.; Buzdar, A.U.; Frye, D.K.; Hortobagyi, G.N. *J. Natl. Cancer Inst.* **1991**, *83*, 1797 - 1805.

32. Seidman, A.; Reichman, B.; Crown, J. *Proc. Amer. Soc. Clin. Oncol.* **1992**, *11*, 64.

33. Chang, A.; Kim, K.; Glick, J. *Proc. Amer. Soc. Clin. Oncol.* **1992**, *11*, 981.

34. Murphy, W.K.; Winn, R.J.; Fossella, F.V. *Proc. Amer. Soc. Clin. Oncol.* **1992**, *11*, 985.

35. Kingston, D.G.I.; Gunatilaka, A.A.L.; Ivey, C.A. *J. Nat. Prod.* **1992**, *55*, 259 - 261.

36. Blume, E. *J. Natl. Cancer Inst.* **1991**, *83*, 1054 - 1056.

37. Cragg, G.M.; Snader, K.M. *Cancer Cells* **1991**, *3*, 233 - 235.

38. Vidensek, N.; Lim, P.; Campbell, A.; Carlson, C. *J. Nat. Prod.* **1990**, *53*, 1609 - 1610.

39. Witherup, K.M.; Look, S.A.; Stasko, M.W.; Ghiorzi, T.J.; Muschik, G.M.; Cragg, G.M. *J. Nat. Prod.* **1990**, *53*, 1249 - 1255.

40. Wheeler, N.C.; Jech, K.; Masters, S.; Brobst, S.W.; Alvarado, A.B.; Hoover, A.J.;

Snader, K.M. *J. Nat. Prod.* **1992**, *55*, 432 - 440.

41. <ANON>-CHEM-ENG-PR *Chem. Eng. Proc.* **1991**, *87*, 23.

42. Edgington, S.M. *Biotechnology* **9**, *1991*, 933 - 938.

43. Christen, A.A.; Bland, J.; Gibson, G.M. *Proc. Am. Assoc. Cancer Res.* **1989**, *30*, 566, A2252.

44. Sénilh, V.; Blechert, S.; Colin, M.; Guénard, D.; Picot, F.; Potier, P.; Varenne, P. *J. Nat. Prod.* **1984**, *47*, 131 - 137.

45. Chauvière, G.; Guénard, D.; Picot, F.; Sénilh, V.; Potier, P. *C.R. Acad. Sc.* **1981**, *293*, 501 - 514.

46. Guéritte-Voegelein, F.; Sénilh, V.; David, B.; Guénard, D.; Potier, P. *Tetrahedron* **1986**, *42*, 4451 - 4460.

47. Mangatal, L.; Adeline, M.-T.; Guénard, D.; Guéritte-Voegelein, F.; Potier, P. *Tetrahedron* **1989**, *45*, 4177 - 4190.

48. Ringel, I.; Horwitz, S. *J. Natl. Cancer Inst.* **1991**, *83*, 288 - 291.

49. Blume, E. *J. Natl. Cancer Ints.* **1992**, *84*, 673.

50. Denis, J.-N.; Greene, A.E.; Serra, A.A.; Luche, M.-J. *J. Org. Chem.* **1986**, *51*, 46 - 50.

51. Denis, J.-N.; Correa, A.; Greene, A.E. *J. Org. Chem.* **1990**, *55*, 1957 - 1959.

52. Deng, L.; Jacobsen, E.N. *J. Org. Chem.* **1992**, *57*, 4320 - 4323.

53. Palomo, C.; Arrieta, A.; Cossio, F.P.; Aizpurua, J.M.; Mielgo, A.; Aurrekoetxea, N. *Tetrahedron Lett.* **1990**, *31*, 6429 - 6432.

54. Ojima, I.; Habus, I.; Zhao, M.; Georg, G.; Jayasinghe, L.R. *J. Org. Chem.* **1991**,

56, 1681 - 1683.

55. Denis, J.-N.; Correa, A.; Greene, A.E. *J. Org. Chem.* **1991**, *56*, 6939 - 6942.

56. Hönig, H.; Seufer-Wasserthal, P.; Weber, H. *Tetrahedron* **1990**, *46*, 3841 - 3850.

57. Denis, J.-N.; Greene, A.E.; Guénard, D.; Guéritte-Voegelein, F.; Mangatal, L.; Potier, P. *J. Am. Chem. Soc.* **1988**, *110*, 5917 - 5919.

58. Swindell, C.S.; Krauss, N.E.; Horwitz, S.B.; Ringel, I. *J. Med. Chem.* **1991**, *34*, 1176 - 1184.

59. Wender, P.A.; Mucciaro, T.P. *J. Am. Chem. Soc.* **1992**, *114*, 5878 - 5879.

60. Kingston, D.G.I.; Samaranayake, G.; Ivey, C.A. *J. Nat. Prod.* **1990**, *53*, 1 -12.

61. Parness, J.; Kingston, D.G.I.; Powell, R.G.; Harracksingh C.; Horwitz, S.B. *Biochem. Biophys. Res. Commun.* **1982**, *105*, 1082 - 1089.

62. Magri, N.F.; Kingston, D.G.I. *J. Nat. Prod.* **1988**, *51*, 298 - 306.

63. Lataste, H.; Senilh, V.; Wright, M.; Guénard, D.; Potier, P. *Proc. Natl. Acad. Sci.* USA **1984**, *81*, 4090 - 4094.

64. Mellado, W.; Magri, N.F.; Kingston, D.G.I.; Garcia-Arenas, R.; Orr, G.A.; Horwitz, S.B. *Biochem. Biophys. Res. Commun.* **1984**, *124*, 329 - 336.

65. Guéritte-Voegelein, F.; Guénard, D.; Lavelle, R.; Le Goff, M.-T.; Mangatal, L.; Potier, P. *J. Med. Chem.* **1991**, *34*, 992 - 998.

66. Ringel, I.; Horwitz, S.B. *J. Pharmacol. Ther.* **1987**, *242*, 692 - 698.

67. Samaranayake, G.; Magri, N.F.; Jitrangsri, C.; Kingston, D.G.I. *J. Org. Chem.*, **1991**, *56*, 5114 - 5119.

68. Harrison, J.W.; Scrowston, R.M.; Lythgoe, B. *J. Chem. Soc. C* **1966**, 1933 - 1945.

69. Guéritte-Voegelein, F.; Guénard, D.; Potier, P. *J. Nat. Prod.* **1987**, *50*, 9 - 18.

70. Dauben, W.G.; Hubbell, J.P.; Oberhansli, P.; Thiessen, W.E. *J. Org. Chem.* **1979**, *44*, 669 - 673.

71. Begley, M.J.; Jackson, C.B.; Pattenden, G. *Tetrahedron* **1990**, *46*, 4907 - 4924.

72. Kingston, D.G.I. *Pharmacol. Ther.* **1991**, *52*, 1 - 34.

73. Leete, E.; Bodem, G.B. *Tetrahedron Lett.* **1966**, *33*, 3925 - 3927.

74. Platt, R.V.; Opie, C.T.; Haslam, E. *Phytochemistry* **1984**, *23*, 2211 - 2217.

75. Cane, D.E.; Iyengar, R.; Shiao, M.-S. *J. Am. Chem. Soc.* **1981**, *103*, 914 - 931.

76. Coates, R.M.; Ley, D.A.; Cavender, P.L. *J. Org. Chem.* **1978**, *43*, 4915 - 4922.

77. Crombie, L; King, R.W.; Whiting, D.A. *J. Chem. Soc. Perkin I* **1975**, 913 - 915.

78. Cramer, F. *Angew. Chem.* **1959**, *71*, 775 - 779.

79. Cramer, W.D.; Weiman, G. *Chem. Ind. (London)* **1960**, 46 - 54.

80. Cornforth, R.H.; Popjak, G. *Meth. Enzymol.* **1969**, *16*, 359 - 390.

81. Dixit, V.M.; Laskovics, F.M.; Noall, W.I.; Poulter, C.D. *J. Org. Chem.* **1981**, *46*, 1967 - 1969.

82. Davisson, V.J.; Woodside, A.B.; Neal, T.R.; Stremler, K.E.; Muehlbacher, M.; Poulter, D.C. *J. Org. Chem.* **1986**, *51*, 4768 - 4779.

83. Cane, D.E.; Oliver, J.S.; Harrison, P.H.M.; Abell, C.; Hubbard, B.R.; Kane, C.T.; Lattman, R. *J. Am. Chem. Soc.* **1990**, *112*, 4513 - 4524.

84. Sample prepared by Gerri M^{ac}Eachern in the Research Group.

85. Still, W.C.; Kahn, M.; Mitra, A. *J. Org. Chem.* **1978**, *43*, 2923 - 2925.